Title
Exploring the Non-Transcriptional Activity of Thyroid Hormone Derivatives

Permalink
https://escholarship.org/uc/item/1514n1bp

Author
Snead, Aaron Nathan

Publication Date
2008

Peer reviewed|Thesis/dissertation

Exploring the Non-Transcriptional Activity of
Thyroid Hormone Derivatives

by

Aaron Nathan Snead

DISSERTATION

Submitted in partial satisfaction of the requirements for the degree of

DOCTOR OF PHILOSOPHY

in

Chemistry and Chemical Biology

in the

GRADUATE DIVISION

of the

UNIVERSITY OF CALIFORNIA, SAN FRANCISCO

ii

Acknowledgments

Abstract

Exploring the Non-Transcriptional Activity of

Thyroid Hormone Derivatives

This work is premised on the hypothesis that thyroid hormone may be a substrate for the aromatic L-amino acid decarboxylase (AADC) and that the resulting iodothyronamines would have significant structural and perhaps functional similarity with several biogenic amines including the classical monoamine neurotransmitters. Previous reports have shown that several thyronamines are rapid and potent agonists of the trace amine-associated receptor 1 ($TAAR_1$), a G protein-coupled receptor (GPCR). We hypothesized that thyronamines might function physiologically as classical neurotransmitters or neuromodulators. As such, we sought to screen thyronamines for activity with a variety of known monoamine transporters. Additionally we attempted to clone, express and screen the rat TAAR family of GPCRs for activity with thyronamines and a variety of phenethylamine (PEA), thyroid hormone, and amino acid derivatives.

Using our previously reported synthesis of these presumed thyroid hormone metabolites and a radioactive derivative of T_1AM, we found that T_1AM inhibits plasma membrane transport of norepinephrine and dopamine in synaptosomes, and also inhibits biogenic amine vesicular packaging in synaptic vesicles. We further demonstrate that T_1AM is an inhibitor of the plasma membrane neurotransmitter transporters DAT and NET, and an inhibitor of the vesicular transporter VMAT2. This is a novel and exciting result, because T_1AM is the first example of an endogenous substance that inhibits these

transporters and suggests that T_1AM may play a physiological role in regulating synaptic transmission with catecholamine neurons. In addition, we report that several PEA derivatives act as agonists of $rTAAR_4$, both confirming previously identified compounds and discovering several additional agonists. Lastly, we show that a class of clinically used thyroid hormone derivatives act as agonists of $TAAR_1$ with potential therapeutic relevance. Significantly, we expand on our understanding of trace amine-associated receptor ligand recognition and the physiological relevance of thyronamine/GPCR interactions.

Table of Contents

List of Figures, Schemes, and Tables

Chapter 4

Appendix

Chapter 1

Introduction to Thyroid Hormone, Thyronamines, Monoamine Transporters, and Trace Amine-Associated Receptors

Thyroid Hormone

Thyroid hormone (TH) is an important endocrine modulator known to play numerous roles in biology. In vertebrates TH can activate specific nuclear thyroid hormone receptors that regulate transcription of a wide variety of target genes (*1-4*). Deregulation of TH production, both under and over production, results in well-documented developmental problems and adult disease states (*5,6*). Under production, or hypothyroidism, can result in developmental disorders such as cretinism, and problems in adult life including reduction in metabolic rate, body temperature and heart rate, mental disorders like depression, or physical issues like weight gain and goiter formation. Conversely, overproduction in the adult can result in increases in metabolic rate, body temperature and heart rate, as well as decreases in body mass.

TH activity

Thyroid hormone is known to function predominantly in the form of 3,5,3'-triiodo-L-thyronine (T_3). T_3 binds and activates nuclear thyroid hormone receptors that regulate transcription over relatively long time frames (hours to days) (Figure 1). There are two genes, TRα and TRβ, encoding thyroid hormone receptors (*3,7*). Additionally, both genes can have alternative splicing of their transcripts to form two distinct isoforms,

TRα 1 and 2 and TRβ 1 and 2. The transcriptional regulation through these receptors by T$_3$ in target tissues directs many biological processes including development, metabolism, thermogenesis, lipid homeostasis, mood/mental state and cardiac performance.
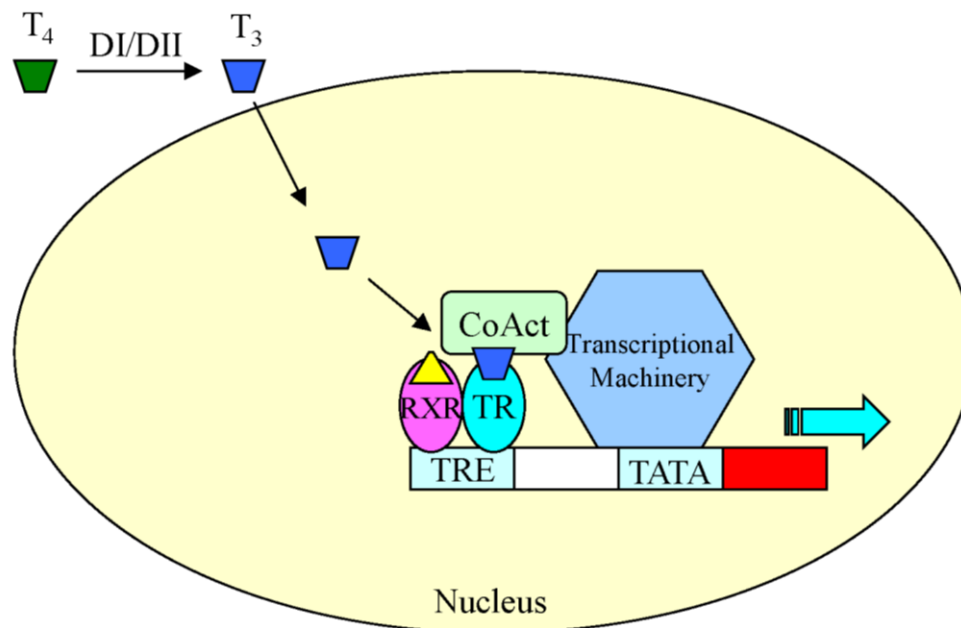
Figure 1. Transcriptional activity of thyroid hormone.

The biosynthesis of TH has been clearly mapped out. TH is initially synthesized in the thyroid gland through a well regulated process of iodination and cross linking of specific tyrosine residues in thyroglobulin by the enzyme thyroperoxidase (TPO) (*3*). TH is biosynthesized covalently bound to thyroglobulin (Tg), and is released by stimulated proteolysis of Tg by thyroid stimulating hormone (TSH), resulting in the largely inactive molecule thyroxine (T$_4$). T$_4$ and a small amount of T$_3$ is then secreted from the thyroid

gland into the circulatory system where the vast majority (> 99%) is bound by carrier

proteins (including thyroxine binding globulin, thyroxine binding prealbumin, and

albumin) to prevent degradation and facilitate delivery of the hormone to target tissues.

In target tissues T_4 is subsequently monodeiodinated by type 1 5'-deiodinase (DI) or type

2 5'-deiodinase (DII) to the more physiologically active T_3 (Figures 1 and 2) (*8*). A third

deiodinase family member, type 3 5-deiodinase (DIII) can also remove an inner ring

iodine from T_4 to produce the inactive 3, 3', 5'- triiodothyronine (rT_3). Enzymatic

combinations of these three deiodinases can remove additional iodine molecules in order

to both inactivate T_3 as well as recycle the iodine for future TH production. This

systematic deiodination can produce 9 possible permutations of iodothyronines from T_4

to T_0.
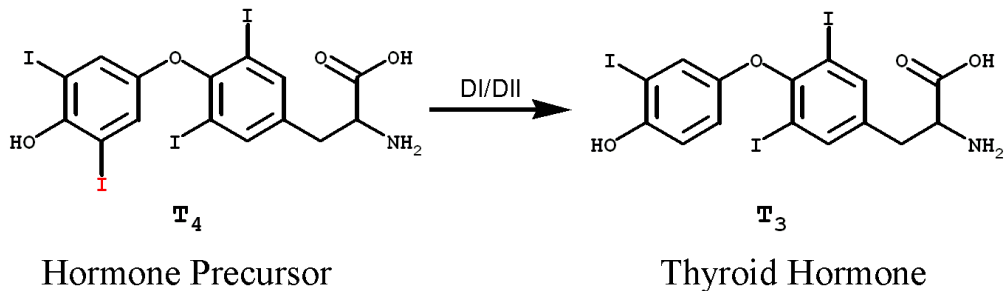
Figure 2. T_3 Biosynthesis.

Non-transcriptional effects

In addition to these well documented transcriptional or genomic effects, rapid

responses to thyroid hormone (seconds to minutes), too fast to be explained by

transcriptional effects, have also been demonstrated (*9-12*). Administration of TH has

been observed to have general effects on ion fluxes and electrophysiological events in

cardiac cells (*13*). These include an increase in 2-deoxyglucose uptake in chick embryo and heart and other organ cells of the rat, transient effects on Ca^{2+} uptake as well as effects on cystolic free Ca^{2+} levels in rat myocytes, PKC-mediated sarcoplasmic reticulum Ca^{2+}-ATPase activity, rapid stimulation of the Na^+/H^+ antiporter, regulation of electrophysiological parameters of rat ventricular myocytes measured using whole cell patch clamp techniques, stimulation of O_2 consumption, and effects on Na+ currents in cardiac myocytes. These rapid responses occur within seconds to minutes but the molecular basis of these non-transcriptional responses remains unknown.

Thyronamine Hypothesis

Over time T_4 and T_3 are metabolized and are known to be discarded as waste; however, these resulting metabolites may have unique and specific biological activities of their own. Our lab hypothesized that TH could be metabolized by one of the enzymes that is involved in the biosynthesis of the biogenic amine neurotransmitters, the aromatic L-amino acid decarboxylase (AADC). AADC is responsible for the removal of the carboxylic acid nonspecifically on aromatic L-amino acids, such as the conversion of tyrosine to tyramine, and is essential for the production of the transmitters dopamine, epinephrine, norepinephrine and serotonin (*14*).

This proposed decarboxylation of TH, which is an aromatic L-amino acid, coupled with the known deiodination pathways for TH suggested a novel class of compounds, the iodothyronamines (Figure 3). The class of thyronamines consists of the nine iodinated derivatives of decarboxylated T_4 (Figure 4). A previous report described

4

the synthesis and pharmacology of this class of compounds (*15*). Additionally, the

presence of endogenous thyronamines was reported in various mammalian tissues.
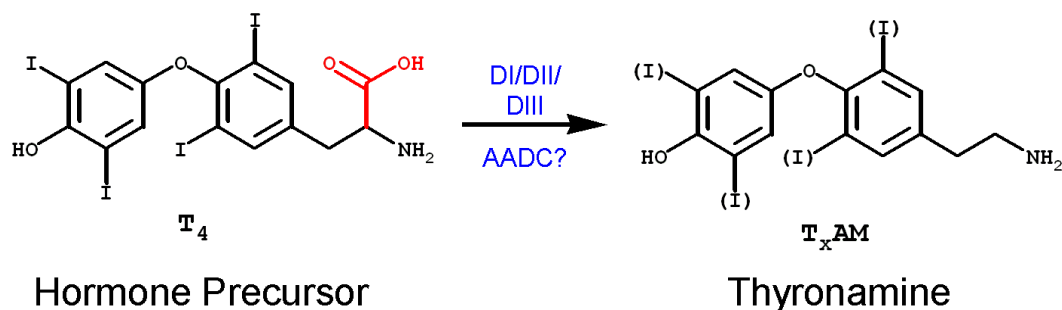
Figure 3. Proposed iodothyronamine biosynthesis.

This work demonstrated that at least two of these compounds, thyronamine

(T_0AM) and 3-iodothyronamine (T_1AM), are present in various vertebrate tissues and

are potent and rapid activators of the rat and mouse trace amine associated receptors 1

($TAAR_1$), members of the G protein-coupled receptor (GPCR) superfamily (*15*). T_1AM,

when administered by intraperitoneal (i.p.) injection in mice, induces profound

hypothermia and bradycardia within minutes, too rapid for a transcriptional mechanism.
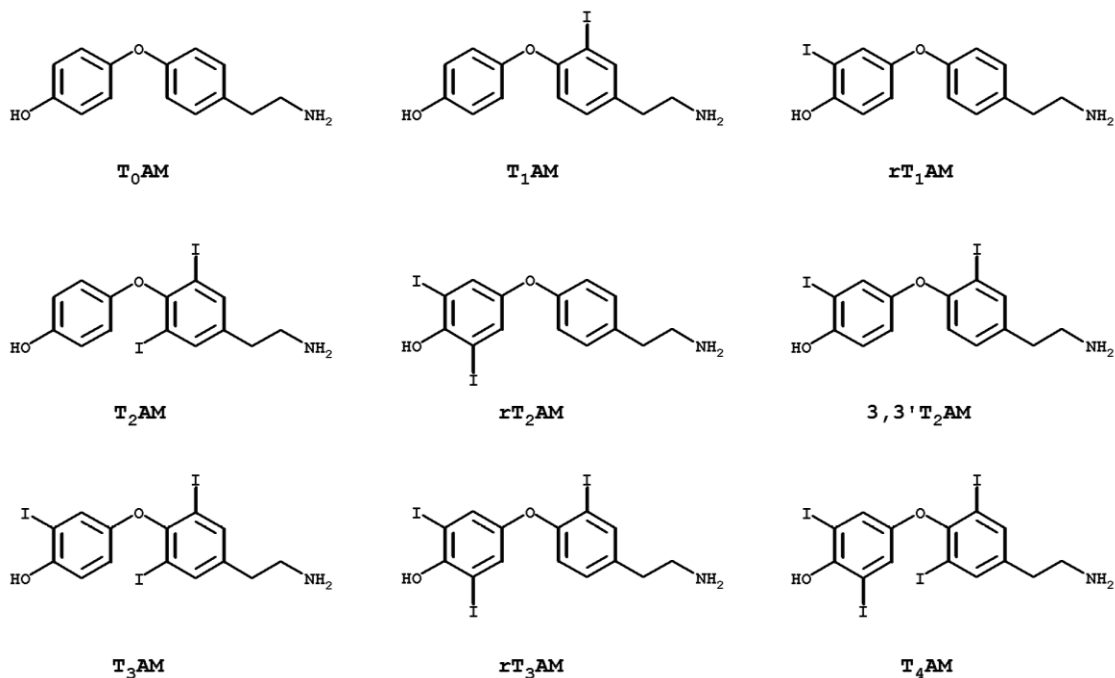
Figure 4. Thyronamine Panel.

TAAR$_1$ is an orphan G protein-coupled receptor (GPCR) that was discovered by two independent groups attempting to clone novel catecholamine and 5-HT receptor family homologs (*16,17*). TAAR$_1$ belongs in the biogenic amine subfamily of class A GPCRs. This receptor is coupled to a stimulatory G protein (G$_S$) and is found in a variety of tissues (*16-19*).

In addition to T$_1$AM, a wide variety of synthetic and naturally occurring trace amines act as potent agonists of the various TAAR$_1$ orthologs. Several groups established that TAAR$_1$ is activated by a wide variety of PEA derivatives with distinct SAR (*16,17,20-25*), including even the drugs of abuse, amphetamines and ecstasy. Work with some of these ligands in cardiac models has suggested that TAAR activity can

influence cardiac performance (*26*). TAAR1 has also been shown capable of negatively

regulating insulin release in pancreatic β-cells (*18*). Additionally, two separate TAAR$_1$

knockout studies in mice have linked the receptor to movement control (*27*), modulation

of catecholaminergic function, and sensitivity to amphetamine with implications for

disorders like Parkinson's disease and schizophrenia (*28*).

TAAR$_1$, however, is only one member of a family of orphan GPCRs. Several

molecular genetic studies have suggested mutations in a variety of TAAR homologs may

be linked with specific disease states. Mutations within the group of TAAR genes on

chromosome 6 suggested correlation with familial instances of cluster headaches (*29*).

Additional studies have offered conflicting reports of a link between mutations in

TAAR6 and instances of schizophrenia and bipolar disorder in specific ethnic

populations (*30-39*).

Independent groups have shown that a wide variety of vertebrates contain the

TAAR family of genes (*40-42*), though the absolute number in a given species varies

widely (as few as 9 in chimpanzee (with 6 being pseudogenes) to as many as 97 in

zebrafish (40 pseudogenes). The disparity in TAAR number per species raised intriguing

questions about the possible function of this receptor family. Are these merely redundant

copies of the same receptor? Do these receptors recognize the same ligands but have

different tissue distribution? Or do these receptors recognize distinct sets of ligands, each

with a unique function? To address these questions we aimed to clone and functionally

express the rat TAAR family members and profile the ligand preference of this set of

TAAR GPCRs.

Another class of molecules that activate TAAR GPCRs is the trace amines (*16,17,43-45*). Like thyronamines, trace amines contain the arylethylamine functionality that is common to the catecholamines; dopamine, norepinephrine, and epinephrine, which are known to also activate GPCRs as classical neurotransmitters. Trace amines are endogenous derivatives of monoamine neurotransmitters and were originally presumed to be transient by-products of neurotransmitter synthesis and metabolism. When added at high concentrations, trace amines had striking pharmacological effects (*46*). This work by Raiteri *et al*. classified this set of molecules as neuromodulators because they were shown to influence neurotransmission by regulating the active transport of monoamine transmitters through monoamine transporters.

Neurotransmission occurs at the synapse by the regulated release of large stores of transmitters from the presynaptic neuron, which can then activate receptors (GPCRs or ion channels) on the postsynaptic neuron. Active transport of the transmitters is essential for neurotransmission, as it is the process by which transmitter stores accumulate. There are two distinct cellular locations where neurotransmitters are transported across membranes (*47-49*). The first is at the membrane of the secretory vesicle where transmitters are accumulated from the cytoplasm in preparation for regulated exocytotic release. The second location is at the plasma membrane where specific transporters for each of the classical neurotransmitters act to terminate signaling and to recycle transmitters for future rounds of release.

Neurotransmitter transporters function by four distinct mechanisms, all of which exploit the strong electrochemical gradients that are maintained at the respective membranes to push transmitters up their concentration gradients (Figure 5) (*50*). At the

plasma membrane, transporters either 1) exchange Na^+ and Cl^- from one side of the membrane for transmitters (GABA, monoamines, glycine, or proline) on the other, or 2) couple the exchange of Na^+ and K^+ with the co-transport of transmitter (glutamate or aspartate) and a proton. At the vesicular membrane, where transport is driven solely by the proton electrochemical gradient established by ATPase activity, transporters either 3) rely on the electrical component where transport is driven by the ability of negatively charged transmitters (GABA or amino acids) crossing the membrane to balance the positively charged vesicle, or 4) rely on the chemical component by exchanging positively charged protons for positively charged transmitters (monoamines or acetylcholine). Mechanisms 1 and 4 are the primary mechanisms for monoamine transport in the central nervous system (CNS). The plasma membrane transporters responsible for cellular uptake of the monoamine neurotransmitters are the dopamine transporter (DAT), the norepinephrine transporter (NET) and the serotonin transporter (SERT), and the sole transporter responsible for vesicular transport of all monoamines in the CNS is the vesicular monoamine transporter 2 (VMAT2) (*51,52*).
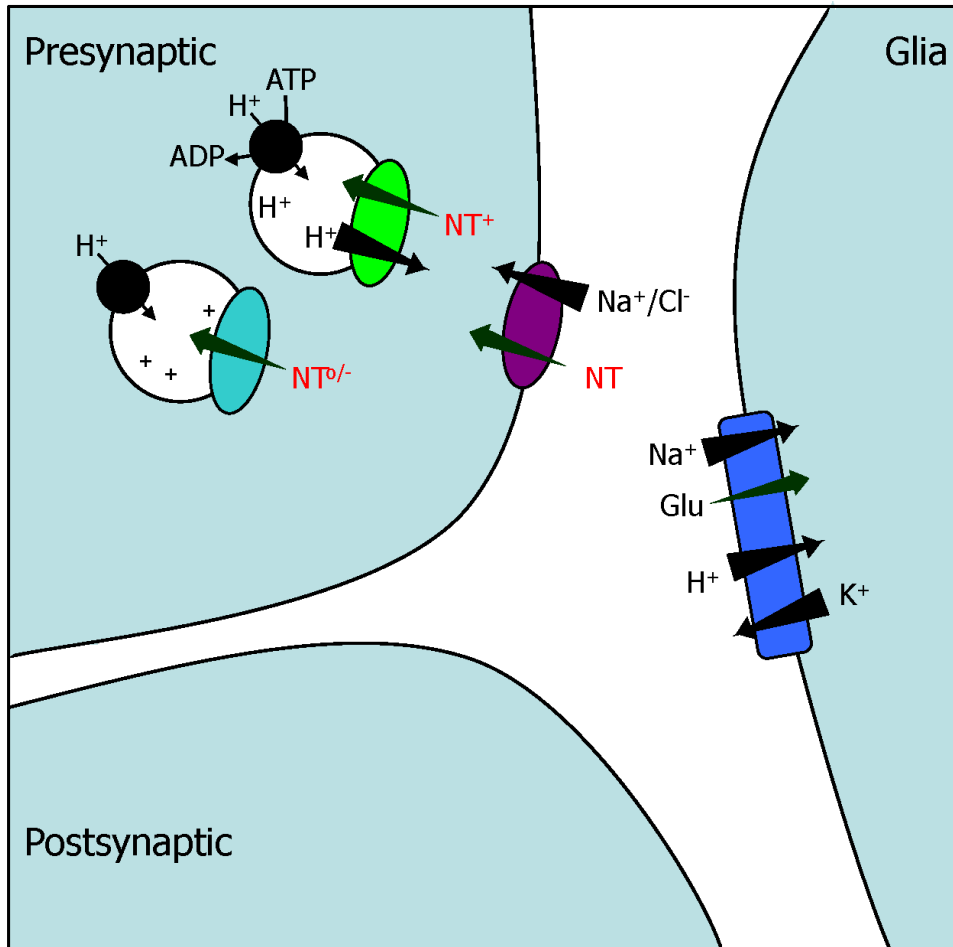
Figure 5. Mechanisms of neurotransmitter transport. Image reproduced from Liu et al. (*50*). Mechanisms of CNS transmitter transport. Mechanism 1 is depicted by the purple oval, mechanism 2 by the blue rectangle, mechanism 3 by the turquoise oval and mechanism 4 by the green oval.

Given the presence of thyronamines in the brain and their structural similarity to the monoamine transmitters and trace amines, we hypothesized that thyronamines might interact with monoamine transporters. Additionally because thyronamines have potent *in vitro* activity with a class of orphan G protein-coupled receptors (GPCRs), the trace amine associated receptors (TAARs), and exhibit activity kinetics that are common to the catecholamine and serotonin neuromodulators and neurotransmitters we hypothesized

that thyronamines may function physiologically as classical neurotransmitters or neuromodulators (Figure 6).

My work sought to expand on our understanding of trace amine-associated receptor ligand recognition and the physiological relevance of thyronamine/GPCR interactions. Additionally we investigated a novel neuromodulatory role for thyronamines, further exploring the role for non-transcriptional effects of thyroid hormone derivatives. This was done by examining several key aspects of neurotransmission; identifying thyronamine activity with specific cellular and vesicular packaging machinery, and characterization of specificity and potency of various thyronamines and TH derivatives with GPCRs. To classify one or more of these molecules as neurotransmitters three criteria must be met; 1) they have a downstream post-synaptic receptor 2) they are selectively packaged for signaled release into the synapse and 3) there is a reuptake mechanism for their recycling. Chapter 2 discusses our work to screen various monoamine transporters (VMAT2, DAT, NET, and SERT) for activity with thyronamines. Chapter 3 shows our effort to clone, express, and evaluate the ligand profiles of the rat family of trace amine-associated receptors. Finally, Chapter 4 presents a screen of several $TAAR_1$ orthologs for activity with another class of clinically used thyroid hormone derivatives, amiodarones.
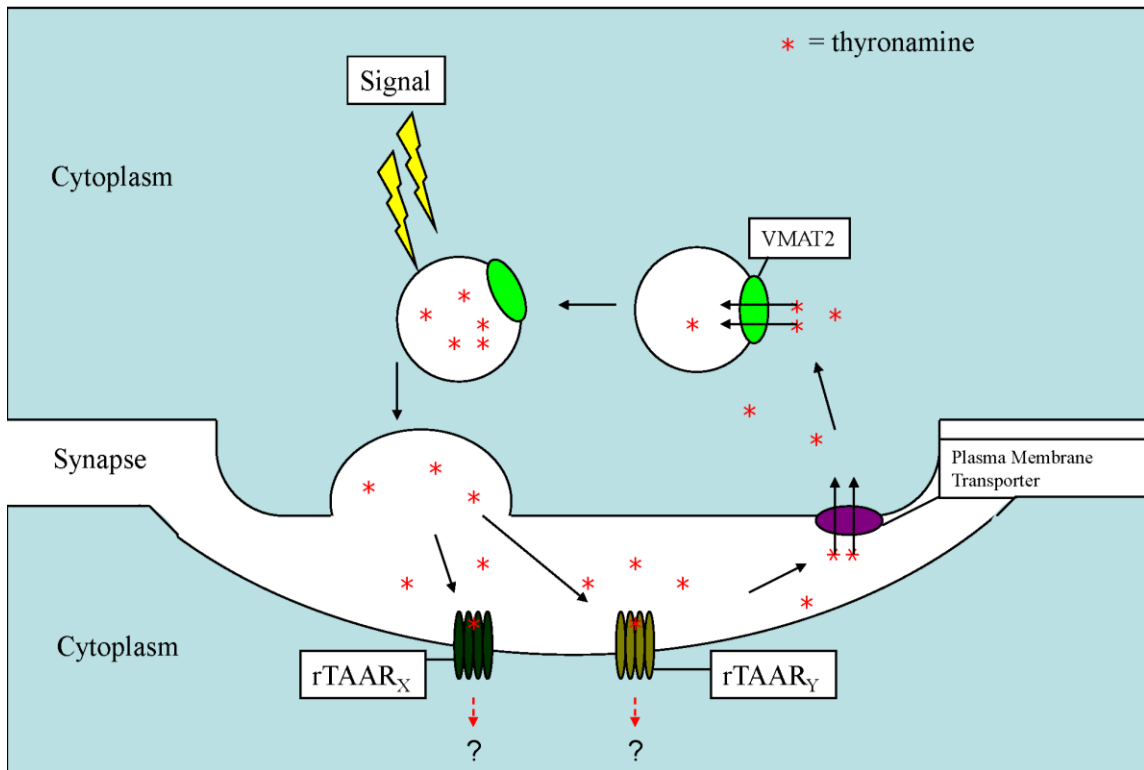
Figure 6. Proposed thyronamine activity.

References

1.   Oppenheimer, J. H. (1979) Thyroid hormone action at the cellular level, *Science 203*, 971-9.

2.   Oppenheimer, J. H.,Schwartz, H. L.,Mariash, C. N.,Kinlaw, W. B.,Wong, N. C.;Freake, H. C. (1987) Advances in our understanding of thyroid hormone action at the cellular level, *Endocr Rev 8*, 288-308.

3.   Yen, P. M. (2001) Physiological and molecular basis of thyroid hormone action, *Physiol Rev 81*, 1097-142.

4.   Harvey, C. B.;Williams, G. R. (2002) Mechanism of thyroid hormone action, *Thyroid 12*, 441-6.

5.   Utiger, R. D. (1995) Thyrotropin-receptor mutations and thyroid dysfunction, *N Engl J Med 332*, 183-5.

6.   Shi, Y. B.,Ritchie, J. W.;Taylor, P. M. (2002) Complex regulation of thyroid hormone action: multiple opportunities for pharmacological intervention, *Pharmacol Ther 94*, 235-51.

7.   Mangelsdorf, D. J.,Thummel, C.,Beato, M.,Herrlich, P.,Schutz, G.,Umesono, K.,Blumberg, B.,Kastner, P.,Mark, M.,Chambon, P.;Evans, R. M. (1995) The nuclear receptor superfamily: the second decade, *Cell 83*, 835-9.

8.   Larsen, P. R.;Berry, M. J. (1995) Nutritional and hormonal regulation of thyroid hormone deiodinases, *Annu Rev Nutr 15*, 323-52.

9.   Davis, P. J.;Davis, F. B. (1996) Nongenomic actions of thyroid hormone, *Thyroid 6*, 497-504.

10. Davis, P. J.;Davis, F. B. (2002) Nongenomic actions of thyroid hormone on the heart, *Thyroid 12*, 459-66.

11. Shih, A.,Zhang, S.,Cao, H. J.,Tang, H. Y.,Davis, F. B.,Davis, P. J.;Lin, H. Y. (2004) Disparate effects of thyroid hormone on actions of epidermal growth factor and transforming growth factor-alpha are mediated by 3',5'-cyclic adenosine 5'-monophosphate-dependent protein kinase II, *Endocrinology 145*, 1708-17.

12. Davis, P. J.,Leonard, J. L.;Davis, F. B. (2008) Mechanisms of nongenomic actions of thyroid hormone, *Front Neuroendocrinol 29*, 211-8.

13. Falkenstein, E.,Tillmann, H. C.,Christ, M.,Feuring, M.;Wehling, M. (2000) Multiple actions of steroid hormones--a focus on rapid, nongenomic effects, *Pharmacol Rev 52*, 513-56.

14. Zhu, M. Y.;Juorio, A. V. (1995) Aromatic L-amino acid decarboxylase: biological characterization and functional role, *Gen Pharmacol 26*, 681-96.

15. Scanlan, T. S.,Suchland, K. L.,Hart, M. E.,Chiellini, G.,Huang, Y.,Kruzich, P. J.,Frascarelli, S.,Crossley, D. A.,Bunzow, J. R.,Ronca-Testoni, S.,Lin, E. T.,Hatton, D.,Zucchi, R.;Grandy, D. K. (2004) 3-Iodothyronamine is an endogenous and rapid-acting derivative of thyroid hormone, *Nat Med 10*, 638-42.

16. Borowsky, B.,Adham, N.,Jones, K. A.,Raddatz, R.,Artymyshyn, R.,Ogozalek, K. L.,Durkin, M. M.,Lakhlani, P. P.,Bonini, J. A.,Pathirana, S.,Boyle, N.,Pu, X.,Kouranova, E.,Lichtblau, H.,Ochoa, F. Y.,Branchek, T. A.;Gerald, C. (2001) Trace amines: identification of a family of mammalian G protein-coupled receptors, *Proc Natl Acad Sci U S A 98*, 8966-71.

17.   Bunzow, J. R.,Sonders, M. S.,Arttamangkul, S.,Harrison, L. M.,Zhang, G.,Quigley, D. I.,Darland, T.,Suchland, K. L.,Pasumamula, S.,Kennedy, J. L.,Olson, S. B.,Magenis, R. E.,Amara, S. G.;Grandy, D. K. (2001) Amphetamine, 3,4-methylenedioxymethamphetamine, lysergic acid diethylamide, and metabolites of the catecholamine neurotransmitters are agonists of a rat trace amine receptor, *Mol Pharmacol 60*, 1181-8.

18.   Regard, J. B.,Kataoka, H.,Cano, D. A.,Camerer, E.,Yin, L.,Zheng, Y. W.,Scanlan, T. S.,Hebrok, M.;Coughlin, S. R. (2007) Probing cell type-specific functions of Gi in vivo identifies GPCR regulators of insulin secretion, *J Clin Invest 117*, 4034-43.

19.   Regard, J. B.,Sato, I. T.;Coughlin, S. R. (2008) Anatomical profiling of G protein-coupled receptor expression, *Cell 135*, 561-71.

20.   Hart, M. E.,Suchland, K. L.,Miyakawa, M.,Bunzow, J. R.,Grandy, D. K.;Scanlan, T. S. (2006) Trace amine-associated receptor agonists: synthesis and evaluation of thyronamines and related analogues, *J Med Chem 49*, 1101-12.

21.   Wainscott, D. B.,Little, S. P.,Yin, T.,Tu, Y.,Rocco, V. P.,He, J. X.;Nelson, D. L. (2007) Pharmacologic characterization of the cloned human trace amine-associated receptor1 (TAAR1) and evidence for species differences with the rat TAAR1, *J Pharmacol Exp Ther 320*, 475-85.

22.   Reese, E. A.,Bunzow, J. R.,Arttamangkul, S.,Sonders, M. S.;Grandy, D. K. (2007) Trace amine-associated receptor 1 displays species-dependent stereoselectivity for isomers of methamphetamine, amphetamine, and para-hydroxyamphetamine, *J Pharmacol Exp Ther 321*, 178-86.

23.   Tan, E. S.,Miyakawa, M.,Bunzow, J. R.,Grandy, D. K.;Scanlan, T. S. (2007) Exploring the structure-activity relationship of the ethylamine portion of 3-iodothyronamine for rat and mouse trace amine-associated receptor 1, *J Med Chem 50*, 2787-98.

24.   Lewin, A. H.,Navarro, H. A.;Mascarella, S. W. (2008) Structure-activity correlations for beta-phenethylamines at human trace amine receptor 1, *Bioorg Med Chem 16*, 7415-23.

25.   Tan, E. S.,Groban, E. S.,Jacobson, M. P.;Scanlan, T. S. (2008) Toward deciphering the code to aminergic G protein-coupled receptor drug design, *Chem Biol 15*, 343-53.

26.   Frascarelli, S.,Ghelardoni, S.,Chiellini, G.,Vargiu, R.,Ronca-Testoni, S.,Scanlan, T. S.,Grandy, D. K.;Zucchi, R. (2008) Cardiac effects of trace amines: pharmacological characterization of trace amine-associated receptors, *Eur J Pharmacol 587*, 231-6.

27.   Sotnikova, T. D.,Zorina, O. I.,Ghisi, V.,Caron, M. G.;Gainetdinov, R. R. (2008) Trace amine associated receptor 1 and movement control, *Parkinsonism Relat Disord 14 Suppl 2*, S99-102.

28.   Wolinsky, T. D.,Swanson, C. J.,Smith, K. E.,Zhong, H.,Borowsky, B.,Seeman, P.,Branchek, T.;Gerald, C. P. (2007) The Trace Amine 1 receptor knockout mouse: an animal model with relevance to schizophrenia, *Genes Brain Behav 6*, 628-39.

29. Aridon, P.,D'Andrea, G.,Rigamonti, A.,Leone, M.,Casari, G.;Bussone, G. (2004) Elusive amines and cluster headache: mutational analysis of trace amine receptor cluster on chromosome 6q23, *Neurol Sci 25 Suppl 3*, S279-80.

30. Duan, J.,Martinez, M.,Sanders, A. R.,Hou, C.,Saitou, N.,Kitano, T.,Mowry, B. J.,Crowe, R. R.,Silverman, J. M.,Levinson, D. F.;Gejman, P. V. (2004) Polymorphisms in the trace amine receptor 4 (TRAR4) gene on chromosome 6q23.2 are associated with susceptibility to schizophrenia, *Am J Hum Genet 75*, 624-38.

31. Ikeda, M.,Iwata, N.,Suzuki, T.,Kitajima, T.,Yamanouchi, Y.,Kinoshita, Y.,Inada, T.;Ozaki, N. (2005) No association of haplotype-tagging SNPs in TRAR4 with schizophrenia in Japanese patients, *Schizophr Res 78*, 127-30.

32. Duan, S.,Du, J.,Xu, Y.,Xing, Q.,Wang, H.,Wu, S.,Chen, Q.,Li, X.,Li, X.,Shen, J.,Feng, G.;He, L. (2006) Failure to find association between TRAR4 and schizophrenia in the Chinese Han population, *J Neural Transm 113*, 381-5.

33. Amann, D.,Avidan, N.,Kanyas, K.,Kohn, Y.,Hamdan, A.,Ben-Asher, E.,Macciardi, F.,Beckmann, J. S.,Lancet, D.;Lerer, B. (2006) The trace amine receptor 4 gene is not associated with schizophrenia in a sample linked to chromosome 6q23, *Mol Psychiatry 11*, 119-21.

34. Venken, T.,Alaerts, M.,Adolfsson, R.,Broeckhoven, C. V.;Del-Favero, J. (2006) No association of the trace amine-associated receptor 6 with bipolar disorder in a northern Swedish population, *Psychiatr Genet 16*, 1-2.

35. Vladimirov, V.,Thiselton, D. L.,Kuo, P. H.,McClay, J.,Fanous, A.,Wormley, B.,Vittum, J.,Ribble, R.,Moher, B.,van den Oord, E.,O'Neill, F. A.,Walsh,

D.,Kendler, K. S.;Riley, B. P. (2007) A region of 35 kb containing the trace amine associate receptor 6 (TAAR6) gene is associated with schizophrenia in the Irish study of high-density schizophrenia families, *Mol Psychiatry 12*, 842-53.

36.   Reiners, J.,Schmidt, M.,Packer, J.,Unger, L.;Wernet, W. (2007) A polymorphism linked to bipolar affective disorder does not alter the CRE activity of constitutively activated trace amine receptor 4, *Mol Psychiatry 12*, 900-2.

37.   Pae, C. U.,Yu, H. S.,Amann, D.,Kim, J. J.,Lee, C. U.,Lee, S. J.,Jun, T. Y.,Lee, C.,Paik, I. H.,Patkar, A. A.;Lerer, B. (2008) Association of the trace amine associated receptor 6 (TAAR6) gene with schizophrenia and bipolar disorder in a Korean case control sample, *J Psychiatr Res 42*, 35-40.

38.   Vladimirov, V. I.,Maher, B. S.,Wormley, B.,O'Neill, F. A.,Walsh, D.,Kendler, K. S.;Riley, B. P. (2008) The trace amine associated receptor (TAAR6) gene is not associated with schizophrenia in the Irish Case-Control Study of Schizophrenia (ICCSS) sample, *Schizophr Res*

39.   Ludewick, H. P.,Schwab, S. G.,Albus, M.,Lerer, B.,Maier, W.,Trixler, M.;Wildenauer, D. B. (2008) No support for an association with TAAR6 and schizophrenia in a linked population of European ancestry, *Psychiatr Genet 18*, 208-10.

40.   Lindemann, L.,Ebeling, M.,Kratochwil, N. A.,Bunzow, J. R.,Grandy, D. K.;Hoener, M. C. (2005) Trace amine-associated receptors form structurally and functionally distinct subfamilies of novel G protein-coupled receptors, *Genomics 85*, 372-85.

41. Gloriam, D. E.,Bjarnadottir, T. K.,Schioth, H. B.;Fredriksson, R. (2005) High Species Variation within the Repertoire of Trace Amine Receptors, *Ann N Y Acad Sci 1040*, 323-7.

42. Gloriam, D. E.,Bjarnadottir, T. K.,Yan, Y. L.,Postlethwait, J. H.,Schioth, H. B.;Fredriksson, R. (2005) The repertoire of trace amine G-protein-coupled receptors: large expansion in zebrafish, *Mol Phylogenet Evol 35*, 470-82.

43. Premont, R. T.,Gainetdinov, R. R.;Caron, M. G. (2001) Following the trace of elusive amines, *Proc Natl Acad Sci U S A 98*, 9474-5.

44. Kim, K. A.;von Zastrow, M. (2001) Old drugs learn new tricks: insights from mammalian trace amine receptors, *Mol Pharmacol 60*, 1165-7.

45. Berry, M. D. (2004) Mammalian central nervous system trace amines. Pharmacologic amphetamines, physiologic neuromodulators, *J Neurochem 90*, 257-71.

46. Raiteri, M.,Del Carmine, R.,Bertollini, A.;Levi, G. (1977) Effect of sympathomimetic amines on the synaptosomal transport of noradrenaline, dopamine and 5-hydroxytryptamine, *Eur J Pharmacol 41*, 133-43.

47. Schuldiner, S.,Shirvan, A.;Linial, M. (1995) Vesicular neurotransmitter transporters: from bacteria to humans, *Physiol Rev 75*, 369-92.

48. Masson, J.,Sagne, C.,Hamon, M.;El Mestikawy, S. (1999) Neurotransmitter transporters in the central nervous system, *Pharmacol Rev 51*, 439-64.

49. Torres, G. E.,Gainetdinov, R. R.;Caron, M. G. (2003) Plasma membrane monoamine transporters: structure, regulation and function, *Nat Rev Neurosci 4*, 13-25.

50. Liu, Y.,Krantz, D. E.,Waites, C.;Edwards, R. H. (1999) Membrane trafficking of neurotransmitter transporters in the regulation of synaptic transmission, *Trends Cell Biol 9*, 356-63.

51. Weihe, E.,Schafer, M. K.,Erickson, J. D.;Eiden, L. E. (1994) Localization of vesicular monoamine transporter isoforms (VMAT1 and VMAT2) to endocrine cells and neurons in rat, *J Mol Neurosci 5*, 149-64.

52. Peter, D.,Liu, Y.,Sternini, C.,de Giorgio, R.,Brecha, N.;Edwards, R. H. (1995) Differential expression of two vesicular monoamine transporters, *J Neurosci 15*, 6179-88.

Chapter 2

Thyronamines Inhibit Plasma Membrane and Vesicular Monoamine Transport

Abstract

Thyroid hormone has long been known to have important transcriptional regulatory activities. Recently, however, the presence of endogenous derivatives of thyroid hormone, thyronamines, has been reported in various mammalian tissues. These derivatives have potent *in vitro* activity with a class of orphan G protein-coupled receptors (GPCRs), the trace amine-associated receptors (TAARs), and profound *in vivo* effects when administered to mice. We report here a novel neuromodulatory role for thyronamines. In synaptosomal preparations and heterologous expression systems, thyronamines act as specific dopamine and norepinephrine reuptake inhibitors. Thyronamines also inhibit the transport of monoamines into synaptic vesicles. These observations expand the non-transcriptional role of thyroid hormone derivatives, and may help to explain the pharmacological effects of thyronamines *in vivo*.

Introduction

A previous report described the synthesis and pharmacology of a class of compounds, thyronamines (*1*) (Supplementary Figure 1), which are presumably decarboxylated metabolites of thyroid hormone, a classic endocrine hormone known to exert its actions by means of transcriptional regulation (*2, 3*). This work demonstrated that at least two of these compounds, thyronamine (T_0AM) and 3-iodothyronamine (T_1AM), are present in various vertebrate tissues and are potent and rapid activators of the rat and mouse trace amine associated receptors 1 ($TAAR_1$), members of the G protein-coupled receptor (GPCR) superfamily. T_1AM, when administered by intraperitoneal (i.p.) injection in mice, induces profound hypothermia and bradycardia within minutes, too rapid for a transcriptional mechanism.

Notably, thyronamines contain the arylethylamine scaffold and exhibit activity kinetics that are common to the catecholamine and serotonin neuromodulators and neurotransmitters. Trace amines, another well described class of molecules with arylethylamine functionality, are endogenous derivatives of monoamine neurotransmitters. Despite their presence in the brain, trace amines were originally presumed to be transient by-products of neurotransmitter synthesis and metabolism, causing striking pharmacological effects, but only at high concentrations. Additionally, trace amines have been shown to influence neurotransmission by regulating the active transport of monoamine transmitters, thus acting as neuromodulators (*4*). However, recent evidence suggests a physiological role for these trace amines. Like thyronamines, they have been shown to activate the TAAR family of GPCRs (*5–9*).

There are two distinct cellular locations where neurotransmitters are transported across membranes. The first is at the plasma membrane where specific transporters for each of the classical neurotransmitters act to terminate signaling and to recycle transmitters for future rounds of release. The second location is at the membrane of the secretory vesicle where transmitters are accumulated from the cytoplasm in preparation for regulated exocytotic release (*10–12*). The plasma membrane transporters responsible for cellular uptake of the monoamine neurotransmitters are the dopamine transporter (DAT), the norepinephrine transporter (NET) and the serotonin transporter (SERT), and the sole transporter responsible for vesicular transport of all monoamines in the central nervous system (CNS) is the vesicular monoamine transporter 2 (VMAT2) (*13, 14*).

Neurotransmitter transport has an important role in normal neurotransmission and in a wide variety of disease states (*11*). However, the specific molecular mechanisms that regulate these activities remain poorly understood. Given the presence of thyronamines in the brain and their structural similarity to the monoamine transmitters and trace amines, we hypothesized that thyronamines might interact with monoamine transporters. Herein we demonstrate that several thyronamines, including T_1AM, act as specific dopamine and norepinephrine reuptake inhibitors, as well as inhibitors of VMAT2. These data shed light on the molecular mechanisms that contribute to the physiological and pharmacological effects of monoamines.

Results and Discussion

The current study tested the ability of a panel of synthetically derived iodothyronamines (*1*) to perturb monoamine neurotransmitter transport, with the goal of expanding the potential physiological roles of thyronamines and understanding the molecular mechanisms of thyronamine pharmacology. This analysis was motivated by the significant structural similarity of thyronamines to the trace amines and monoamine neurotransmitters, as well as the demonstrated GPCR activity with TAARs. T_1AM became the primary focus of this work due to its profound pharmacological activity *in vivo* and its potent ability to activate rat and mouse $TAAR_1$ relative to other trace amines *in vitro* (*1, 5, 6*). Herein, we demonstrate that T_1AM is a DAT, NET, and VMAT2 inhibitor with low μM potencies. This novel neuromodulatory role for T_1AM indicates a potentially expanded physiological role for thyroid hormone derivatives, distinct from transcriptional regulation, and adds to the complexity of thyronamine pharmacology.

T_1AM Inhibition of Synaptosomal Monoamine Transport

To study the effect of T_1AM on plasma membrane monoamine transport, we prepared rat brain synaptosomes. Synaptosomal preparations have been used previously to study plasma membrane neurotransmitter transport (*4, 15*). Membranes were assayed with or without either T_1AM (10 μM) or the reuptake inhibitor mazindol (3 μM). At this concentration, T_1AM significantly inhibited dopamine, norepinephrine and serotonin transport (77.6%, 72.1%, and 42.2% inhibition respectively, as compared with no T_1AM controls) (Fig. 1A). This mirrors the activity of mazindol, a potent inhibitor of dopamine, norepinephrine and serotonin transporters (*12*), which at 3 μM inhibited transport of the

24

respective radioligands in this assay by 92.5%, 76.4%, and 15.5%. Both T_1AM and mazindol demonstrated specificity for inhibition of monoamine transport, as neither had any significant effect on glutamate transport.

Several of the classical trace amines and pharmacological ligands which are structurally similar to T_1AM, are known both to inhibit neurotransmitter transport and also to be recognized as substrates (*16, 17*). To distinguish between a role as an inhibitor or a substrate, $[^{125}I]T_1AM$ was synthesized and used to directly measure T_1AM transport (*18*). Membranes incubated with $[^{125}I]T_1AM$ demonstrated no significant uptake above background binding (Fig. 1B). Additionally, increasing concentrations of unlabeled T_1AM had no effect on the relative uptake (data not shown), indicating that T_1AM is not a substrate.
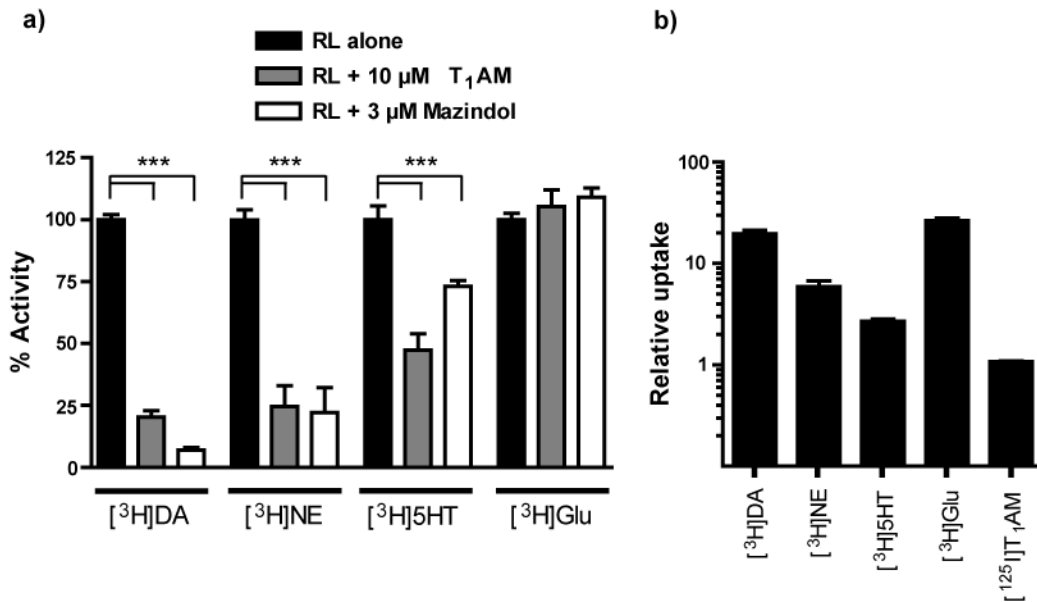
Figure 1 T$_1$AM Inhibition of Synaptosomal Transport of Monoamines. a) Uptake is shown as percent activity normalized for each of the tritiated radioligands [^{3}H]5HT, [^{3}H]DA, [^{3}H]NE, and [^{3}H]Glu. Statistical significance was determined using the paired two-tailed t test. ***, statistically significant, $p < 0.001$. b) Alternately, uptake of these radioligands or [^{125}I]T$_1$AM at 37 °C for 5 min is shown relative to uptake at time 0 min, in which membranes were held on ice and the reaction mixture was immediately quenched with cold KRH buffer. Membranes treated with radioligand and 1% DMSO showed no significant difference in uptake compared with cells incubated with radioligand alone (data not shown). The mean values reported are from three separate experiments performed in triplicate.

DAT, NET, and SERT inhibition by thyronamines

The dopamine transporter (hDAT), norepinephrine transporter (hNET), and serotonin transporter (hSERT), were expressed in HeLa cells to identify the specificity of T$_1$AM for each of the plasma membrane monoamine transporters, and to screen for activity of the other thyronamines. Heterologous expression of the various plasma membrane transporters has been demonstrated (*19*) and provides an excellent means of selectively analyzing transport by each of the known transporters outside the nervous

system. To determine the effects of various thyronamines on each of the transporters, transfected cells were assayed for uptake of their preferred substrates ([^{3}H]5HT for SERT, [^{3}H]DA for DAT, and [^{3}H]NE for NET) in the presence of each of the nine thyronamines at a single concentration (10 μM). Consistent with the rat synaptosomal uptake, hDAT and hNET were sensitive to T$_1$AM, with transport inhibited by 76.5% and 67.7% respectively, as compared with non-T$_1$AM treated controls (Fig 2A, B). Additionally, both hDAT and hNET had varying sensitivities to the other thyronamines at 10 μM. In the case of hNET transport we found that several thyronamines, T$_2$AM, T$_3$AM, and rT$_3$AM, increased NE transport (33 to 75%). In contrast to the synaptosomal results, however, heterologously expressed hSERT was insensitive to T$_1$AM and most of the thyronamines at 10 μM (Fig. 2C). Only 3,3'T$_2$AM demonstrated any significant inhibition of hSERT (~50% inhibition at 10 μM 3,3'T$_2$AM). Controls with mazindol showed near complete inhibition, indicating that hSERT was fully sensitive to a known inhibitor. Furthermore, identical experiments performed with rDAT and rSERT showed similar overall activity and thyronamine sensitivity (data not shown). Additionally, neither DAT, NET, nor SERT demonstrated detectable uptake of [^{125}I]T$_1$AM under a variety of conditions (Fig 2D).
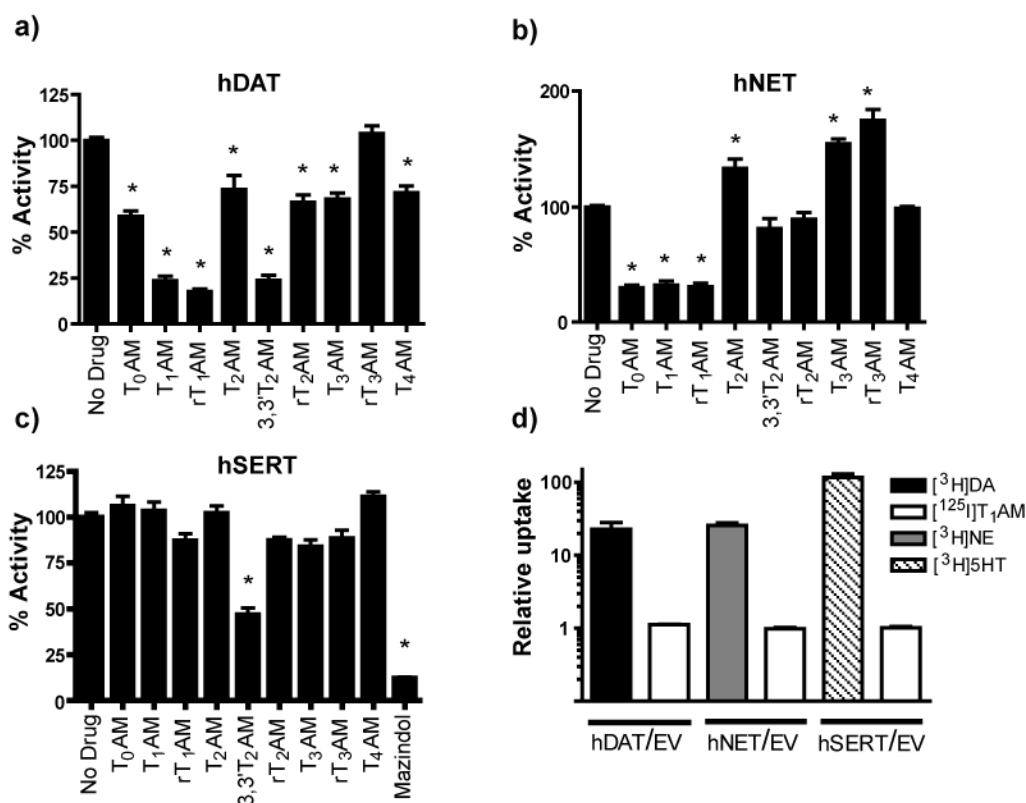
Figure 2 DAT, NET, and SERT Inhibition by Thyronamines. a–c) Results are shown as percent uptake normalized to 100% for hDAT, hNET, and rSERT with radioligand alone. d) Alternatively uptake is shown relative to empty pBSK or empty pcDNA3 transfected cells. Statistical significance was determined using the paired two-tailed t test. *, statistically significant, $p < 0.001$. Cells treated with radioligand and 1% DMSO showed no significant difference in uptake compared with cells incubated with radioligand alone (data not shown). The mean values reported are from three separate experiments performed in triplicate.

To characterize more thoroughly the potency of T_1AM inhibition, a dose response was performed with hDAT and hNET, varying the T_1AM concentrations from 10 nM to 100 μM. The analysis yielded IC_{50}s for T_1AM of 3.6 μM in the case of hDAT and 4.4 μM in the case of hNET (Fig. 3A, B, Table 1). The mode of T_1AM inhibition was then assessed by measuring the effects of T_1AM on the K_m and V_{max} of DA transport by DAT and NE transport by NET. hDAT transfected HeLa cells were incubated with 20 nM to

100 μM [³H]DA with or without 5 μM T$_1$AM. 5 μM T$_1$AM increased the K$_m$ (from ~5

μM to ~16 μM) and decreased (by ~25%) the V_{max} (Fig. 3C, Table 1), suggesting that

T$_1$AM acts by mixed inhibition, with competitive and noncompetitive components. The

kinetic analysis was repeated for hNET-transfected cells incubated with 10 nM to 100

μM [³H]NE with or without 5 μM T$_1$AM. T$_1$AM addition resulted in a nearly three-fold

increase (1.8 μM to ~5.0 μM) in K$_m$ (Fig. 3D, Table 1), but had no significant effect on

V_{max}, indicating that T$_1$AM behaves as a competitive inhibitor of hNET.
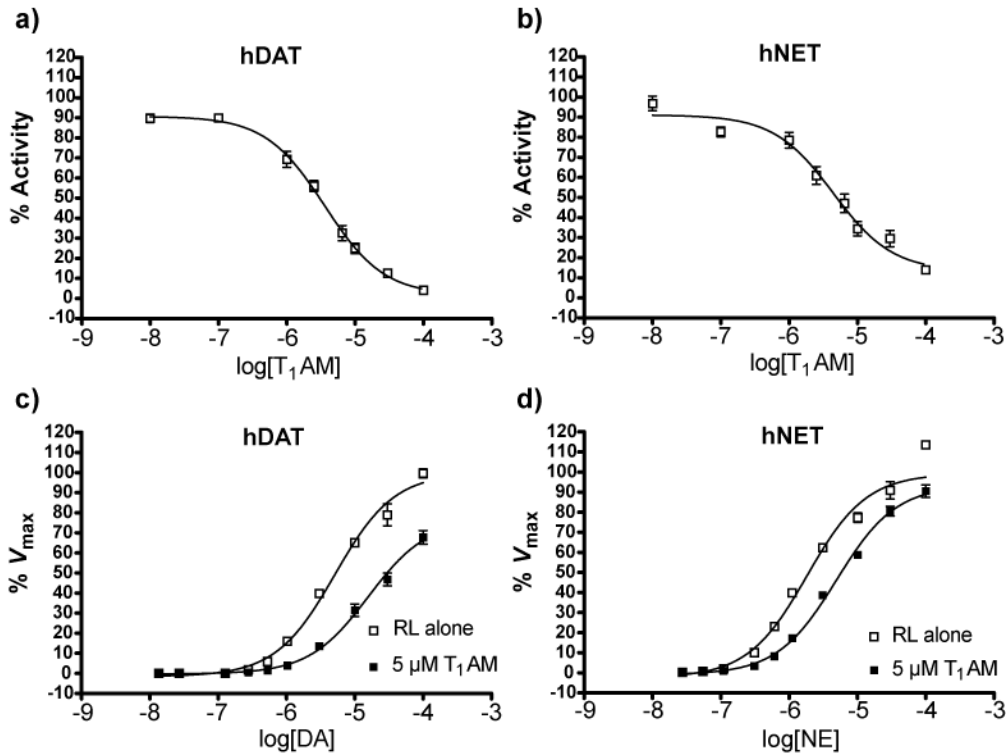
Figure 3. DAT, NET Dose Responses to T$_1$AM Treatment. a–b) Data are shown as percent uptake of cells incubated with radioligand alone. c–d) Data are shown as percent V_{max} of non- T$_1$AM treated cells as calculated by Prism 4.0. The mean values reported are from three separate experiments performed in triplicate.

Synaptosomal preparations and heterologous expression systems allowed us to assess the pharmacological effects of thyronamines on the plasma membrane transport of monoamines and generated a detailed analysis of thyronamine sensitivities and T_1AM inhibition kinetics. In synaptosomal uptake assays, T_1AM demonstrated near complete inhibition of DA and NE uptake at 10 μM, with limited effects on 5HT uptake and no effects on glutamate transport. Coupling this with data from heterologous expression systems for DAT, NET, and SERT, T_1AM selectively inhibits DAT and NET at concentrations similar to those demonstrated for several of the trace amines (*4*). Although DAT and NET are both inhibited by T_1AM, there are subtle differences in their overall thyronamine structure-activity relationships (SAR), with DAT showing additional sensitivity to rT_1AM and $3,3'T_2AM$, and NET to T_0AM and rT_1AM. Surprisingly, we found that T_2AM, T_3AM, and rT_3AM hyper-activate NET (33 to 75%) by an unknown mechanism. Given the similarity of DAT and NET in sequence (65% identity) and substrate preference, it is noteworthy that structural changes as small as the presence and location of a single iodide atom can lead to differences in recognition by these two transporters.

In contrast to the consistent inhibition of DAT and NET in synaptosomes and heterologous expression systems, T_1AM inhibits uptake of $[^3H]$5HT into rat synaptosomal preparations but has no effect on transport of $[^3H]$5HT by hSERT. Although these observations seem contradictory, there are possible SERT-independent sources of 5HT uptake in the synaptosome assay. Thus, considering the relatively low level of synaptosomal uptake seen for 5HT (2.7 fold over background), compared to that for DA (19.6 fold), NE (5.9 fold), and Glu (26.5 fold), the poor ability of mazindol to

block 5HT uptake in this assay, as well as the inability of T_1AM to inhibit recombinant

hSERT, we conclude that T_1AM is not a SERT inhibitor.

Effects of T_1AM on Synaptic Vesicle Transport

Since we found that T_1AM may modulate plasma membrane monoamine

transport we sought to determine its effect on vesicular monoamine transport, as this is

often a coupled process. To assess the effects of T_1AM on synaptic vesicle amine

transport, synaptic vesicles were purified from crude synaptosomal preparations by

means of differential centrifugation. Using vesicle preparations, the uptake of $[^3H]$5HT

was measured with or without T_1AM or tetrabenazine, a known VMAT2 inhibitor (IC_{50}

of 460 nM) (*20*). Tetrabenazine (TBZ) is an appropriate positive control for inhibition

because TBZ-sensitive VMAT2 is the only known vesicular transporter for monoamines

in the CNS (*13, 14*). $[^3H]$5HT was used as the test substrate because it is recognized with

high apparent affinity by VMAT2 (K_m ~0.29 μM). We observed that T_1AM (10 μM)

inhibited vesicular transport of 5HT by 62% (Fig. 4A). In the same assay saturating

levels of TBZ inhibited monoamine transport by 87%. However, no transport of

$[^{125}I]T_1AM$ could be detected under a variety of conditions (Fig. 4B).

31
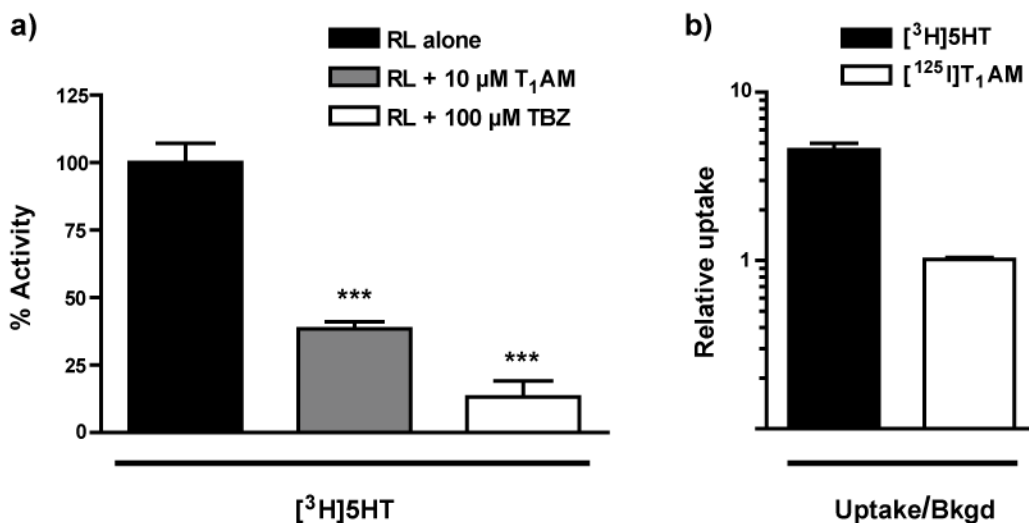
Figure 4. Effects of T$_1$AM on Synaptic Vesicle Transport. a) Uptake is shown as percent activity normalized for the uptake of 20–30 nM [^{3}H]5HT alone. Statistical significance was determined using the paired two-tailed t test. ***, statistically significant, p < 0.001. b) Alternately, uptake of [^{3}H]5HT or [^{125}I]T$_1$AM at 37 °C for 5 min is shown relative to uptake at time 0 min, in which membranes were held on ice and the reaction mixture was immediately quenched with cold SH buffer. Membranes treated with radioligand and 1% DMSO showed no significant difference in uptake compared with cells incubated with radioligand alone (data not shown). The mean values reported are from three separate experiments performed in duplicate.

VMAT2 inhibition by thyronamines

To understand the interaction of T$_1$AM with vesicular monoamine transport, we assayed 5HT uptake in the presence of thyronamines (10 μM final concentration) into endosomal membranes prepared from rVMAT2-transfected HEK293 cells. Consistent with the effects seen in synaptic vesicles, T$_1$AM significantly inhibited VMAT2 (by 80%) (Fig 5A). In addition to T$_1$AM, all thyronamines except T$_4$AM inhibited VMAT2 mediated transport of [^{3}H]5HT to varying degrees. The potency we observed for T$_1$AM (IC$_{50}$ of 3.2 μM) is comparable to several well characterized VMAT2 inhibitors (*21, 22*) (Fig. 6A, Table 1). To address the possible recognition of T$_1$AM as a VMAT2 substrate,

32

we also assayed the uptake of $[^{125}I]T_1AM$. No $[^{125}I]T_1AM$ transport could be detected in membranes prepared from cells transfected with VMAT2 (Fig. 5B).
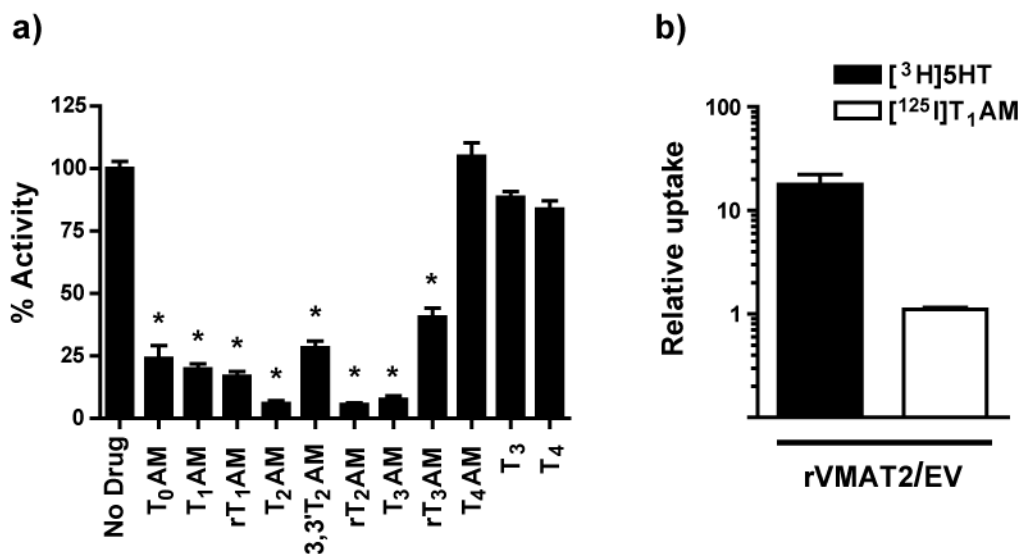
Figure 5. VMAT2 Activity with Thyronamines. a) Uptake is shown as percent activity normalized for 20 nM $[^3H]5HT$ alone. Statistical significance was determined using the paired two-tailed t test. *, statistically significant, p < 0.001. b) Additionally for $[^3H]5HT$ and $[^{125}I]T_1AM$, uptake is shown as a uptake relative to WT HEK293 cell membrane preparation treated as described above. Membranes treated with radioligand and 1% DMSO showed no significant difference in uptake compared with cells incubated with radioligand alone (data not shown). The mean values reported are from three separate experiments performed in triplicate.

To determine the mode of T_1AM inhibition, kinetic analyses were performed using 20 nM to 100 μM $[^3H]5HT$ with or without 5 μM T_1AM. 5 μM T_1AM resulted in a more than two-fold increase in K_m (450 nM to 1.1 μM) and a 26% reduction in V_{max} (Fig. 6B, Table 1), suggesting that T_1AM inhibits VMAT2 by mixed inhibition, with both competitive and noncompetitive components.
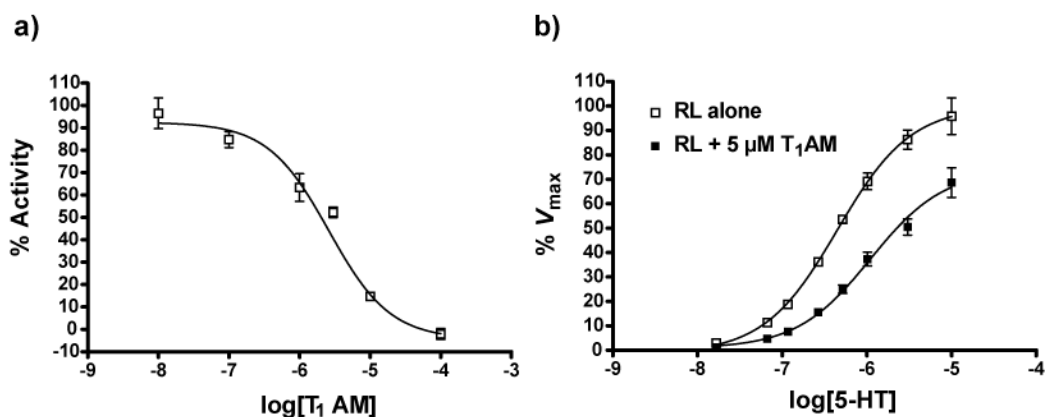
Figure 6. Mode of T$_1$AM Inhibition. a) Data are shown as % uptake of non-T1AM treated cells. b) Similarly, membrane preparations of VMAT2 transfected cells were assayed as described in Fig. 5 with various concentrations of non-radioactive 5HT (20 nM to 10 μM) with or without 5 μM T$_1$AM. Data are shown as percent V_{max} of untreated VMAT2 membranes, as calculated by Prism 4.0. The mean values reported are from three separate experiments performed in triplicate.

	T$_1$AM	0 T$_1$AM		5 μM T$_1$AM	
	IC$_{50}$ (μM)	K$_m$ (μM)	% V_{max}	K$_m$ (μM)	% V_{max}
hDAT	3.59	5.11	100 ± 2.1	15.79	76.8 ± 2.9
hNET	4.41	1.83	100 ± 1.9	4.95	94.1 ± 1.4
rVMAT2	3.20	0.45	100 ± 3.1	1.10	74.0 ± 3.5

Table 1. T$_1$AM Effects on Neurotransmitter Transport. Cells and membranes were prepared, assayed with radioligand, and uptake determined for each transporter as described in methods. To assess T$_1$AM sensitivity, the amount of ligand required to inhibit DA, NE, or 5HT transport by 50% (IC$_{50}$) was determined. The K$_m$ values for dopamine, norepinephrine, and serotonin were calculated using Prism 4.0 software using a range of ligand concentrations. The mean values reported are from three separate experiments performed in triplicate. The standard error of the log of the IC$_{50}$ or K$_m$ values was <1.5% for all values. % V_{max} values are presented ± SE.

Unlike the plasma membrane monoamine transporters, the vesicular monoamine transporter, VMAT2, tolerates a variety of monoamine substrates (*21, 23*), and this tolerance translated into a broader sensitivity to thyronamines. All thyronamines except T_4AM demonstrate significant inhibition of VMAT2 and the potency of T_1AM (3.2 μM) is comparable to the trace amines and other VMAT2 inhibitors (*21, 22*). Notably, compounds with fewer than two iodines in their phenolic ring showed greater VMAT2 inhibition. Most significantly, our data revealed inhibition of neurotransmitter transport by T_1AM, but no detectable uptake of radiolabeled T_1AM, under a variety of conditions, by either the synaptic vesicle preparations or by membranes heterologously expressing VMAT2. This is surprising given the wide variety of substrates transported by VMAT2. Thus, T_1AM is the only known endogenous phenethylamine examined to date that inhibits VMAT2 but fails to be recognized as a substrate.

Implications of T1AM modulation of monoamine transport

Given T_1AM's ability to inhibit DAT, NET, and VMAT2 mediated transport, one might expect T_1AM inhibition of plasma membrane monoamine traffic to cause a significant accumulation of extracellular monoamines and other downstream effects (*24, 25*). Additionally, inhibition of vesicular monoamine transport would likely deplete neurotransmitter stores, reducing further monoamine transmission. This would produce effects in the CNS similar to, but perhaps distinct from, supra-physiological levels of trace amines and other neuromodulators like cocaine and amphetamines. Although, the observed potencies of thyronamine inhibition (low μM IC_{50}s) are lower than that of the pharmacological reuptake inhibitors cocaine and mazindol (low–mid nM IC_{50}s, K_is)

they are comparable to the potencies of the biogenic trace amines (low μM) and known

VMAT2 inhibitor tetrabenazine (< 1 μM).

Despite the differences in potencies, aminergic agents that regulate monoamine

neurotransmission have been associated with thermoregulatory and cardiac effects (*26–*

28). Although not as rapidly acting as T_1AM, the hypothermic induction by reserpine

administration highlights such an effect (*29, 30*). Thus, T_1AM effects on monoamine

transport may contribute to the observed hypothermia and reduction in cardiac

performance *in vivo*. There is evidence, however, that activation of $TAAR_1$ correlates

with the hypothermic induction by T_1AM and related derivatives (*31*). This led to the

supposition that TAAR-mediated activity may be the underlying molecular mechanism of

the observed T_1AM pharmacology.

Evidence for three possibilities now exists. The first is that thyronamine activity

with TAAR GPCRs alone leads to the observed pharmacological effects, and the

neuromodulatory effects on monoamine transport have an as yet undiscovered effect on

mammalian physiology. Second, the neuromodulatory activities of thyronamines are

responsible for the hypothermic and cardiac effects. This could be consistent with the

TAAR studies if the synthetic thyronamine derivatives tested for GPCR activity also

inhibit monoamine transport with the same SAR. Lastly, it is possible that the

thyronamine effects on monoamine transport and activity with $TAAR_1$ synergistically

lead to the observed pharmacology. This would be possible if thyronamines

simultaneously block monoamine transport leading to higher extracellular levels of

monoamines, as well as activate TAAR GPCRs to regulate neurotransmission through

intracellular mechanisms (*32*). Such dual activity with transporters and GPCRs is

common for neuromodulators and other pharmacological agents such as MDMA (*7, 33*).

This synergistic mechanism is the most feasible given the complex nature of the effects

seen coupled with the recent demonstration of the feedback between $TAAR_1$ and DAT

activity (*34, 35*).

Beyond their pharmacological properties, thyronamines may also have unique

physiological roles. T_0AM and T_1AM are present in a variety of mammalian tissues

including the brain, as well as in circulation (*1*). The hypothesis of a physiological role

for thyroid hormone derivatives is not new. Specifically, Dratman *et al.* hypothesized

that thyroid hormone metabolites may be active neurotransmitters or neuromodulators

(*36*). They demonstrated that intravenous administration of radiolabeled thyroid

hormone is efficiently localized to, concentrated, retained, and metabolized in

synaptosomal components of rat brains, specifically regions associated with

noradrenergic signaling (*37–40*). T_1AM was not specifically identified in these studies,

but metabolites with complete phenolic ring deiodination, as in T_1AM, were not

observed due to location of the $[^{125}I]$ tag in the radioligand used. Despite the discovery of

thyroid hormone localization and subsequent metabolism in the brain, determination of

local concentrations of the hormone or its metabolites has, to our knowledge, not been

quantified.

Evidence for specific active transport of physiological levels of thyroid hormone,

the presumed parent compound for thyronamines, into synaptosomes raises the

physiological potential of thyronamine effects on neurotransmitter transport above that of

the other trace amines, for which no active transport mechanism at physiological levels

has been described (*8*). Despite the unknown synaptosomal concentrations of thyroid

hormone or its derivatives, it is widely appreciated that, given active localization mechanisms such as demonstrated for thyroid hormone by Dratman *et al.*, local concentrations can far exceed circulating levels (*41*). As an extension of the demonstrated trafficking and subsequent metabolism of thyroid hormone (*37–40*), it is feasible that local concentrations of thyronamines in specific brain regions may reach levels determined here to be sufficient to affect catecholamine transport. This supports the hypothesis of a specific physiological mechanism for thyroid hormone transport, metabolism, and neuromodulation by means of thyronamine activity in the mammalian CNS.

In summary, several thyronamines, including T_1AM, inhibit neuronal transport of DA and NE, as well as vesicular transport of biogenic amines. The vesicular activity of T_1AM is particularly interesting because it is the only demonstrated instance of an endogenous monoamine inhibitor of VMAT2 that is itself not a substrate. The now expanded role of T_1AM highlights its potentially novel mechanism of action as a physiologically relevant neuromodulator, consistent with the definition supplied by Berry (*8*), and raises the possibility of a unique pharmacology in the CNS distinct from the known activity of the monoamine neurotransmitters, any of the other endogenous trace amines, or known pharmacological agents including cocaine and amphetamines. Though this demonstrated neuromodulatory activity of T_1AM can explain some of the previously observed pharmacology, these effects are highly complex and may have multiple underlying causes.

METHODS:

Synaptosome Purification

Crude synaptosomes were prepared as previously described (*42*). Briefly, brains, avoiding myelin-rich areas, were removed from freshly decapitated Sprague-Dawley rats greater than 10 weeks of age and placed into ice-cold homogenization buffer (320 mM sucrose, 4 mM Hepes-NaOH, pH 7.3 (10 mL per brain)) with protease inhibitors (Complete protease inhibitor tablet, Roche) plus 200 μM Phenylmethanesulfonyl fluoride (PMSF) and 1 μg mL^{-1} Pepstatin A), homogenized in a glass-Teflon homogenizer at 900 rpm, and centrifuged for 10 min at 1000Xg. The supernatant was then centrifuged for 15 min at 12000Xg. The pellet was resuspended in homogenization buffer (10 mL per brain) (avoiding the dark brown bottom of the pellet) and re-centrifuged for 15 min at 13,000Xg. The resulting pellet was carefully resuspended in homogenization buffer to yield the crude synaptosomal preparation.

Synaptosomal Transport Assay

For each experiment 75 μg of protein of the synaptosome preparation was added to 200 μL of KRH buffer (125 mM NaCl, 4.8 mM KCl, 1.3 mM CaCl$_2$, 1.2 mM MgSO$_4$, 1.2 mM KH$_2$PO$_4$, 25 mM HEPES, 5.6 mM Glucose, pH 7.3) containing 100 μM sodium ascorbate (Sigma), 100 μM pargyline (Sigma) and either 40 nM 5-[1,2-^{3}H] Hydroxytryptamine ([^{3}H]serotonin, [^{3}H]5HT), 20 nM 3,4-[Ring-2,5,6-^{3}H]-Dihydroxyphenethylamine ([^{3}H]dopamine, [^{3}H]DA) (Perkin Elmer), 180 nM DL-[7-^{3}H(N)]- norepinephrine ([^{3}H]norepinephrine, [^{3}H]NE) (Perkin Elmer), 40 nM L-[3,4, ^{3}H]-Glutamic Acid ([^{3}H]Glu) (Perkin Elmer), or several non-radioactive T$_1$AM

concentrations (from 100 nM to 10 μM) doped with [^{125}I]T$_1$AM (*18*). To determine the

effect of compounds on uptake of radioligands either non-radioactive T$_1$AM (10 μM

final concentration) (*31*), or mazindol (3 μM final concentration, Research Biochemicals

International- Sigma) was added to the reaction solution, and the solution was incubated

for 5 min at 37 °C. The transport reaction was terminated by rapid dilution with two 1.5

mL aliquots of cold KRH buffer and filtration through 0.2 μm HT 200 Tuffryn

membranes (Pall Life Sciences). The filters were then dried and bound radioactivity

measured by scintillation counting in cytoscint (ICN) scintillation fluid. Transport

activity for each condition was measured in triplicate on at least three separate occasions.

The protein concentration of each synaptosome prep was measured using a Coomassie

protein assay (Pierce) (*20*). In order to determine background measurements for each

radioligand, membranes in the reaction mixture were held on ice and the mixture was

immediately quenched with cold KRH buffer and filtered as described above.

Cell Transfection

For transfection of hNET, hDAT (Susan G. Amara Lab, University of Pittsburgh,

Pittsburgh, PA), hSERT (Randy D. Blakely Lab, Vanderbilt University, Nashville, TN),

empty pBluescript SKII(-) (pBSK) and empty pcDNA3, HeLa cells were grown to

confluency in 15 cm plates in DMEH21 containing 10% (v/v) heat inactivated fetal

bovine serum (FBS) (Hyclone Laboratories) and 1% (v/v) pen/strep. Cells were seeded

into 24 well plates at ~100,000 cells per well 16 hours prior to transfection and were

transfected using the vaccinia/T7 transient expression system, described previously (*19*).

For rVMAT2 expressing stable HEK293 cell lines, HEK293 cells were transfected with rVMAT2 pcDNA3 plasmid. HEK293 cells were grown to confluency in 15 cm plates in DMEH21 media containing 10% (v/v) heat inactivated FBS and 1% (v/v) pen/strep. 16 hours prior to transfection cells were split 1:2. Cells were transfected with Lipofectamine (Invitrogen) using standard protocol, placed in G418 selective media 48 hours after transfection and propagated until harvest.

Membrane Preparation

HEK293 cells expressing VMAT2 or untransfected HEK293 cells from 15 cm plates were washed in pre-warmed (37 °C) PBS, manually detached from the plate with a cell scraper (Fisherbrand, Fisher Scientific), collected by centrifugation (5 min at 1000Xg), and resuspended in cold SH buffer (0.32 M sucrose, 10 mM HEPES, pH 7.4) containing protease inhibitors (Complete protease inhibitor tablet, Roche). The cell suspension was then sonicated in an ice-cooled bath sonicator (Branson) at medium intensity twice for 20 seconds, and the cell debris removed by sedimentation at 1300Xg for 5 min at 4 °C. All membranes were frozen and used within 60 days with no significant reduction in transport activity. The protein concentration of each membrane preparation was measured using a Coomassie protein assay.

DAT/NET/SERT Transport Assay

For each experiment, 24 well plates with HeLa cells transiently expressing either hNET, hDAT, hSERT, empty pBSK, or empty pcDNA3 (described above) were assayed as previously described (*19*). Briefly, cells were washed and preincubated with pre-

warmed KRTH (120 mM NaCl, 4.7 mM KCl, 2.2 mM CaCl$_2$, 1.2 mM MgSO$_4$, 1.2 mM

KH$_2$PO$_4$, 5 mM Tris, 10 mM HEPES, pH 7.4) containing 100 µM ascorbate (500 µL per

well) for 30 min at 37°C. Uptake was initiated by the addition of 55 nM [^{3}H]NE, 20 nM

[^{3}H]DA, 30 nM [^{3}H]5HT, or several non-radioactive T$_1$AM concentrations (from 100

nM to 10 µM) doped with [^{125}I]T$_1$AM. To determine the effect of each of the

thyronamines on transport of radioligands, thyronamines (*31*) dissolved in DMSO were

added to the reaction to a 10 µM final concentration, or mazindol to a final concentration

of 3 µM, and transport measured after incubation for 20 min at 37 °C. To determine the

effects of T$_1$AM on K$_m$ for dopamine, non-radioactive DA (Sigma) dissolved in 100 µM

ascorbate was added to the reaction solution at concentrations ranging from 10 nM to 100

µM, with or without 5 µM non-radioactive T$_1$AM. Transport was measured after

incubation for 20 min at 37 °C. To determine effects of T$_1$AM on the K$_m$ for

norepinephrine, non-radioactive NE (Sigma) dissolved in 100 µM ascorbate was added to

the reaction solution at concentrations ranging from 100 nM to 100 µM, with or without 5

µM non-radioactive T$_1$AM. Transport was measured after incubation for 20 min at 37

°C. Following incubation, the transport reaction was terminated (cells were washed three

times with 0.5 mL cold (4 °C) KRTH and solubilized in 1% (w/v) SDS), and

radioactivity measured by scintillation counting in cytoscint scintillation fluid (ICN).

Transport activity for each condition was measured in triplicate on at least three separate

occasions. Data given for relative uptake of hDAT and hNET show representative uptake

for a single experiment done in triplicate. In order to determine background

measurements for each ligand, membranes from cells transfected with empty pBSK

vector were added to the reaction mixture and treated as described above.

Synaptic Vesicle Purification

Synaptic vesicles were prepared as previously described (*42*). Briefly, synaptic vesicles were released from synaptosomes in a crude synaptosome preparation. Synaptosomes were resuspended with 9 volumes of cold water with protease inhibitors ((Complete protease inhibitor tablet, Roche), plus 200 μM PMSF and 1μg mL^{-1} Pepstatin A) and lysed with a glass-Teflon homogenizer at 2000 rpm. The homogenate suspension was centrifuged for 20 min at 33,000Xg, and the resulting supernatant was removed and centrifuged for 2 hr at 260,000Xg. The remaining supernatant was discarded, and the pellet was carefully resuspended to yield the crude synaptic vesicle preparation.

Synaptic Vesicle and VMAT2 Transport Assay

Membrane preparations were assayed as described previously (*20*). For each experiment an aliquot of membranes (50–100 μg of protein), either frozen rVMAT2 membranes thawed on ice or fresh synaptic vesicle preparation, was added to 200 μL of SH buffer containing 4 mM KCl, 2 mM MgSO$_4$, 2.5 mM ATP, and either 20–30 nM [^{3}H]5HT or [^{125}I]T$_1$AM (from 100 nM to 10 μM). To determine the effect of each of the thyronamines on transport of radioligands, 10 μM final concentration of either thyronamines, 3,5,3'-triiodothyronine (Thyroid Hormone, T$_3$), or thyroxine (T$_4$) (all dissolved in DMSO), or 100 μM tetrabenazine were added to the reaction. To determine the concentration of compounds needed to inhibit serotonin transport by 50% (IC$_{50}$), T$_1$AM dissolved in DMSO was added to the reaction solution to final concentrations ranging from 10 nM to 100 μM. To determine effects of T$_1$AM on the K$_m$ for 5HT, non-

radioactive 5HT dissolved in SH buffer was added to the reaction solution at

concentrations ranging from 10 nM to 10 μM, with or without 5 μM non-radioactive

T_1AM. After incubation for 5 min at 37 °C, the transport reaction was terminated by

rapid dilution with two 1.5 mL aliquots of cold SH buffer and filtration through 0.2 μm

HT 200 Tuffryn membranes (Pall Life Sciences). The filters were then dried, and bound

radioactivity was measured by scintillation counting in cytoscint scintillation fluid.

Transport activity for each condition was measured in triplicate (duplicate for the

synaptic vesicle assay) on at least three separate occasions (*20*). To determine

background measurements for synaptic vesicle transport, purified vesicles were added to

the reaction mixture, held on ice and the mixture was immediately quenched with cold

SH buffer and filtered as described above. To determine background measurements for

recombinant VMAT2 transport, membranes from cells transfected with empty pcDNA3

vector were added to the reaction mixture were held on ice and the mixture was

immediately quenched with cold KRH buffer and treated as described above.

Statistical Analysis

Statistical analyses were performed with the GraphPad Prism version 4.00

software, with values expressed as means ± SEM. Statistical significance was

determined using the paired two-tailed t test.

a)
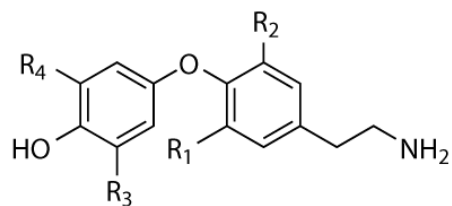
	R1	R2	R3	R4
T0AM	H	H	H	H
T1AM	I	H	H	H
rT1AM	H	H	I	H
T2AM	I	I	H	H
3,3' T2AM	I	H	I	H
rT2AM	H	H	I	I
T3AM	I	I	I	H
rT3AM	I	H	I	I
T4AM	I	I	I	I

b)
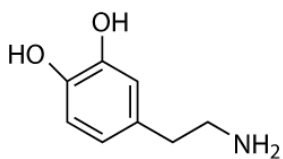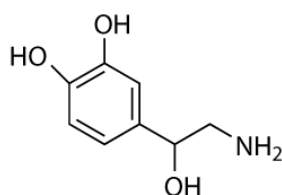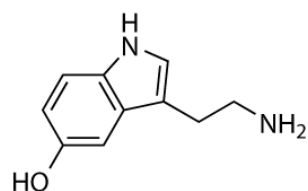
Dopamine   Norepinephrine   Serotonin

Supplemental Figure 1. Structures of Iodothyronamines. Chemical scaffold is shown for all nine iodothyronamines. Structures vary in iodine, number from 0–4 iodines, and ring position resulting in nine unique iodothyronamine permutations. Also shown for structural comparison are the biogenic amine neurotransmitters dopamine, norepinephrine and serotonin.

References

1. Scanlan, T. S., Suchland, K. L., Hart, M. E., Chiellini, G., Huang, Y., Kruzich, P. J., Frascarelli, S., Crossley, D. A., Bunzow, J. R., Ronca-Testoni, S., Lin, E. T., Hatton, D., Zucchi, R., and Grandy, D. K. (2004) 3-Iodothyronamine is an endogenous and rapid-acting derivative of thyroid hormone, *Nat Med 10*, 638–42.

2. Yen, P. M. (2001) Physiological and molecular basis of thyroid hormone action, *Physiol Rev 81*, 1097–142.

3. Harvey, C. B., and Williams, G. R. (2002) Mechanism of thyroid hormone action, *Thyroid 12*, 441–6.

4. Raiteri, M., Del Carmine, R., Bertollini, A., and Levi, G. (1977) Effect of sympathomimetic amines on the synaptosomal transport of noradrenaline, dopamine and 5-hydroxytryptamine, *Eur J Pharmacol 41*, 133–43.

5. Borowsky, B., Adham, N., Jones, K. A., Raddatz, R., Artymyshyn, R., Ogozalek, K. L., Durkin, M. M., Lakhlani, P. P., Bonini, J. A., Pathirana, S., Boyle, N., Pu, X., Kouranova, E., Lichtblau, H., Ochoa, F. Y., Branchek, T. A., and Gerald, C. (2001) Trace amines: identification of a family of mammalian G protein-coupled receptors, *Proc Natl Acad Sci U S A 98*, 8966–71.

6. Bunzow, J. R., Sonders, M. S., Arttamangkul, S., Harrison, L. M., Zhang, G., Quigley, D. I., Darland, T., Suchland, K. L., Pasumamula, S., Kennedy, J. L., Olson, S. B., Magenis, R. E., Amara, S. G., and Grandy, D. K. (2001) Amphetamine, 3,4-methylenedioxymethamphetamine, lysergic acid diethylamide, and metabolites of the catecholamine neurotransmitters are agonists of a rat trace amine receptor, *Mol Pharmacol 60*, 1181–8.

7.   Premont, R. T., Gainetdinov, R. R., and Caron, M. G. (2001) Following the trace of elusive amines, *Proc Natl Acad Sci U S A 98*, 9474–5.

8.   Berry, M. D. (2004) Mammalian central nervous system trace amines. Pharmacologic amphetamines, physiologic neuromodulators, *J Neurochem 90*, 257–71.

9.   Kim, K. A., and von Zastrow, M. (2001) Old drugs learn new tricks: insights from mammalian trace amine receptors, *Mol Pharmacol 60*, 1165–7.

10.   Schuldiner, S., Shirvan, A., and Linial, M. (1995) Vesicular neurotransmitter transporters: from bacteria to humans, *Physiol Rev 75*, 369–92.

11.   Masson, J., Sagne, C., Hamon, M., and El Mestikawy, S. (1999) Neurotransmitter transporters in the central nervous system, *Pharmacol Rev 51*, 439–64.

12.   Torres, G. E., Gainetdinov, R. R., and Caron, M. G. (2003) Plasma membrane monoamine transporters: structure, regulation and function, *Nat Rev Neurosci 4*, 13–25.

13.   Weihe, E., Schafer, M. K., Erickson, J. D., and Eiden, L. E. (1994) Localization of vesicular monoamine transporter isoforms (VMAT1 and VMAT2) to endocrine cells and neurons in rat, *J Mol Neurosci 5*, 149–64.

14.   Peter, D., Liu, Y., Sternini, C., de Giorgio, R., Brecha, N., and Edwards, R. H. (1995) Differential expression of two vesicular monoamine transporters, *J Neurosci 15*, 6179–88.

15.   Whipple, M. R., Reinecke, M. G., and Gage, F. H. (1983) Inhibition of synaptosomal neurotransmitter uptake by hallucinogens, *J Neurochem 40*, 1185–8.

16. Baldessarini, R. J., and Vogt, M. (1971) The uptake and subcellular distribution of aromatic amines in the brain of the rat, *J Neurochem 18*, 2519–33.

17. Horn, A. S., and Snyder, S. H. (1972) Steric requirements for catecholamine uptake by rat brain synaptosomes: studies with rigid analogs of amphetamine, *J Pharmacol Exp Ther 180*, 523–30.

18. Miyakawa, M., and Scanlan, T. S. (2006) Synthesis of [125I]-,[2H]-, and [3H]-Labeled 3-Iodothyronamine (T1AM), *Synth Commun 36*, 891–902.

19. Buck, K. J., and Amara, S. G. (1994) Chimeric dopamine-norepinephrine transporters delineate structural domains influencing selectivity for catecholamines and 1-methyl-4-phenylpyridinium, *Proc Natl Acad Sci U S A 91*, 12584–8.

20. Finn, J. P., 3rd, and Edwards, R. H. (1997) Individual residues contribute to multiple differences in ligand recognition between vesicular monoamine transporters 1 and 2, *J Biol Chem 272*, 16301–7.

21. Peter, D., Jimenez, J., Liu, Y., Kim, J., and Edwards, R. H. (1994) The chromaffin granule and synaptic vesicle amine transporters differ in substrate recognition and sensitivity to inhibitors, *J Biol Chem 269*, 7231–7.

22. Liu, Y., Peter, D., Roghani, A., Schuldiner, S., Prive, G. G., Eisenberg, D., Brecha, N., and Edwards, R. H. (1992) A cDNA that suppresses MPP+ toxicity encodes a vesicular amine transporter, *Cell 70*, 539–51.

23. Erickson, J. D., Schafer, M. K., Bonner, T. I., Eiden, L. E., and Weihe, E. (1996) Distinct pharmacological properties and distribution in neurons and endocrine

cells of two isoforms of the human vesicular monoamine transporter, *Proc Natl Acad Sci U S A 93*, 5166–71.

24. O'Connor K, A., Porrino, L. J., Davies, H. M., and Childers, S. R. (2005) Time-Dependent Changes in Receptor/G-Protein Coupling in Rat Brain following Chronic Monoamine Transporter Blockade, *J Pharmacol Exp Ther 313*, 510–7.

25. O'Connor, K. A., Gregg, T. C., Davies, H. M., and Childers, S. R. (2005) Effects of long-term biogenic amine transporter blockade on receptor/G-protein coupling in rat brain, *Neuropharmacology 48*, 62–71.

26. Clark, W. G. (1979) Changes in body temperature after administration of amino acids, peptides, dopamine, neuroleptics and related agents, *Neurosci Biobehav Rev 3*, 179–231.

27. Clark, W. G., and Clark, Y. L. (1980) Changes in body temperature after administration of adrenergic and serotonergic agents and related drugs including antidepressants, *Neurosci Biobehav Rev 4*, 281–375.

28. Backs, J., Bresch, E., Lutz, M., Kristen, A. V., and Haass, M. (2005) Endothelin-1 inhibits the neuronal norepinephrine transporter in hearts of male rats, *Cardiovasc Res 67*, 283–90.

29. Beim, H. J. (1956) The pharmacology of rauwolfia, *Pharmacol Rev 8*, 435–483.

30. Frances, H., and Simon, P. (1987) Reserpine-induced hypothermia: participation of beta 1 and beta 2 adrenergic receptors, *Pharmacol Biochem Behav 27*, 21–4.

31. Hart, M. E., Suchland, K. L., Miyakawa, M., Bunzow, J. R., Grandy, D. K., and Scanlan, T. S. (2006) Trace Amine-Associated Receptor Agonists: Synthesis and

Evaluation of Thyronamines and Related Analogues, *J Med Chem 49*, 1101–1112.

32. Sotnikova, T. D., Budygin, E. A., Jones, S. R., Dykstra, L. A., Caron, M. G., and Gainetdinov, R. R. (2004) Dopamine transporter-dependent and -independent actions of trace amine beta-phenylethylamine, *J Neurochem 91*, 362–73.

33. Bexis, S., and Docherty, J. R. (2005) Role of alpha2A-adrenoceptors in the effects of MDMA on body temperature in the mouse, *Br J Pharmacol 146*, 1–6.

34. Xie, Z., and Miller, G. M. (2007) Trace Amine-Associated Receptor 1 is a Modulator of the Dopamine Transporter, *J Pharmacol Exp Ther*.

35. Xie, Z., Westmoreland, S., Bahn, M. E., Chen, G. L., Yang, H., Vallender, E., Yao, W. D., Madras, B. K., and Miller, G. M. (2007) Rhesus monkey trace amine-associated receptor 1 signaling: enhancement by monoamine transporters and attenuation by the D2 autoreceptor in vitro, *J Pharmacol Exp Ther*.

36. Dratman, M. B. (1974) On the mechanism of action of thyroxin, an amino acid analog of tyrosine, *J Theor Biol 46*, 255–70.

37. Dratman, M. B., Crutchfield, F. L., Axelrod, J., Colburn, R. W., and Thoa, N. (1976) Localization of triiodothyronine in nerve ending fractions of rat brain, *Proc Natl Acad Sci U S A 73*, 941–4.

38. Dratman, M. B., and Crutchfield, F. L. (1978) Synaptosomal [125I]triiodothyronine after intravenous [125I]thyroxine, *Am J Physiol 235*, E638–47.

39.   Dratman, M. B., Futaesaku, Y., Crutchfield, F. L., Berman, N., Payne, B., Sar, M., and Stumpf, W. E. (1982) Iodine-125-labeled triiodothyronine in rat brain: evidence for localization in discrete neural systems, *Science 215*, 309–12.

40.   Rozanov, C. B., and Dratman, M. B. (1996) Immunohistochemical mapping of brain triiodothyronine reveals prominent localization in central noradrenergic systems, *Neuroscience 74*, 897–915.

41.   Cooper, J. R., Bloom, F. E., and Roth, R. H. (1996) *The Biochemical Basis of Neuropharmacology*, 7th ed., Oxford University Press.

42.   Jahn, J. w. H. a. R. (1994) *Preparation of Synaptic Vessicles from Mammalian Brain*, Academic Press, Inc.

Chapter 3

Cloning, Expression, and Ligand Profiling of rTAARs

Introduction

It has been demonstrated that a wide variety of synthetic and naturally occurring trace amine ligands act as potent agonists of the trace amine-associated receptor 1 (TAAR$_1$) (*1-7*). TAAR$_1$ is an orphan G protein-coupled receptor (GPCR) that was discovered by two independent groups attempting to clone novel catecholamine and 5-HT receptor family homologs (*1,2*). TAAR$_1$ belongs in the biogenic amine subfamily of class A GPCRs. This receptor is coupled to a stimulatory G protein (G$_s$) and is found in a variety of tissues including brain, heart, pancreas, kidney, stomach, small intestine, skeletal muscle, prostate, liver, and spleen (*1,2,8,9*).

TAAR$_1$, however, is only one member of a family of orphan GPCRs. Several independent studies have shown that a wide variety of vertebrates contain this TAAR family of genes (*1,2,10,11*), though the absolute number in a given species varies widely (as few as 9 in chimpanzee (with 6 being pseudogenes) to as many as 97 in zebrafish (40 pseudogenes). The disparity in TAAR number per species raised intriguing questions about the possible function of this receptor family. Are these merely redundant copies of the same receptor? Do these receptors recognize the same ligands but have different tissue distribution? Or do these receptors recognize distinct sets of ligands each with a unique function? To address these questions we aimed to clone and functionally express

the rat TAAR family members and profile the ligand preference of this set of TAAR

GPCRs. The rat TAAR family contains 17 TAAR genes and 2 pseudogenes (*10*).

Cloning strategy 1- TOPO-TA vector

Our initial attempt to clone rat TAAR genes focused on just 5 TAARs 4, 6, 7d, 8c,

and 9 (trace amine receptors (TARs) 2,4,15,10, and 3 respectfully, under the prior

nomenclature, see Figure 1). These were chosen to span the sequence diversity of the rat

TAAR family. The genes were amplified by polymerase chain reaction (PCR) from rat

genomic DNA (primer sets shown in methods). Amplification from genomic DNA was

possible since all the rTAAR family members, besides rTAAR$_2$, contain no introns. A

signal sequence-FLAG tag was added to each TAAR PCR product by sequential PCR

reactions with overlapping primers and the resulting products were ligated into a

pcDNA3.1/V5-His TOPO TA expression vector (Invitrogen). Several attempts were

made to generate HEK293 cells lines stably expressing each of the correct TAAR

constructs (complete methods below). Stably transfected HEK293 cell lines were

screened for TAAR expression by probing a western blot with ANTI-FLAG M1

Monoclonal Antibody (Sigma). We observed low or undetectable expression of the

TAARs (data not shown), which led us to use an alternate expression strategy.

a)

Early rTAAR nomenclature	Current rTAAR nomenclature
TAR	TAAR
1	1
2	4
3	9
4	6
6	7h
7	8b
8	7a
9	7g
10	8c
11	8a
12	7b
13	7f
14	7e
15	7d
Previously unknown	2, 3, 5, 7c, 7i

b)
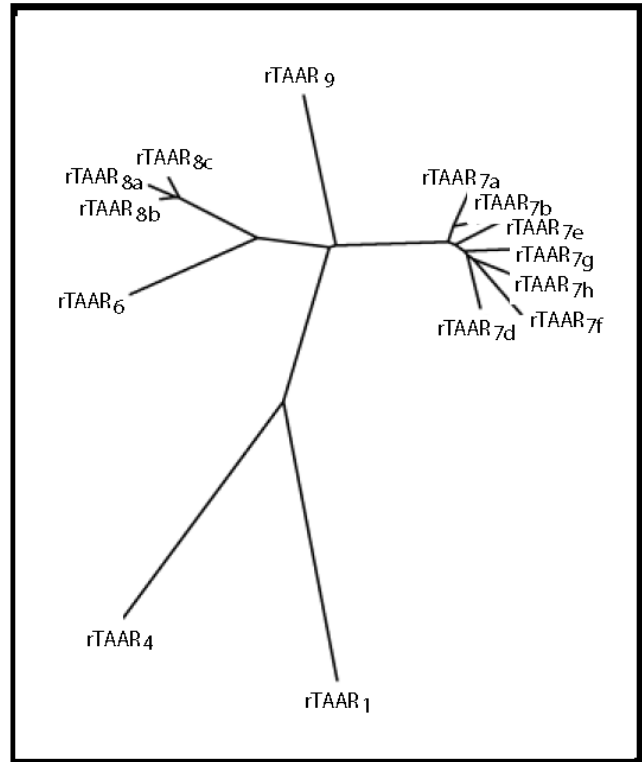
Figure 1. rTAAR family nomenclature and tree diagram.
a) Comparison of the old versus the current nomenclature for the rTAAR family of GPCRs. **b)** CLustalW sequence alignment of the rTAARs. Linear distance between receptors is proportional to difference in sequence identity of the receptors.

Cloning strategy 2- pIRESneo

In order to maximize our chances of successfully cloning and functionally expressing the TAAR genes in stable cell lines, the expression plasmid was changed from pcDNA3.1/V5-His TOPO TA to pIRESneo (Genbank U89673, Figure 2). This plasmid was chosen because the G418 selection marker is expressed from an internal ribosomal entry sequence, increasing the likelihood that G418 selection results in clones with detectable TAAR expression. Following the failed attempt to clone and express a small

subset of the rTAARs using the TOPO TA cloning method we attempted to clone the

entire rTAAR family of GPCRs. Our strategy was to amplify each of the TAAR genes

from rat genomic DNA using standard PCR techniques followed by the addition of a

signal sequence and flag tag epitope using overlapping PCR primers (as described in the

methods). The primers incorporated restriction sites specific to each of the rTAARs for

insertion into the pIRESneo vector, which could be used to transiently or stably express

the genes in mammalian cell lines. Using the primer pairs listed in the methods, PCR

products for all 15 known rTAAR genes were generated with an N-terminal SSF epitope

and were ligated into the pIRESneo vector. Complete and correct sequences were

obtained for TAARs 1, 4, 6, 7a, 7g, 8a, 8c, and 9. Since several groups have reported

difficulty expressing the receptors (*1,2*), especially with localization to the plasma

membrane, we sought to evaluate the relative expression of these TAAR constructs with

immunofluorescent microscopy in a variety of commonly used cell lines to find optimal

conditions for plasma membrane expression.
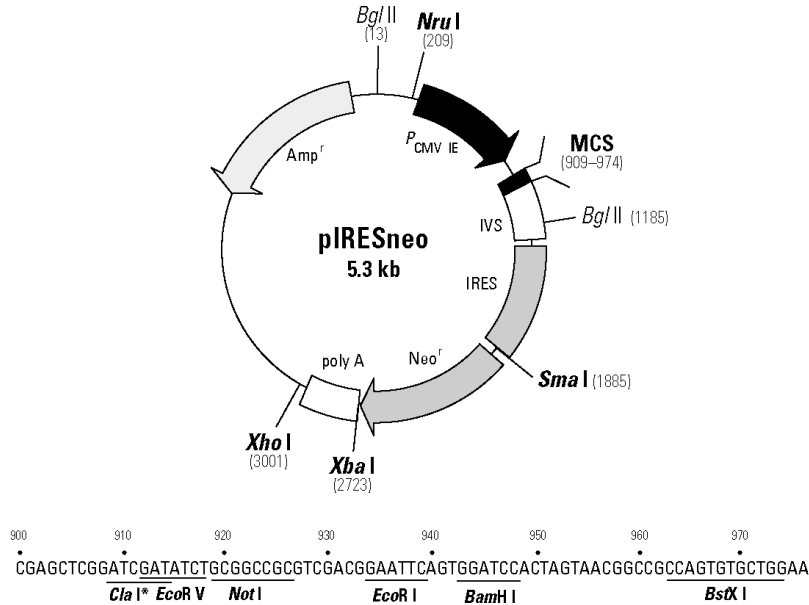
Restriction Map and Multiple Cloning Site (MCS) of pIRESneo Vector. Unique restriction sites are in bold. The *Cla* I site in the MCS is methylated in the DNA provided by CLONTECH. If you wish to digest the vector with this enzyme, you will need to transform the vector into a *dam⁻* host and make fresh DNA.

Figure 2. pIRESneo vector map. Originally published (Clonetech PR93695, 18 March 1999)

Transient Expression- immunofluorescent microscopy

Expression of each of the successfully cloned TAAR receptors was evaluated by immunofluorescent microscopy. Three commonly used mammalian cell lines (HEK293, Cos7, and CHO-K1) were initially screened for transient expression of each of the receptors. rTAAR constructs were transfected in 10 cm plates with Lipofectamine 2000 (Invitrogen) following the recommended protocol. 24 hours after the transfection the cells were analyzed for expression. To compare total expression versus cell surface

localization each of the three cell lines was fixed in formaldehyde and probed for expression of each of the receptors with and without triton-X 100 (Figure 3). $rTAAR_1$, followed by $rTAAR_4$ consistently exhibited the highest expression levels at the plasma membrane. The remaining receptors all had approximately the same low level of surface localization but high internal expression. Amongst the cell backgrounds, the best expression was detected in HEK293 cells (as previously reported for $TAAR_1$ expression) and CHO-K1 cells. The levels observed in Cos7 cells were markedly lower. The observed receptor expression/localization was sufficient for proceeding to the generation of cell lines stably expressing each of the receptors for screening potential TAAR ligands in functional assays. HEK293 cells were chosen for stable expression of the TAAR constructs to retain consistency with previous experiments with $rTAAR_1$. Similar to the protocol for the TOPO TAAR construct stable cell line generation, HEK293 cells were transfected with each TAAR construct (see methods below). The constructs used were empty pIRESneo vector, and each of TAARs 1, 4, 6, 7a, 7g, 8a, 8c, and 9. About a dozen independent stable cell lines were made for each construct and were frozen in 1.5 mL stocks for future evaluation of expression and TAAR mediated activity. Cell lines were labeled and stored in liquid nitrogen as recorded in methods (see appendix for complete inventory).
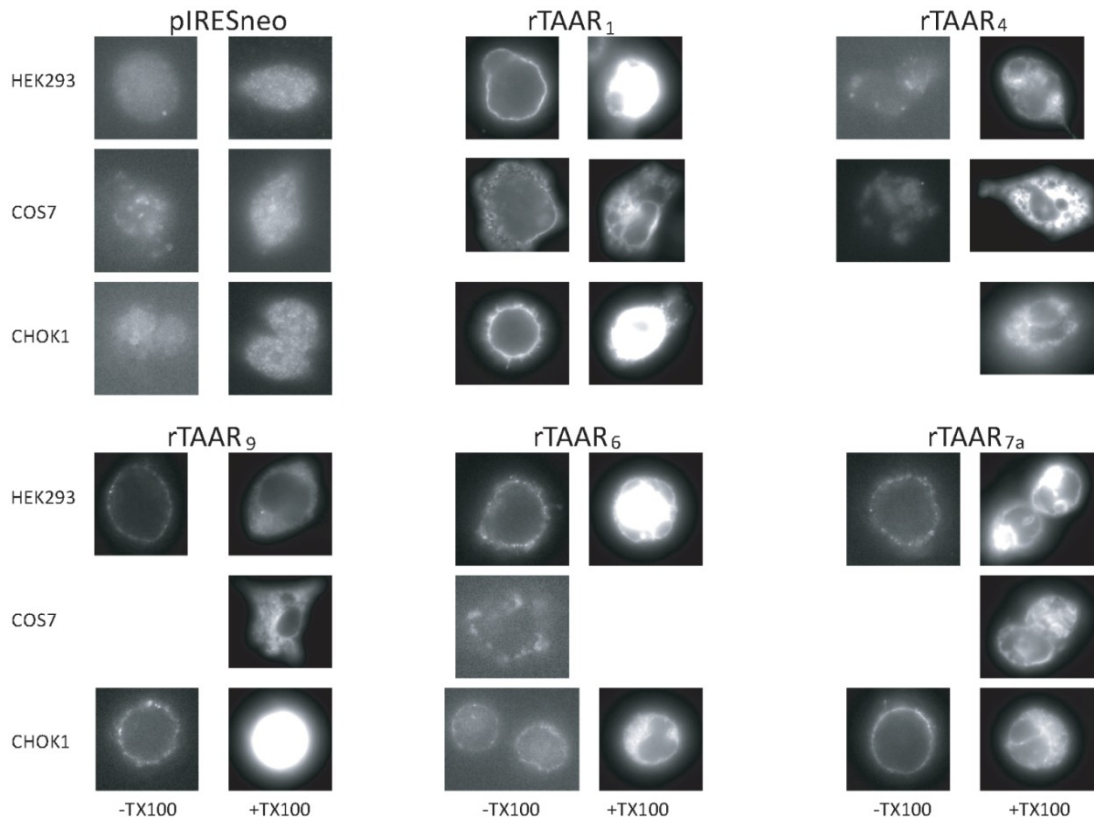
Figure 3. Transient Expression of rTAARs.

rTAAR$_4$ activity assays

Having obtained stable cell lines expressing each of a representative panel of rat

TAAR GPCRs we sought to initiate functional assays. Our aim was to screen a wide

variety of PEA thyroid hormone and thyronamine derivatives. First TAAR$_4$-expressing

cells lines were evaluated. TAAR$_4$ was selected for preliminary screens because Liberles

et al. previously demonstrated that a number of phenethylamine derivatives activated

TAAR$_4$ in a G$_S$ coupled manner (*12*). These results suggested that the arylethylamine

scaffold, also present in thyronamines, was reasonably likely to produce other active

molecules. Additionally because rTAAR$_4$ was found to be G$_s$ coupled, we could utilize

the experimental setup previously established in our lab for TAAR$_1$ screens.

Eleven TAAR$_4$ cell lines were screened for activity with three compounds

phenethylamine (PEA), N-methyl phenethylamine (N-Me-PEA) and 3-methoxy

phenethylamine (3-MeO-PEA). PEA, N-Me-PEA and a mixture of isomers of methoxy

phenethylamine were all previously reported rTAAR$_4$ agonists (*12*). Functional assays

were performed instead of screening the lines for total TAAR$_4$ expression levels because

maximal functional activity was ideal for subsequent pharmacological screening. The 11

TAAR$_4$ cell lines were thawed and grown under G418 selective conditions for at least

three passages and then evaluated for TAAR$_4$ dependent ligand activity as described in

the methods. The lines were screened with PEA, N-Me-PEA and 3-MeO-PEA at final

concentrations of 100 nM, 1 μM, and 10 μM. The difference between our experimental

setup and the screen reported by Liberles et al. (*12*), was that our drug treatment was for

1 hour followed by a direct measurement of changes in intracellular cAMP concentration,

as opposed to a 24-48 hour treatment with a CRE-luciferase readout, which is an indirect

measure of cAMP levels.

Unexpectedly, there was no agonist activity for any of the compounds with any of

the TAAR$_4$ cell lines (Figure 4a). We reasoned that a false negative result in this assay

could be explained if an increase in cAMP levels induced by agonist treatment remained

below the sensitivity of the assay due to low-level rTAAR$_4$ expression or low efficacy of

the receptor on adenylyl cyclase. As shown cAMP concentrations up to even 10 nM

resulted in baseline measurements (Figure 5a). To test the idea that changes in

intracellular cAMP were staying below the limit of detection we repeated the experiment

described above with the addition of an EC_{30} concentration of forskolin (a direct agonist of adenylyl cyclase, dose curve shown in Figure 5b) in all conditions (~ 2 µM). Under these conditions, concentration dependent agonist activity was detected for all the reported agonists in the vast majority of the $TAAR_4$ cell lines with varying levels of efficacy relative to cAMP changes induced by saturating forskolin concentrations (Figure 4b).

a)   b)
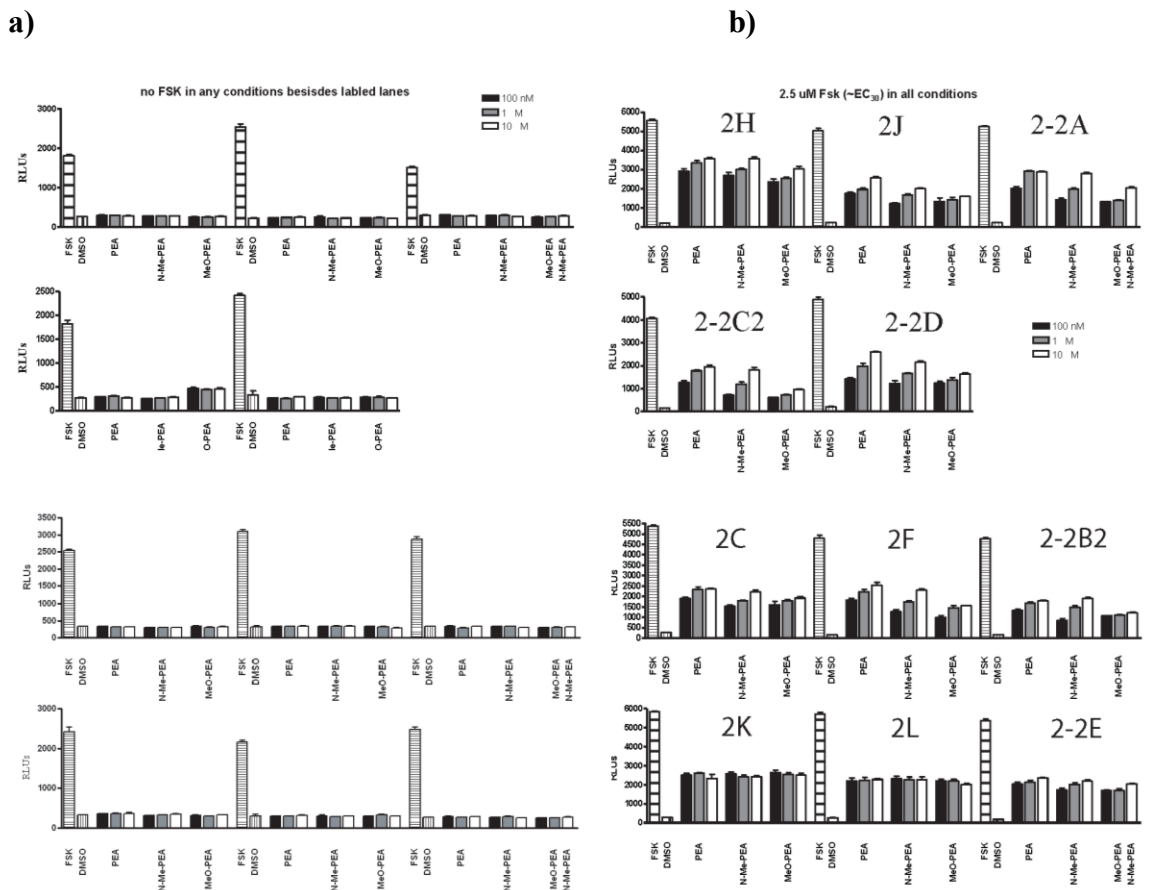
Figure 4. Screening rTAAR4 cell lines. Eleven HEK293 cell lines stably transfected with rTAAR4 (2H through 2-2E) were assayed as described in the methods (in vitro cAMP assay) with additionally either **a)** vehicle or **b)** 2 µM FSK added to the reaction mixture with test ligands. Data were reported as relative light units (RLUs) for each condition tested. Data were plotted and analyzed with Prism software (GraphPad, San Diego, CA). Standard error of the mean was calculated for at least three separate experiments performed in triplicate.

That $TAAR_4$ dependent cAMP induction by known $TAAR_4$ agonists was observed only in the presence of EC_{30} concentrations of forskolin raised a number of questions: Why is forskolin necessary? Is it simply a matter of raising the cAMP concentration into detectable limits for our screen, which was the rational used for its inclusion, or is it 'priming' the cells for $TAAR_4$ activation? If the FSK is acting as a priming agent can we determine its mechanism and can we reduce the FSK concentration needed to levels that would not on their own change cellular cAMP concentrations?

To determine whether the observed $TAAR_4$ activity was simply an issue of raising cAMP levels above the limit of detection or if FSK treatment was eliciting an unintended cellular response, the previous experiment was repeated both with and without EC_{30} concentrations of FSK and the lysate was collected as described previously. If this were simply a cAMP concentration issue, adding a fixed amount of cAMP to the cell lysate after the experiment should recapitulate the effect of adding FSK during the assay? Therefore, to the lysate from cells not treated with FSK we added cAMP standard to the lysate to a concentration of ~50 nM in addition to any cAMP present from the cells. Under this setup agonist induced and $TAAR_4$ dependent cAMP generation was observed only under conditions when FSK (EC_{30}) was present during the drug treatment (Figure 5c). This suggests that FSK is facilitating the $TAAR_4$ activity; simply increasing the levels of detectable cAMP does not follow from the data.
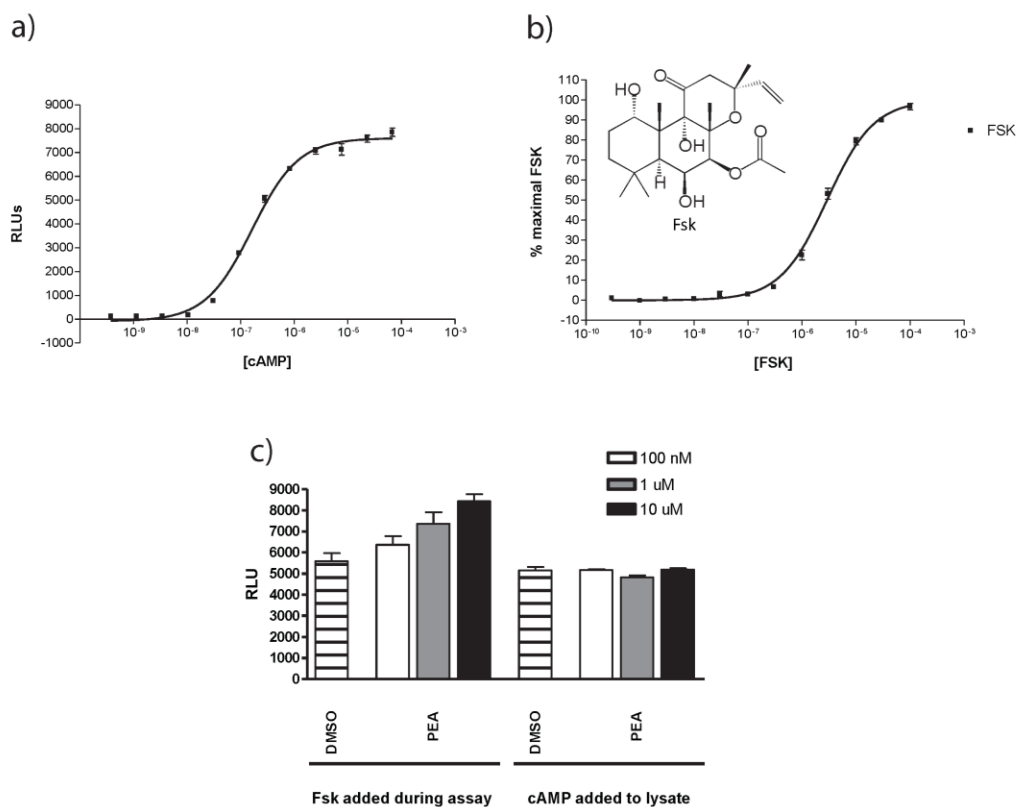
Figure 5. Exploring rTAAR4 FSK dependent activity. cAMP content analyzed by use of the Hithunter cAMP XS kit (DiscoveRX, Fremont, CA). **a)** cAMP standard curve (384 pM to 68.1 μM) or **b)** HEK293 cells stably transfected with rTAAR4 treated with concentration range of FSK (200 pM to 100 μM). **c)** HEK293 cells stably transfected with rTAAR4 were assayed as described in the methods (in vitro cAMP assay) with additionally either vehicle or 2 μM FSK added to the reaction mixture with test ligands. Lysate was collected and analyzed for cAMP content with and without the addition of 50 nM cAMP. Data were reported as relative light units (RLUs) for each condition tested. Data were plotted and analyzed with Prism software (GraphPad, San Diego, CA). Standard error of the mean was calculated for at least three separate experiments performed in triplicate.

To expand upon this finding we sought to determine the minimal FSK concentration necessary for TAAR4 activity. We screened the TAAR4 cell line with an

8 point concentration curve of FSK (from 1 nM to 3 µM) (Figure 6a). FSK was added

either with the vehicle/agonist or 30 min prior to addition of vehicle/agonist to determine

if preincubation enhances the effect of FSK (Figure 6b). The agonist used was PEA at 1

µM final concentration (reported EC_{50} for PEA). The results showed a minimal

concentration of FSK necessary to observe $TAAR_4$ dependent activity with 1 µM PEA to

be ~300 nM. 30 min preincubation with FSK had no effect on the minimal FSK

concentration needed.
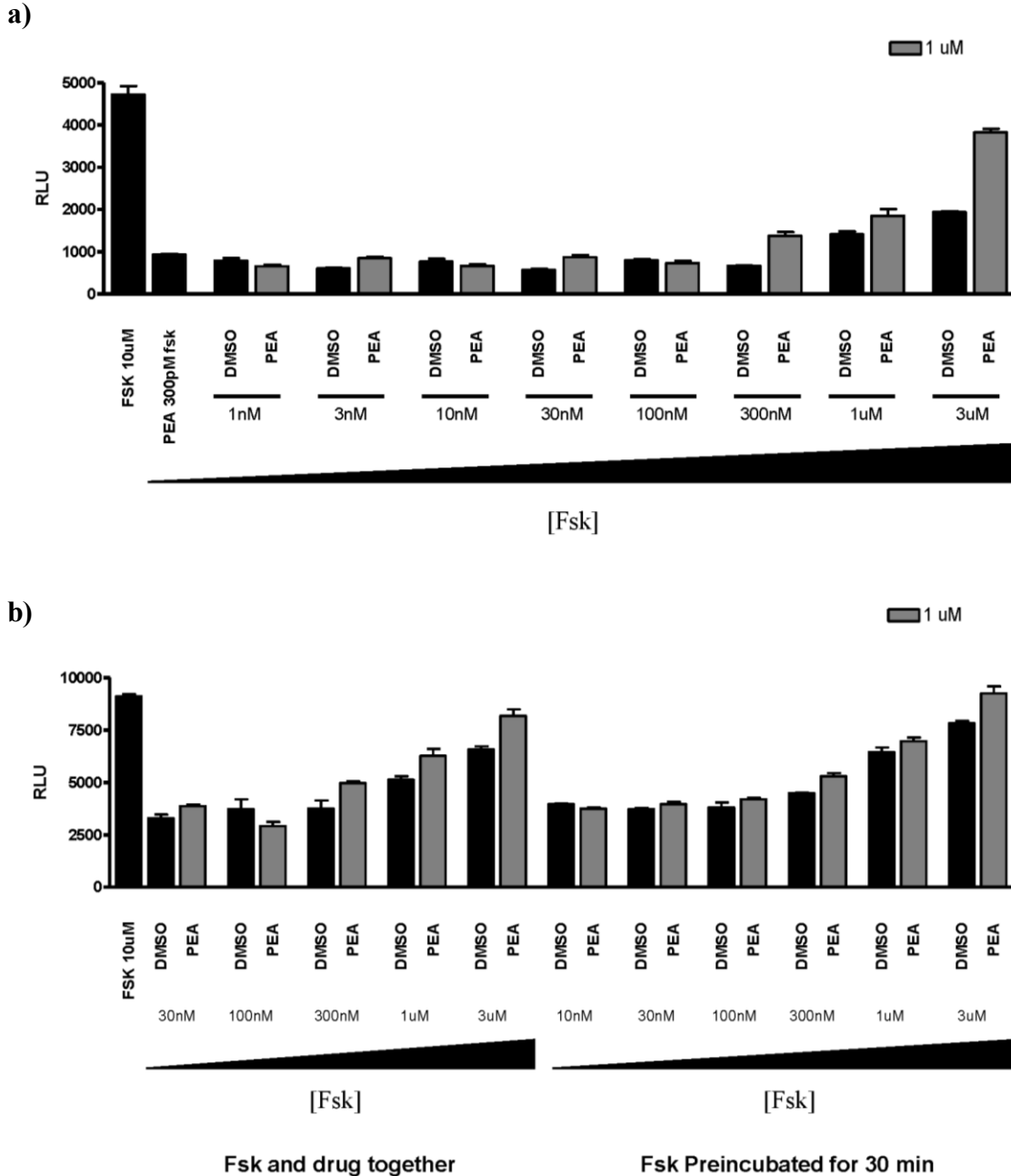
Figure 6. Determining minimal necessary FSK concentration. a) HEK293 cells stably transfected with rTAAR$_4$ treated with concentration range of FSK (1nM to 3 μM) with either vehicle or 1μM PEA. **b)** HEK293 cells stably transfected with rTAAR$_4$ were assayed as described in **a)** with FSK added to the reaction mixture either with test ligands or 30 min prior to test ligands. Data were reported as relative light units (RLUs) for each condition tested. Data were plotted and analyzed with Prism software (GraphPad, San Diego, CA). Standard error of the mean was calculated for at least three separate experiments performed in triplicate.

Finally we aimed to determine the mechanism by which FSK acts as a priming agent for $TAAR_4$ activity. We disrupted a number of known signaling mechanisms using a panel of both specific broad spectrum kinase inhibitors to determine if the priming effect of FSK was abolished. The pathways we attempted to disrupt were PKA dependent signaling, PKC signaling, PI3K signaling, the MAP kinase cascade and finally all general kinase signaling. The kinase inhibitors we used for this were H-89 (10 µM), Ro32-0432 (10 µM), wortmannin (100 nM), PD 98059 (50 µM), and staurosporine (1 µM), respectively. Disruption of kinase activity with this panel of inhibitors had no significant effect on the FSK dependent $TAAR_4$ activity (Figure 7), thus these kinase signaling pathways do not mediate the effect of FSK on $TAAR_4$ function.
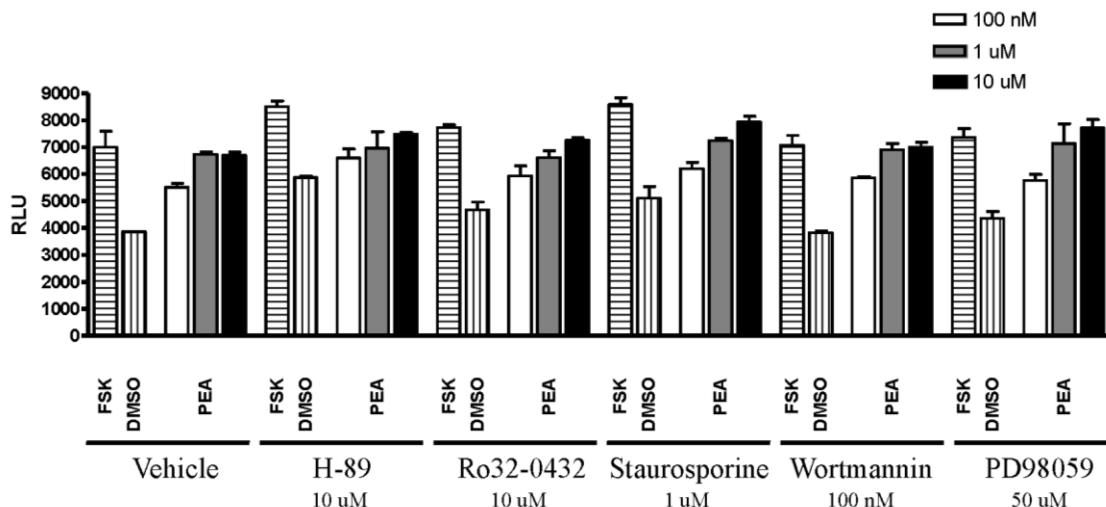
Figure 7. Effects of kinase inhibitors on FSK dependant rTAAR4 signaling.
HEK293 cells stably transfected with rTAAR4 were assayed as described in methods
with 2 μM FSK added to the reaction mixture were treated with either saturating FSK,
DMSO, or PEA in addition to either vehicle or one of the selected kinase inhibitors (H-89, Ro32-0432, staurosporine, wortmannin, or PD98059) which were added 30 min prior
to test ligands at the indicated final concentration. Data were reported as relative light
units (RLUs) for each condition tested. Data were plotted and analyzed with Prism
software (GraphPad, San Diego, CA). Standard error of the mean was calculated for at
least three separate experiments performed in triplicate.

Selbie and Hill (*13*) suggested that "Many 'silent' GPCR agonists, which have

little effect on their own, can stimulate measurable receptor function only when assayed

in the presence of coincident activation of a GPCR that mediates more direct or

pronounced effects on particular second messengers. For example, the Gβγ-subunit-

mediated stimulation of adenylate cyclase by Gαq-coupled receptors requires co-

stimulation of $G_{\alpha s}$...." Perhaps in our TAAR4 assays, FSK was simply generating a

modest level of turnover of adenylyl cyclase, as would the coincident GPCR activity

described above, that the minimal or weak TAAR4 dependent signaling could further

increase cAMP production.   To test this idea we asked if FSK could be replaced by

weakly activating adenylyl cyclase through the addition of a known agonist of a GPCR

that is endogenous to HEK293 cells. We chose to exploit the presence of β_2AR with the

addition of its known agonist isoproterenol. We were able to replicate the priming effects

of FSK by replacing 2 μM FSK with 10 μM isoproterenol in our assay (Figure 8 a, b).

With the addition of 10 μM isoproterenol we were able to see weak PEA induced

$TAAR_4$ dependent activity in a concentration dependent manner.

a)   b)
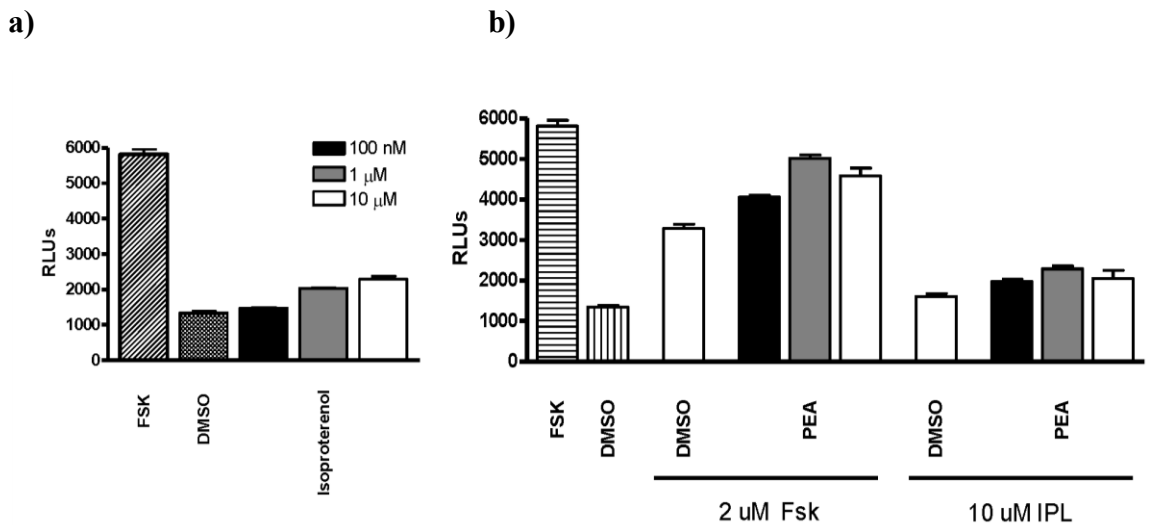
**Figure 8. Replacing FSK dependence with agonist of endogenous Gs couple
receptor. a)** HEK293 cells stably transfected with $rTAAR_4$ were treated with three
concentrations of isoproterenol and analyzed for cAMP content. **b)** HEK293 cells stably
transfected with $rTAAR_4$ were assayed as described in the methods (in vitro cAMP
assay) with additionally either 2 μM FSK or 10 μM isoproterenol (IPL) added to the
reaction mixture with vehicle or agonist PEA at three separate concentrations. Data were
reported as relative light units (RLUs) for each condition tested. Data were plotted and
analyzed with Prism software (GraphPad, San Diego, CA). Standard error of the mean
was calculated for at least three separate experiments performed in triplicate.

After establishing a TAAR$_4$ assay system with the known agonist, PEA, we then screened a number of thyroid hormone and thyronamine derivatives for activity with TAAR$_4$. As shown in figure 9 we screened a wide variety of PEA and thyronamine derivatives for both G$_s$ and G$_i$ (not shown) agonistic activity as well as antagonist activity in competition with 1 μM PEA (not shown). Several compounds PEA, phenyl tyramine, tyramine, napthylethylamine, tryptamine, and both L and D amphetamine, and D methamphetamine were rTAAR$_4$ agonists. Only one compound tested, T$_3$AM, was a weak antagonist when tested in competition with 1 μM PEA. PEA activated TAAR$_4$ with an approximate EC$_{50}$ of 300 nM, although the dose response best fit a biphasic trend line (R^2= 0.86 vs R^2= 0.92) suggesting dual rTAAR$_4$ binding modes for PEA with EC$_{50}$s of 100 nM and ~ 30 μM (Figure 10).
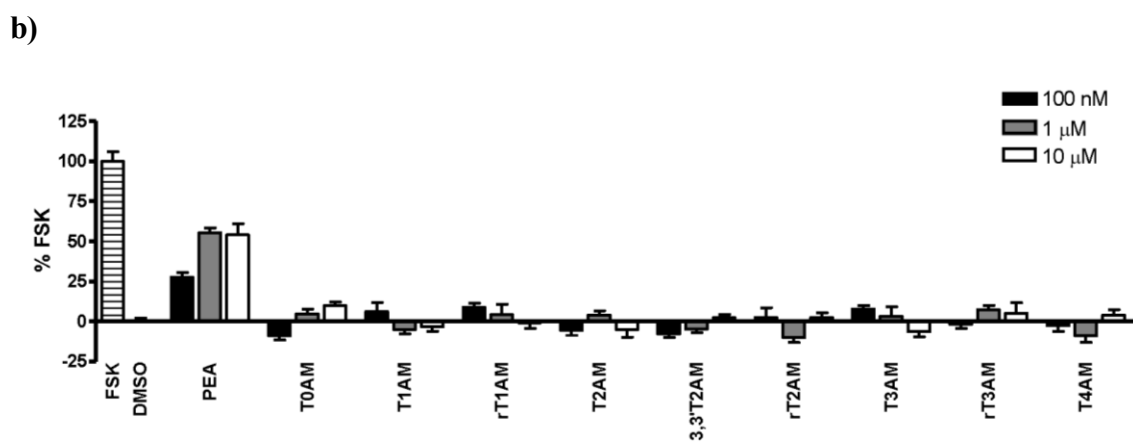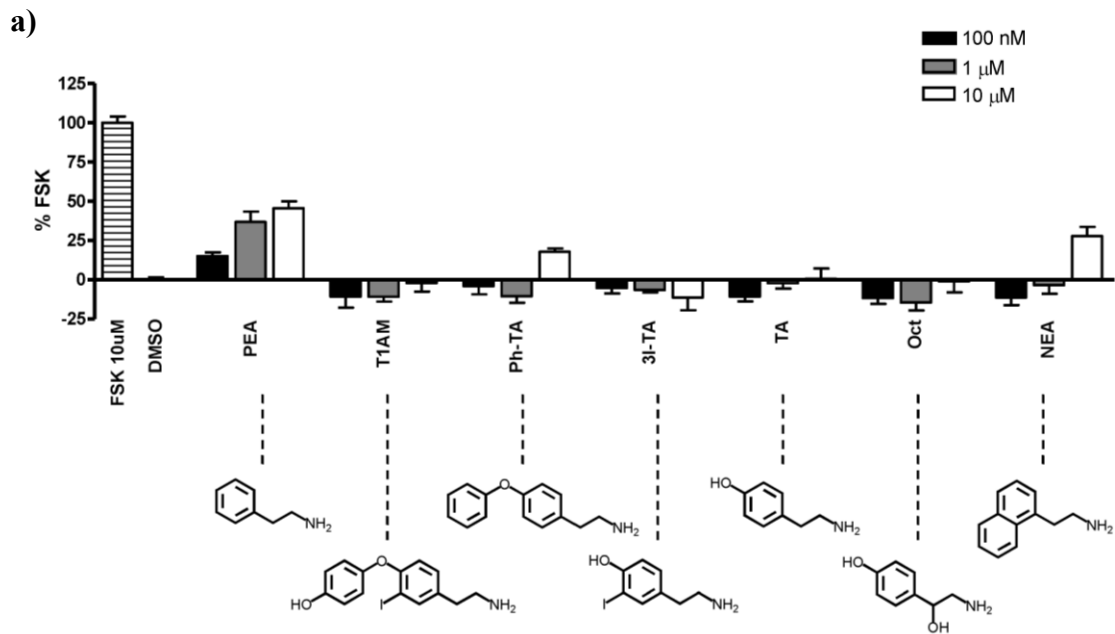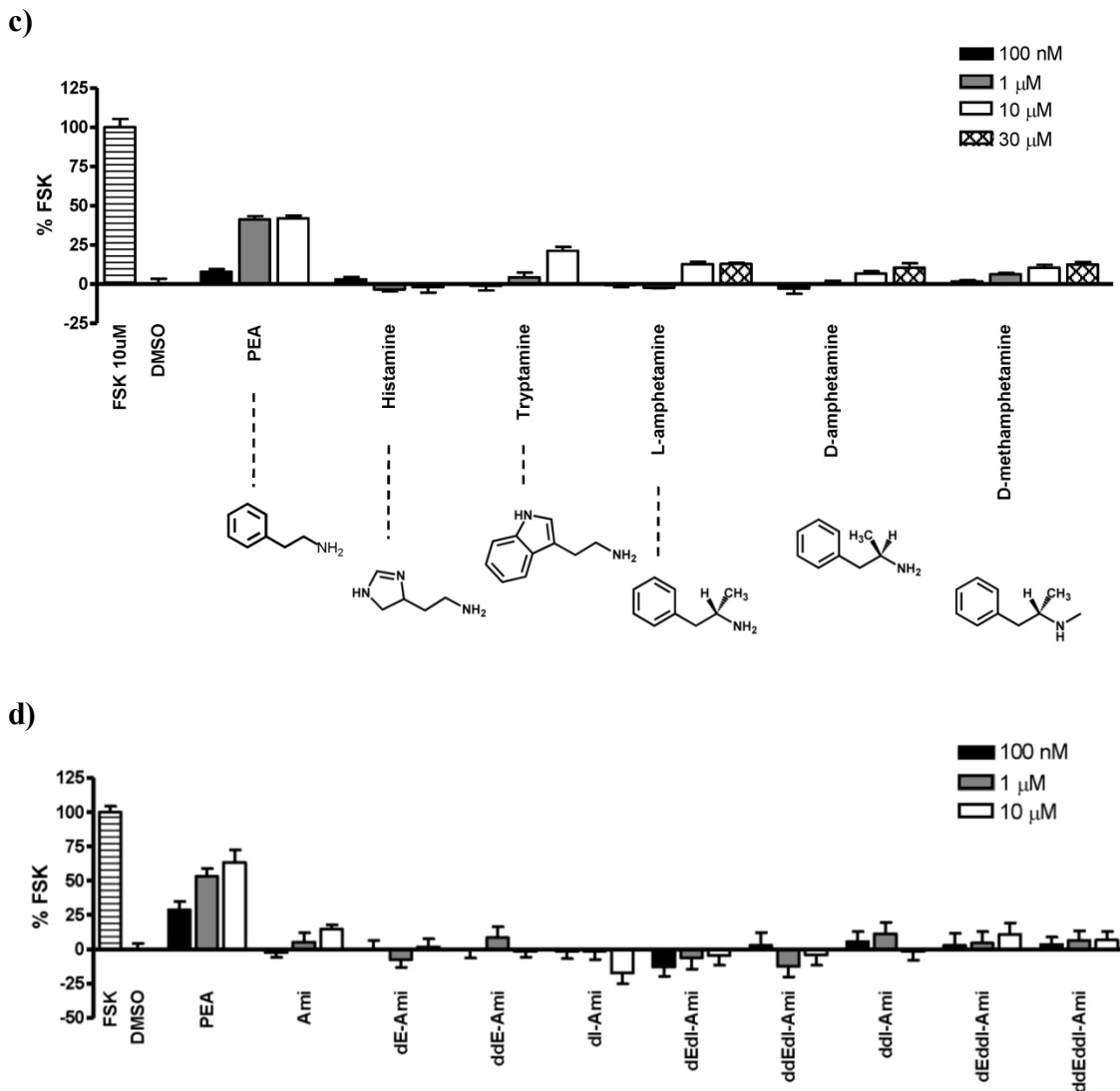
Figure 9. Screening compounds for rTAAR$_4$ dependent activity. HEK293 cells stably transfected with rTAAR$_4$ were assayed as described in the methods (in vitro cAMP assay) with the addition of 2 μM FSK added to the reaction mixture with vehicle or a variety of test ligands **a)** PEA derivatives, **b)** thyronamines, **c)** amphetamine derivatives and **d)** amiodarone derivatives at three separate concentrations (100 nM, 1 μM, and 10 μM). Data were reported as relative light units (RLUs) for each condition tested. Data were plotted and analyzed with Prism software (GraphPad, San Diego, CA). Standard error of the mean was calculated for at least three separate experiments performed in triplicate.
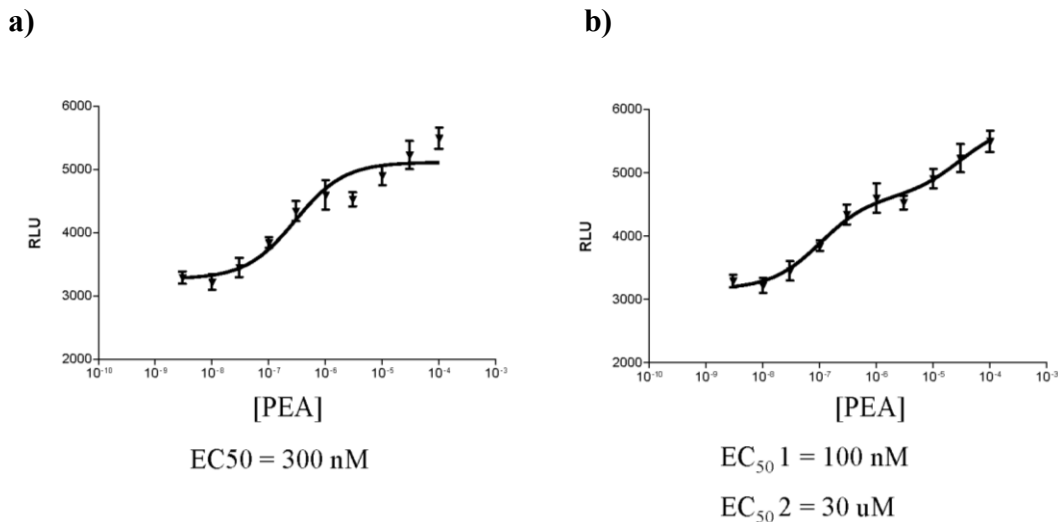
a)   b)

EC50 = 300 nM

$EC_{50}1 = 100$ nM

$EC_{50}2 = 30$ uM

Figure 10. Determining the potency of PEA with rTAAR4. HEK293 cells stably transfected with rTAAR4 were assayed as described in the methods (in vitro cAMP assay) with the addition of 2 µM FSK added to the reaction mixture with PEA at ten concentrations (3 nM to 100µM) Data were reported as relative light units (RLUs) for each condition tested. Data were plotted and analyzed with Prism software (GraphPad, San Diego, CA). The data set was fit with either **a)** a standard sigmoidal dose-response curve or **b)** a two site competition binding curve. Standard error of the mean was calculated for at least three separate experiments performed in triplicate.

Based on the work by Liberles et al. (*12*) another hypothesis about the possible role for TAARs was developed. Because of the variable activity of the PEA derivatives and the smaller volatile amines with a number of the TAAR family members, we reasoned that TAARs may function biologically as sensors for decarboxylated derivatives of the 20 natural L- amino acids. To test this idea, commercially available decarboxylated derivatives of the amino acids were purchased (Figure 11). Derivatives were available for all but 3 of the amino acids (Tyr, Gly, and Trp). These compounds were tested as above for TAAR4-dependent activity at 3 doses (100 nM, 1 µM, and 10 µM) in the presence of 2 µM FSK. The only compounds from this group that

71

demonstrated any TAAR$_4$-specific activity were the previously reported agonists

tryptamine and PEA suggesting a fairly limited ligand profile among the amino acid

derivatives (data not shown).
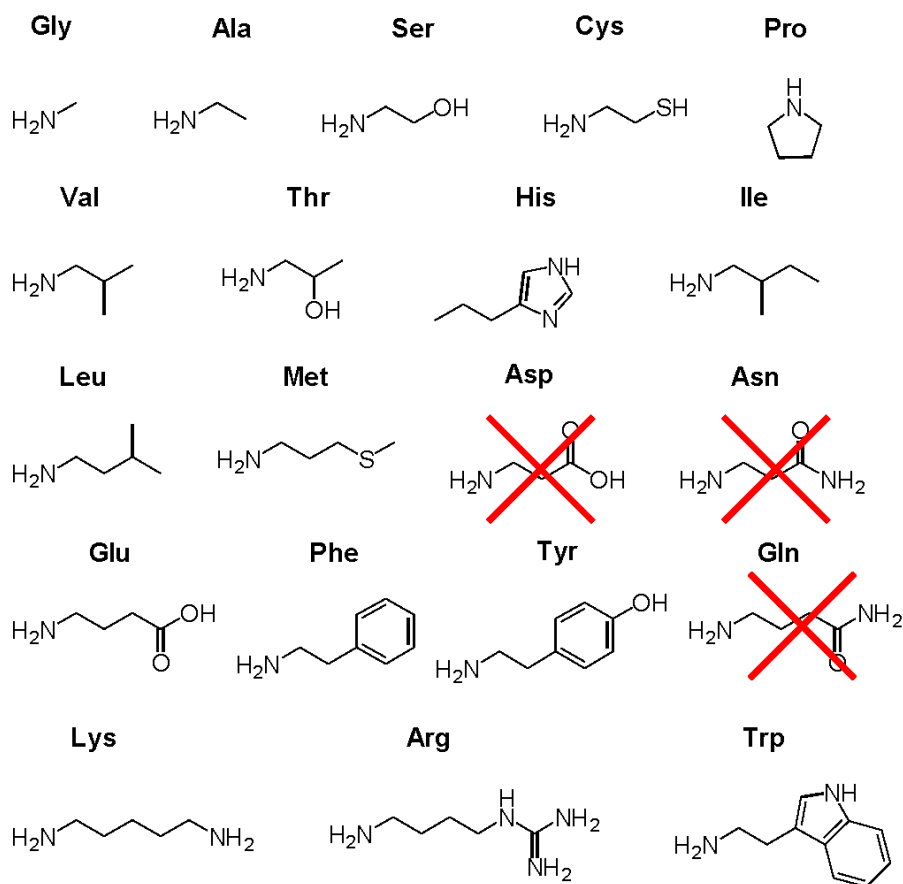
Figure 11. Commercially available decarboxylated Amino Acid Derivatives.
Structures are shown of the decarboxylation products for the 20 listed amino acids.
Derivatives of Asp, Asn, and Gln are marked off with red Xs to indicate lack of
commercial availability.

In summary, $rTAAR_4$ was successfully cloned and functionally expressed in a stable expression construct in HEK293 cells. $rTAAR_4$ is functionally coupled through a G_S coupled G protein resulting in cAMP production upon activation. In order to observe the $TAAR_4$-dependent activity, the cells needed to be primed for adenylyl cyclase activity (accomplished either through the addition of a direct agonist of the cyclase, FSK, or through activation of an endogenous G_S coupled GPCR, such as β2AR with isoproterenol, coincident with agonist treatment). The minimal FSK concentration needed to observe $TAAR_4$-dependent signaling was 300 nM, and pretreatment with FSK prior to addition of test ligands had no significant effect. In an attempt to elucidate the FSK priming mechanism, a panel of known kinase inhibitors was screened but none had any significant effect on the $TAAR_4$ activity. This suggested that FSK was priming by activating adenylyl cyclase at a low level that allowed for amplification of a weaker $TAAR_4$ signal.

Many PEA, TH, and amino acid derivatives were screened for activity with $TAAR_4$, and several acted as agonists including the previously reported compounds PEA, N-Me PEA, 3-methoxy PEA, and tryptamine as well as the newly identified agonists phenyl tyramine, napthylethylamine, and weak agonists L, D amphetamine, and D methamphetamine. The most potent agonist identified was PEA, which activated $rTAAR_4$ with an EC_{50} of approximately 300 nM. However, the PEA concentration curve had a distinct biphasic shape suggesting multiple binding modes. Additionally, rT_3AM was identified as a weak antagonist of $rTAAR_4$ when tested in competition with 1 μM PEA.

rTAAR$_6$ activity assays

After completing the screen of rTAAR$_4$ we sought to expand our study to include a screen of rTAAR$_6$. rTAAR$_6$ was chosen next because it has been suggested that mutations associated with TAAR$_6$ may correlate with schizophrenia in certain patient populations (*14-16*). As with rTAAR$_4$, 12 cell lines stably expressing the rTAAR$_6$ construct were generated. These 12 lines were thawed and propagated for three passages under the standard G418 selective growth media conditions described in the methods. After three passages a membrane preparation was made from each of the lines following the protocol supplied by Dr. Ben Lin (see methods). Whole membranes were resuspended in the prescribed buffer and stored at -80 °C for evaluation of rTAAR$_6$ expression levels. Since no TAAR$_6$ agonists were known, cell lines had to be evaluated for total expression of TAAR$_6$ rather than by a functional assay as for TAAR$_4$.

rTAAR$_6$ expression levels were evaluated by western blot (Figure 12). The membrane preparations were thawed on ice and ~30 µg of total protein from each in a total of 40 µL of sample buffer was run on 10% Criterion Precast SDS PAGE gels. The gels were transferred to PVDF membranes and probed with Anti FLAG M1 monoclonal antibody (Sigma) according to the manufacturers recommended protocol. This blot allowed us to select the line with the highest TAAR$_6$ expression levels (cell line 4-2 J was selected, see ASII pg. 99 for nomenclature) to proceed with functional assays.
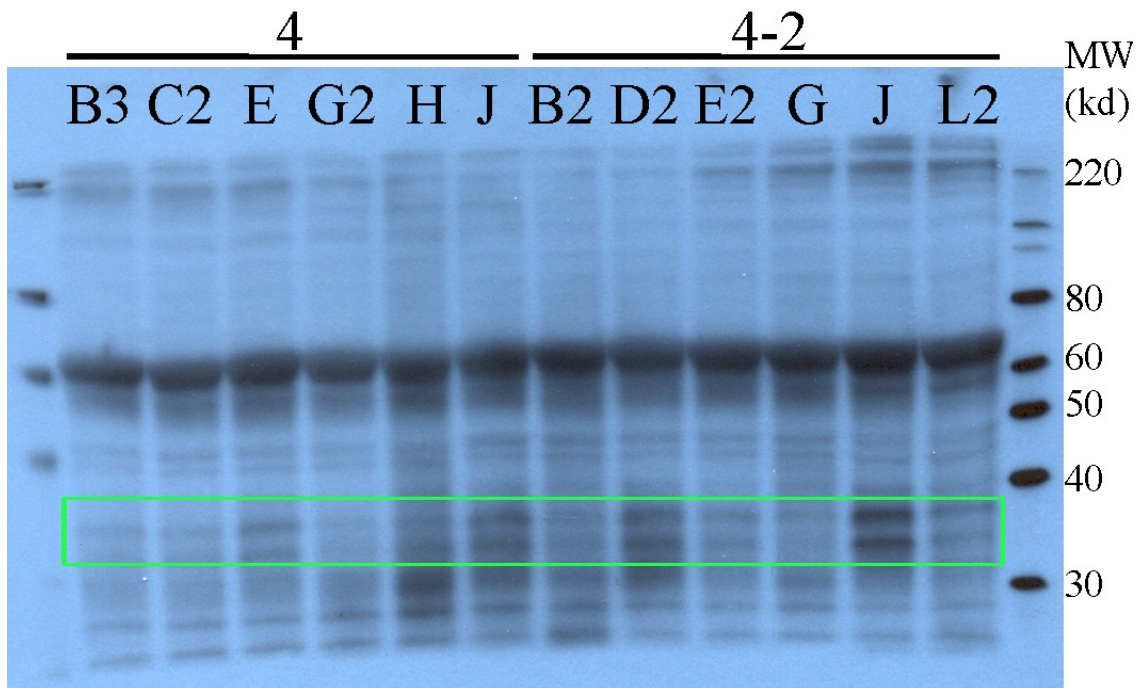
Figure 12. Screening cell lines for expression of rTAAR$_6$. The 12 cell lines stably transfected with rTAAR$_6$ expression constructs were screened for rTAAR$_6$ expression and analyzed by western blot. This blot was probed with an anti FLAG M1 monoclonal antibody (Sigma). Each lane represents one cell line from 4-B3 to 4-2 L2. Cell line 4-2 J (lane 11) shows the highest level of rTAAR$_6$ expression.

The selected cell line stably expressing rTAAR$_6$ 4-2 J was screened for G$_S$ and G$_i$ coupled activity with the entire panel of thyronamine, PEA, amiodarone, and amino acid derivatives described in the rTAAR$_4$ screen. None of the compounds tested demonstrated any significant TAAR$_6$-dependent agonist activity with or without FSK present (Figure 13). Published work by Reiners et al.(*17*) describing the generation of a constitutively active TAAR$_6$ mutant showed this GPCR to be G$_S$ coupled. This work validated the second messenger readout of our screen despite a failure to observe any TAAR$_6$-dependent activity. Additionally, these negative results were independently

confirmed for a representative population of the compounds tested by Xie et al. (*18*). In summary, rTAAR$_6$ was successfully cloned and expressed as a stable expression construct in HEK293 cells. However, a variety of PEA, thyronamine, TH, and amino acid derivatives none demonstrated any rTAAR$_6$-dependent agonist activity.

a)

b)
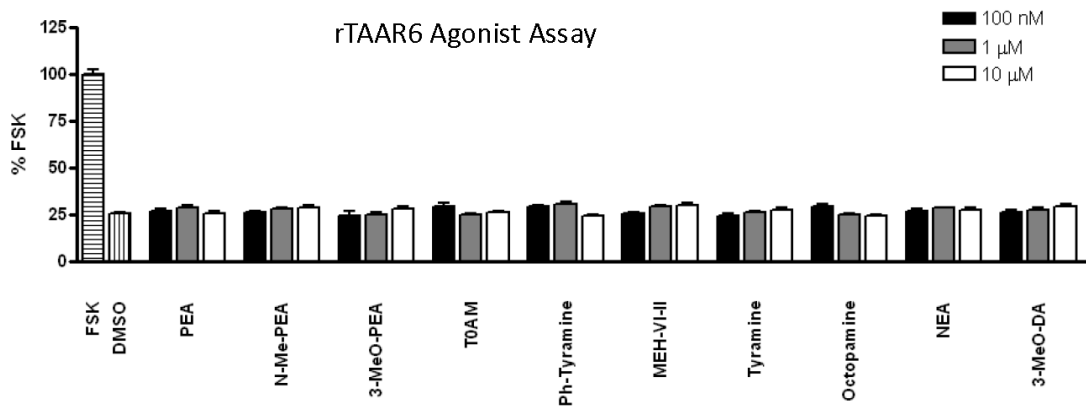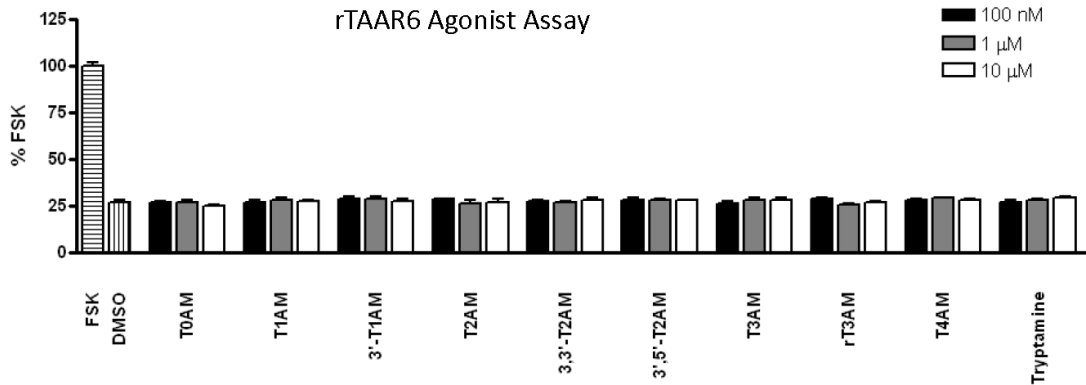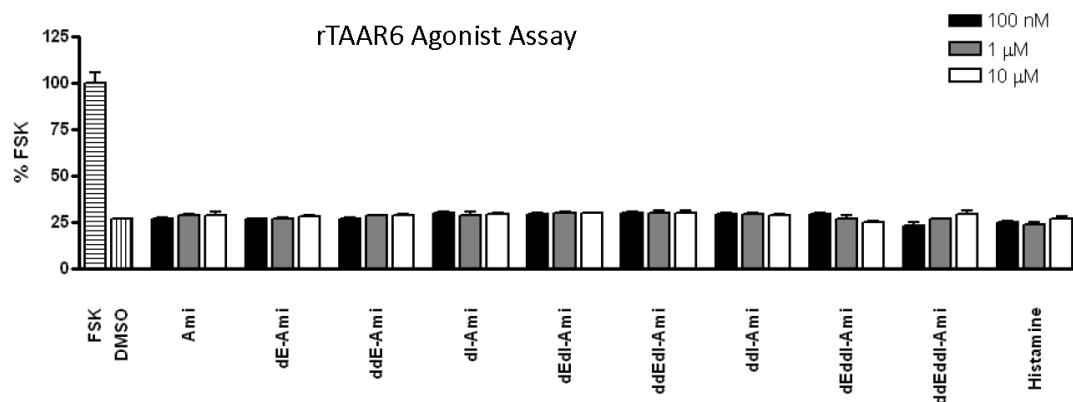
Figure 13. Screening compounds for rTAAR$_6$ dependent activity. HEK293 cells stably transfected with rTAAR$_6$ were assayed as described in the methods (in vitro cAMP assay) with vehicle or a variety of test ligands **a)** PEA derivatives, **b)** thyronamines, and **c)** amiodarone derivatives at three separate concentrations (100 nM, 1 µM, and 10 µM). Data were reported as percent maximal FSK stimulation for each condition tested. Data were plotted and analyzed with Prism software (GraphPad, San Diego, CA). Standard error of the mean was calculated for at least three separate experiments performed in triplicate.

Methods

Topo TA cloning

Primers were all ordered salt-free from Qiagen and diluted to 100 µM. Reaction

mixtures were all 100 µL and composed of 3 µL template DNA (rat genomic DNA, SSF

containing plasmids, or PCR products), 10 µL 10X PCR buffer, 2 µL each of sense and

antisense primers for each TAAR, 2.5 µL 25 mM dNTP mixture, water 79.5 µL and Vent

polymerase 1 µL. PCR products were all purified by gel electrophoresis in 1% agarose

gels followed by extraction with Qiaex II Gel Extraction Kit (Qiagen). The resulting

PCR products were inserted into the pcDNA3.1/V5-His TOPO TA expression vector by

first incubating all products with Taq polymerase to 3' adenylate the products followed

by incubation with the provided salt solution, water, and Topo Vector in a 3:1:1:1 ratio

following the recommended conditions. The resulting products were then transformed

into subcloning efficiency DH5α cells and plated on LB-ampicillin plates overnight. For

each TAAR up to 10 colonies were picked and grown overnight in 6 ml LB-amp media

for Qiagen miniprep isolation of the plasmid DNA. Each DNA prep was screened for

proper insert orientation using standard restriction digestion conditions.   Enzymes used

were BspE1 and Xhb1, HinD III, Xcm1 and HinD III, Ssp1 and HinD III, and HinD III

for each of the respective TAARs.   Plasmids with correctly oriented inserts were

sequenced. Correct sequences were obtained for TAARs 4, 6, and 7d.

rTAR$_2$

sense –   ATGAATTCACCTGACCTCTGG

381 CTCAGTGGACCGCCACTATGC

antisense – CTAAGGATGTGCAGGATGCAA

rTAR$_3$

sense – ATGGAGCTCTGCTACGAGAAC

380 CACTGACCTATCCGACCAAGT

antisense – TTAACCTGCACCTGCTTCTTC

rTAR$_4$

sense – ATGGGTAGTAACTCGTCTCCT

380 CCATTGACAGATACATCGCTG

antisense – TTATATTTGCTCAGAGAACAA

rTAR$_{10}$

sense – ATGACAAGCAACTTTTCCCAA

379 GTGGACAGGTACATCGCTGTC

antisense – TTATTCTGAAAACAAACTTGT

rTAR$_{15}$

sense – ATGCGTGTAGATGATGACCGT

379 GATGTCTCGTTCTGCTATTGT

antisense – CTACTCAGGGAACAAATTGAT

PCR methods

94°C 1 min

(94°C 1 min, 47°C 1 min, 72°C 2 min) 30 cycles

72°C 10 min

4°C hold

pIRESneo cloning strategy

The restriction sites used for the subcloning varied for each TAAR (see below).

Full length SSF-TAAR PCR products and pIRESneo vector were digested with the

appropriate combination of restriction enzymes and ligated using T4 DNA ligase using

recommended conditions. Immediately following the ligation reaction 2 μL of each

reaction was transformed into subcloning efficiency DH5α cells and plated on LB-Amp

agarose plates. Approximately 10 colonies per TAAR were picked and grown overnight

in 6 mL LB-Amp medium for Qiagen miniprep isolation of plasmid DNA. All of the

isolated DNA was screened for 1.2 kb inserts using the appropriate set of restriction

enzymes for each TAAR. Plasmids containing inserts were sequenced to confirm the

exact composition of each TAAR construct. The primers used for sequencing are shown

below.

Restriction sites used for rTAAR insertion into the pIRESneo vector

rTAAR$_1$ EcoR1 - BamH1

rTAAR$_4$ EcoRV - BamH1

rTAAR$_6$ EcoR1 - BamH1

rTAAR$_{7a}$ EcoR1 - Not1

rTAAR$_{7b}$ EcoRV - BamH1

rTAAR$_{7c}$ EcoR1 - BamH1

rTAAR$_{7d}$ EcoRV - BamH1

rTAAR$_{7e}$ EcoRV - BamH1

rTAAR$_{7f}$ EcoR1 - BamH1

rTAAR$_{7g}$ EcoRV - BamH1

rTAAR$_{7h}$ EcoR1 - BamH1

rTAAR$_{7i}$ EcoRV - BamH1

rTAAR$_{8a}$ EcoR1 - BamH1

rTAAR$_{8b}$ EcoR1 - BamH1

rTAAR$_{8c}$ EcoR1 - BamH1

rTAAR$_9$ EcoR1 - BamH1

Primers used

rTAR$_2$

5-Cla1-rTAR$_2$-3s CCATCGATATGAATTCACCTGACCTCTGGT

5-BamH1-rTAR$_2$-3as CGCGGATCCCTAAGGATGTGCAGGATGCAA

5-SSF-rTAR$_2$-3s – AAGGACGATGATGACGCCATGAATTCACCTGACCTC

5-rTAR$_2$-SSF-3as - GAGGTCAGGTGAATTCATGGCGTCATCATCGTCCTT

rTAR$_3$

5-BamH1-rTAR$_3$-3as CGCGGATCCTTAACCTGCACCTGCTTCTT

5-SSF-rTAR$_3$-3s – AAGGACGATGATGACGCCATGGAGCTCTGCTACGAG

5-rTAR$_3$-SSF-3as - CTCGTAGCAGAGCTCCATGGCGTCATCATCGTCCTT

rTAR$_4$

5-Cla1-rTAR$_4$-3s CCATCGATATGGGTAGTAACTCGTCTCCTC

5-BamH1-rTAR$_4$-3as CGCGGATCCTTATATTTGCTCAGAGAACAA

5-SSF-rTAR$_4$-3s – AAGGACGATGATGACGCCATGGGTAGTAACTCGTCT

5-rTAR$_4$-SSF-3as - AGACGAGTTACTACCCATGGCGTCATCATCGTCCTT

rTAR$_{10}$

5-SSF-rTAR$_{10}$-3s – AAGGACGATGATGACGCCATGACAAGCAACTTTTCC

5-rTAR$_{10}$-SSF-3as - GGAAAAGTTGCTTGTCATGGCGTCATCATCGTCCTT

rTAR$_{15}$

5-Cla1-rTAR$_{15}$-3s CCATCGATATGGCTACAGATAATGACAGTT

5-BamH1-rTAR$_{15}$-3as CGCGGATCCCTACTCAGGAAACAAGTTGGT

5-SSF-rTAR$_{15}$-3s –   AAGGACGATGATGACGCCATGCGTGTAGATGATGAC

5-rTAR$_{15}$-SSF-3as - GTCATCATCTACACGCATGGCGTCATCATCGTCCTT

rTAR$_6$

sense-   ATGGCTACAGATGATGAGAGTTTTC

antisense-   CTACTCAGAAACAGGTTGGTGGTT

rTAR$_7$

sense-   ATGACAAGCAACTTTTCCCAAGCAA

antisense-   TTATTCTGAAAACAAACTAGTAGTT

rTAR$_8$

sense-   ATGGACAAGTTGGTTGACAATTTCC

antisense-   CTATTCAGGAAACAGGTTGGTGACT

rTAR$_9$

sense-   ATGGCTACAGATGATGGCAGTTTTC

antisense-   CTACTCAGGGAACAAATTGATGGTT

rTAR$_{11}$

sense-   ATGGAGTGCATTTCTTTCATTTTTG

antisense-   TTACTCTGAAAACAAACTCATGGTA

83

rTAR$_{12}$

sense-   ATGCAGCTGTGCTATGAGAAACTGA

antisense-   CTACTCAGGAAACAGGTTGGTGGCT

rTAR$_{13}$

sense-   ATGCCTGTAGATGATGAGAGTTTTC

antisense-   CTACTCAGGAAACAGGTTGGTGGTT

rTAR$_{14}$

sense-   ATGGCTACAGATGATGCCAGTTTTC

antisense-   CTACTCAGGAAACAGGTTGGTGGCT

Evaluation of transient expression by immunofluorescent microscopy

Expression of each of the correctly cloned TAAR receptors was evaluated by immunofluorescent microscopy. Initial work was done with three commonly used mammalian cell lines (HEK293, Cos7, and CHO-K1) transiently expressing each of the receptors. Transfection of the TAAR constructs was done in 10 cm plates with Lipofectamine 2000 (Invitrogen) following the recommended protocol. 24 hours after the transfection the cells were trypsonized, centrifuged and resuspended with 10 mL of media. From the suspension 500 µL was added to 2 wells of a 6 well plate containing

microscope coverslips on the bottom of the well. The cells mounted on coverslips were fixed and stained with and without triton-X 100 for evaluation of total versus surface expression (see below for immunofluorescence protocol).

With TX100- Cells were split 1:2 onto coverslips 24 hours prior to staining. After 24 hours on the coverslips the cells were washed three times with PBS. Cells were then fixed by addition of 1 mL formaldehyde solution (1:10 mixture of 37% formaldehyde:PBS with Ca2+ and Mg2+) for 20 min at room temperature. Fixed cells were then washed three times with TBS for 5 min each. Cells were permeabilized by addition of 1 mL Blotto (TBS with Ca2+ and Mg2+, 0.1 % Triton X-100, and 3% w/V dry milk powder) and were incubated for 30 min at RT. Blotto was removed and Primary antibody was then added to the cells 1:1000 in blotto solution for 45 min at room temperature. The coverslips were then washed with TBS three times for 5 min each. Secondary antibody was applied to the slides 1:2000 in Blotto solution for 30 min at room temperature. The coverslips were again washed with TBS three times for 5 min each. The slips were then mounted on slides using VectaShield (Vector Laboratories) and fixed in place with wax. Slides were then stored overnight at 4°C for microscopy.

Without TX100- Cells were split 1:2 onto coverslips 24 hours prior to staining. Medium was changed 1 hour prior to staining. Primary antibody was then added 1:1000 to medium for 20 min at room temperature. Cells were washed with PBS 1 time for 5 min. Cells were then fixed by addition of 1 mL formaldehyde solution (1:10 mixture of 37% formaldehyde:PBS with Ca2+ and Mg2+) for 20 min at room temperature. Fixed cells were then washed three times with TBS for 5 min each. Secondary antibody was applied to the slides 1:2000 in TBS for 30 min at room temperature. The coverslips were

again washed with TBS three times for 5 min each. The slips were then mounted on slides using VectaShield and fixed in place with wax. Slides were then stored overnight at 4°C for microscopy.

Stable cell line generation

Several attempts were made to generate HEK293 cells lines stably expressing each of the correct TAAR constructs. WT HEK293 cells were initially transfected with Lipofectamine 2000 reagent (Invitrogen) using recommended conditions. Cells were transfected and left for two days in standard growth medium. After two days the media was replaced with growth medium containing 1 mg/mL G418.   After about 7 days in selective media several isolated colonies were visible. Approximately 15 colonies for each TAAR were removed and placed in separate wells of 6 well plates. Colonies were trypsonized and grown under standard cell culture conditions under selective media until screened for expression (see notebook AS II pg 15).

Cell lines were screened for TAAR expression by western blot probing with ANTI-FLAG M1 Monoclonal Antibody (Sigma). Overall there was very poor expression of all the TAARs which led to the need for an alternate expression strategy, expression from pIRESneo constructs.

In order to screen each of the TAARs for activity with a variety of thyroid hormone derivatives HEK293 cell lines were made to stably express each individual TAAR. Similar to the protocol for the TOPO TAAR construct stable cell line generation HEK293 cells were transfected with each TAAR construct using the Fugene 6 reagent.

HEK293 cells were split into 6 well plates 24 hours prior to transfection following recommended cell densities. 18 separate wells were transfected with either no DNA or one of the 8 TAAR constructs at 2 concentrations each. The constructs used were empty pIRESneo vector, and each of TAARs 4, 6, 7a, 7g, 8a, 8c, and 9. 48 hours after transfection the medium was changed to medium containing 1 mg/mL G418. 24 hours later the wells were trypsonized and transferred into 10 cm plates still containing medium with 1 mg/ml G418. Media was then changed daily for the next 9 days until all cells in the nontransfected HEK293 line were dead and washed off.

In the plates transfected with either empty vector or one of the TAAR containing constructs many visible colonies were present. From each of these plates 24 colonies were transferred to individual wells in 24 well plates. Once these colonies had grown to approximately 1mm diameter they were trypsonized and transferred to another well of a 24 well plate. These cells were sequentially amplified and split into larger diameter plates as they approached confluency under standard cell culture conditions all under G418 selection. After about 4 passages cells were trypsonized, centrifuged, resuspended in Media with 10% DMSO and frozen in 1.5 mL stocks for future evaluation of expression and TAAR mediated activity. Cell lines were labeled and stored in liquid nitrogen as recorded in AS-II pg 99-100.

Membrane Preparation (Hypotonic Lysis)

HEK293 cells stably transfected with either $rTAAR_1$, $mTAAR_1$, $r-hTAAR_1$, or empty pcDNA3 vector were grown according to standard cell culture conditions in DME-H21 media containing 10% fetal bovine serum 1X penicillin/streptomycin, and 1X

Geneticin. After incubation in fresh medium for at least 2 h, cells were washed with PBS

and harvested in 5mLKrebs-Ringer-Hepes buffer (KRH). Cells were pelleted and

resuspended in 2 mL ice cold buffer (50 mM Tris-Cl, pH 7.4, 1 mM EDTA, protease

inhibitor cocktail). Suspension was transferred to a dounce homogenizer and lysed with

20 strokes. Homogenized cells were centrifuged at 3000 rpm for 10 min to pellet

insoluble material. Supernatant was saved and the pellet was resuspended as above and

the process repeated a second time. The supernatants from both steps were combined and

centrifuged at 35,000 rpm for 30 min at 4 ºC. The supernatant was aspirated and the

resulting membranes were resuspended in 1 mL binding buffer (50 mM Tris-Cl, pH 7.4,

5 mM KCl, 5 mM NaCl, 0.75 mM $CaCl_2$, 2 mM $MgCl_2$, 0.5 mg/mL BSA) and stored at -

80 ºC.

In Vitro cAMP Assays

HEK293 cells stably transfected with either $rTAAR_4$, $rTAAR_6$ or empty

pcDNA3 vector were grown according to standard cell culture conditions in DME-H21

media containing 10% fetal bovine serum 1X penicillin/streptomycin, and 1X Geneticin.

After incubation in fresh medium for at least 2 h, cells were harvested in Krebs-Ringer-

Hepes buffer (KRH) and preincubated with 200 μM 3-isobutyl-1-methylxanthine (IBMX)

for 30 min at 37 °C. For agonist assays cells were then incubated in KRH with 133 μM

IBMX and 3 μL of the test compound, forskolin (10 μM), or vehicle (dimethyl sulfoxide,

DMSO) for 1 h at 37 °C (300 μL total volume). The cells were boiled for 20 min after

addition of 100 μL of 0.5 mM sodium acetate buffer (pH ~ 6.4). The cell lysate was

centrifuged (14000 rpm for 3 min) to remove cellular debris and stored at –20 °C for later

analysis. For antagonist assays the cells were treated as above but with the addition of a 30 min pretreatment step with test compounds just prior to the agonist addition as described.

cAMP measurement

Cell lysate stored at -20 °C was thawed and an aliquot (30 μL) was transferred to an opaque, flat bottom 96-well plate (Corning 3917). The cAMP content of the aliquot was measured by use of the Hithunter cAMP XS kit (DiscoveRX, Fremont, CA). The plate was shaken on a titer plate shaker for 2 min after addition of 20 μL of cAMP XS antibody/lysis mix. After incubation in the dark for 1 h, 20 μL of cAMP XS ED reagent was added and the plate was shaken for 2 min. After another hour of incubation in the dark, 40 μL of cAMP XS EA/CL substrate mix was added and the plate was shaken for 2 min. The plate was allowed to incubate for 15 h at room temperature before luminescence was measured (three readings/well at 0.33 s/reading) on a Packard Fusion microplate reader. Data were reported as percent maximal stimulation of reported agonists of each $TAAR_1$ homolog (T_1AM for rat and mouse $TAAR_1$ and phenethylamine (PEA) for r-$hTAAR_1$). Data were plotted and analyzed with Prism software (GraphPad, San Diego, CA). Standard error of the mean was calculated for at least three separate experiments performed in triplicate.

The $TAAR_4$ cells were thawed and grown under G418 selective conditions for 3 passages before experiments were conducted. As described previously HEK293 cells stably transfected with either $rTAAR_4$ or empty pcDNA3 vector were grown according to standard cell culture conditions in DME-H21 media containing 10% fetal bovine

serum 1X penicillin/streptomycin, and 1X Geneticin. After incubation in fresh medium for at least 2 h, cells were harvested in Krebs-Ringer-Hepes buffer (KRH) and preincubated with 200 μM 3-isobutyl-1-methylxanthine (IBMX) for 30 min at 37 °C. For agonist assays cells were then incubated in KRH with 133 μM IBMX and 3 μL of the test compound, forskolin (10 μM), or vehicle (dimethyl sulfoxide, DMSO) for 1 h at 37 °C (300 μL total volume). Test compounds were evaluated at final concentrations of either 100 nM, 1 μM, or 10 μM. The cells were boiled for 20 min after addition of 100 μL of 0.5 mM sodium acetate buffer (pH ~ 6.4). The cell lysate was centrifuged (14000 rpm for 3 min) to remove cellular debris and stored at –20 °C for later analysis. For antagonist assays the cells were treated as above but with the addition of a 30 min pretreatment step with putative antagonists just prior to the agonist addition as described. The differences between this experimental setup and the reported $TAAR_4$ assay were that this was a 1 hour drug treatment followed by a direct measurement of changes in cAMP concentration as opposed to a 24-48 hour drug treatment looking at a CRE-luciferase readout which is an indirect measure of cAMP concentration.

References

1.   Borowsky, B.,Adham, N.,Jones, K. A.,Raddatz, R.,Artymyshyn, R.,Ogozalek, K. L.,Durkin, M. M.,Lakhlani, P. P.,Bonini, J. A.,Pathirana, S.,Boyle, N.,Pu, X.,Kouranova, E.,Lichtblau, H.,Ochoa, F. Y.,Branchek, T. A.;Gerald, C. (2001) Trace amines: identification of a family of mammalian G protein-coupled receptors, *Proc Natl Acad Sci U S A 98*, 8966-71.

2.   Bunzow, J. R.,Sonders, M. S.,Arttamangkul, S.,Harrison, L. M.,Zhang, G.,Quigley, D. I.,Darland, T.,Suchland, K. L.,Pasumamula, S.,Kennedy, J. L.,Olson, S. B.,Magenis, R. E.,Amara, S. G.;Grandy, D. K. (2001) Amphetamine, 3,4-methylenedioxymethamphetamine, lysergic acid diethylamide, and metabolites of the catecholamine neurotransmitters are agonists of a rat trace amine receptor, *Mol Pharmacol 60*, 1181-8.

3.   Scanlan, T. S.,Suchland, K. L.,Hart, M. E.,Chiellini, G.,Huang, Y.,Kruzich, P. J.,Frascarelli, S.,Crossley, D. A.,Bunzow, J. R.,Ronca-Testoni, S.,Lin, E. T.,Hatton, D.,Zucchi, R.;Grandy, D. K. (2004) 3-Iodothyronamine is an endogenous and rapid-acting derivative of thyroid hormone, *Nat Med 10*, 638-42.

4.   Hart, M. E.,Suchland, K. L.,Miyakawa, M.,Bunzow, J. R.,Grandy, D. K.;Scanlan, T. S. (2006) Trace amine-associated receptor agonists: synthesis and evaluation of thyronamines and related analogues, *J Med Chem 49*, 1101-12.

5.   Wainscott, D. B.,Little, S. P.,Yin, T.,Tu, Y.,Rocco, V. P.,He, J. X.;Nelson, D. L. (2007) Pharmacologic characterization of the cloned human trace amine-associated receptor1 (TAAR1) and evidence for species differences with the rat TAAR1, *J Pharmacol Exp Ther 320*, 475-85.

6.   Tan, E. S.,Miyakawa, M.,Bunzow, J. R.,Grandy, D. K.;Scanlan, T. S. (2007) Exploring the structure-activity relationship of the ethylamine portion of 3-iodothyronamine for rat and mouse trace amine-associated receptor 1, *J Med Chem 50*, 2787-98.

7.   Reese, E. A.,Bunzow, J. R.,Arttamangkul, S.,Sonders, M. S.;Grandy, D. K. (2007) Trace amine-associated receptor 1 displays species-dependent stereoselectivity for isomers of methamphetamine, amphetamine, and para-hydroxyamphetamine, *J Pharmacol Exp Ther 321*, 178-86.

8.   Regard, J. B.,Kataoka, H.,Cano, D. A.,Camerer, E.,Yin, L.,Zheng, Y. W.,Scanlan, T. S.,Hebrok, M.;Coughlin, S. R. (2007) Probing cell type-specific functions of Gi in vivo identifies GPCR regulators of insulin secretion, *J Clin Invest 117*, 4034-43.

9.   Regard, J. B.,Sato, I. T.;Coughlin, S. R. (2008) Anatomical profiling of G protein-coupled receptor expression, *Cell 135*, 561-71.

10.   Lindemann, L.,Ebeling, M.,Kratochwil, N. A.,Bunzow, J. R.,Grandy, D. K.;Hoener, M. C. (2005) Trace amine-associated receptors form structurally and functionally distinct subfamilies of novel G protein-coupled receptors, *Genomics 85*, 372-85.

11.   Gloriam, D. E.,Bjarnadottir, T. K.,Yan, Y. L.,Postlethwait, J. H.,Schioth, H. B.;Fredriksson, R. (2005) The repertoire of trace amine G-protein-coupled receptors: large expansion in zebrafish, *Mol Phylogenet Evol 35*, 470-82.

12.   Liberles, S. D.;Buck, L. B. (2006) A second class of chemosensory receptors in the olfactory epithelium, *Nature 442*, 645-50.

13. Selbie, L. A.;Hill, S. J. (1998) G protein-coupled-receptor cross-talk: the fine-tuning of multiple receptor-signalling pathways, *Trends Pharmacol Sci 19*, 87-93.

14. Vladimirov, V.,Thiselton, D. L.,Kuo, P. H.,McClay, J.,Fanous, A.,Wormley, B.,Vittum, J.,Ribble, R.,Moher, B.,van den Oord, E.,O'Neill, F. A.,Walsh, D.,Kendler, K. S.;Riley, B. P. (2007) A region of 35 kb containing the trace amine associate receptor 6 (TAAR6) gene is associated with schizophrenia in the Irish study of high-density schizophrenia families, *Mol Psychiatry 12*, 842-53.

15. Pae, C. U.,Yu, H. S.,Amann, D.,Kim, J. J.,Lee, C. U.,Lee, S. J.,Jun, T. Y.,Lee, C.,Paik, I. H.,Patkar, A. A.;Lerer, B. (2008) Association of the trace amine associated receptor 6 (TAAR6) gene with schizophrenia and bipolar disorder in a Korean case control sample, *J Psychiatr Res 42*, 35-40.

16. Vladimirov, V. I.,Maher, B. S.,Wormley, B.,O'Neill, F. A.,Walsh, D.,Kendler, K. S.;Riley, B. P. (2008) The trace amine associated receptor (TAAR6) gene is not associated with schizophrenia in the Irish Case-Control Study of Schizophrenia (ICCSS) sample, *Schizophr Res*

17. Reiners, J.,Schmidt, M.,Packer, J.,Unger, L.;Wernet, W. (2007) A polymorphism linked to bipolar affective disorder does not alter the CRE activity of constitutively activated trace amine receptor 4, *Mol Psychiatry 12*, 900-2.

18. Xie, Z.,Vallender, E. J.,Yu, N.,Kirstein, S. L.,Yang, H.,Bahn, M. E.,Westmoreland, S. V.;Miller, G. M. (2008) Cloning, expression, and functional analysis of rhesus monkey trace amine-associated receptor 6: evidence for lack of monoaminergic association, *J Neurosci Res 86*, 3435-46.

Chapter 4

Trace Amine-Associated Receptor 1 (TAAR$_1$) is Activated by

Amiodarone Metabolites

Abstract

Amiodarone (Cordarone, Wyeth-Ayerst Pharmaceuticals) is a clinically available drug used to treat a wide variety of cardiac arrhythmias. We report here the synthesis and characterization of a panel of potential amiodarone metabolites that have significant structural similarity to thyroid hormone and its metabolites the iodothyronamines. Several of these amiodarone derivatives act as specific agonists of the G protein-coupled receptor (GPCR) trace amine-associated receptor 1 (TAAR$_1$). This result demonstrates a novel molecular target for amiodarone derivatives with potential clinical significance.

Introduction

Amiodarone (Cordarone, Wyeth-Ayerst Pharmaceuticals) has been available in the United States since 1985 and its biological activity and pharmacokinetics have been well studied. It blocks myocardial potassium channels and inhibits adrenergic receptors as well as type-1 and type-2 5'deiodinases (*1,2*). Despite what is known, there are numerous side effects of amiodarone use in humans that suggest additional activities beyond the identified targets of amiodarone. Amiodarone is known to be a substrate of the cytochrome P450 enzyme group. One major observed metabolite of amiodarone, desethylamiodarone, has antiarrhythmic properties of its own (*3-5*) as well as distinct antagonistic effects on the thyroid hormone receptor (*6-8*).

By comparison to the biosynthesis and metabolism of thyroxine, thyroid hormone (TH), we hypothesized that amiodarone treatment may result in multiple other amiodarone metabolites with potential biological activity. The hypothetical amiodarone metabolites would result as products of known deiodination and desethylation pathways in the body (*3,4*). As iodinated benzofuran derivatives, these amiodarones contain significant structural similarity to TH, and a recently described class of thyroid hormone metabolites, iodothyronamines (*9*).

Iodothyronamines rapidly and potently activate a novel family of orphan G protein-coupled receptors (GPCRs) the trace amine-associated receptors (TAARs). The most thoroughly characterized of the thyronamines, T_1AM, is an endogenous compound with dramatic and rapid pharmacological properties in rodents when administered exogenously (*9*), including significant effects on cardiac performance. While no direct link has been made between T_1AM action with $TAAR_1$ and the observed pharmacology,

a correlation between the potency of several T_1AM derivatives against $TAAR_1$ and their

ability to induce T_1AMs pharmacological effects has been noted (*10*). This suggests

T_1AM activity with $TAAR_1$ may result in the observed pharmacology.

Given that amiodarone and thyronamines are both known to have a variety of

cardiac effects and both share significant structural similarities we sought to understand

whether this clinically used TH derivative, amiodarone or its potential metabolites, may

also target $TAAR_1$. To test this idea, a panel of eight potential amiodarone metabolites

was synthesized (Scheme 1 and Supplemental Information). These derivatives include all

possible permutations of amiodarone desethylation and deiodination (Table 1). The total

panel of eight amiodarone derivatives (compounds **2-9**) plus the parent compound

amiodarone **1** was then screened against several mammalian homologs of $TAAR_1$.

Specifically, we tested these compounds for both agonist and antagonist activity against

mouse, rat and a chimeric human $TAAR_1$. This screen evaluated the amount of

intracellular cAMP levels induced by the amiodarone analogs by stimulation of $TAAR_1$,

a GPCR coupled to a stimulatory G-protein (G_S).
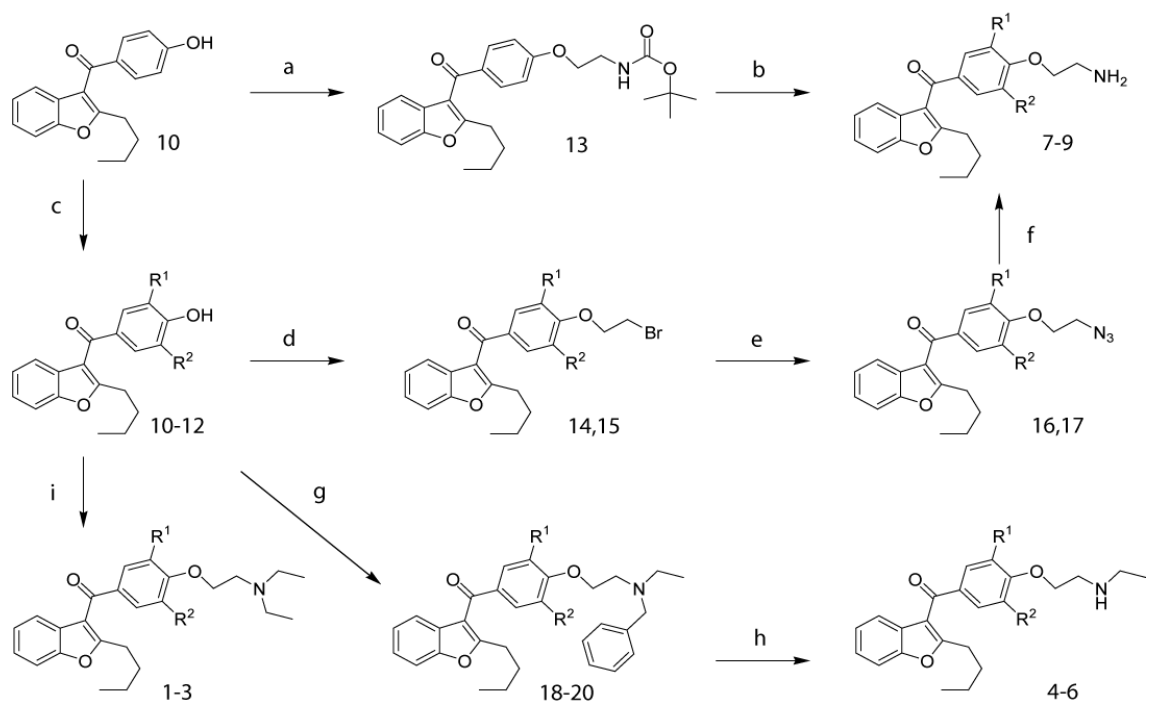
Scheme 1. Synthesis of Amiodarone Panel. For compounds **1**, **4**, **7**, **12**, **15**, **17**, and **20**, $R^1 = R^2 = I$. For compounds **2**, **5**, **8**, **11**, **14**, **16**, and **19**, $R^1 = H$ and $R^2 = I$. For compounds **3**, **6**, **9**, **10**, and **18**, $R^1 = R^2 = H$. **a)** Cs_2CO_3, BocNHCH$_2$CH$_2$OMs, DMF, 50ºC; **b)** 3N anhydrous HCl in EtOAc; **c)** NaI, NaOCl, 5M KOH, MeOH; **d)** EtBr$_2$, K_2CO_3, DMF; **e)** NaN$_3$, DMF; **f)** PPh$_3$, THF/H$_2$O; **g)** N-(2-Chloroethyl)-N-ethylbenzylamine HCl, NaI, K_2CO_3, DMF; **h) (i)** 5, 1-chloroethyl carbonochloride, EtCl$_2$, reflux, 2hr; (ii) MeOH, reflux, 1hr, 3N HCl/EtOAc; **i)** NaI, Et$_2$NCH$_2$CH$_2$Cl·HCl, K_2CO_3, DMF, RT.
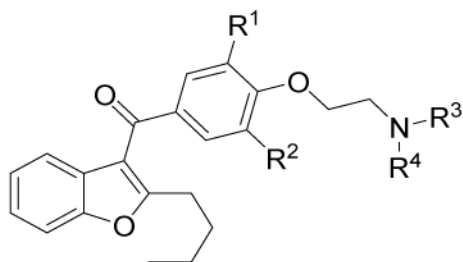
	Compound	R^1	R^2	R^3	R^4
Ami	1	I	I	Et	Et
dE-Ami	4	I	I	Et	H
ddE-Ami	7	I	I	H	H
dI-Ami	2	I	H	Et	Et
dEdI-Ami	5	I	H	Et	H
ddEdI-Ami	8	I	H	H	H
ddI-Ami	3	H	H	Et	Et
dEddI-Ami	6	H	H	Et	H
ddEddI-Ami	9	H	H	H	H

Table 1. Amiodarone Panel.

When screened against rat $TAAR_1$ ($rTAAR_1$) four of the potential amiodarone metabolites, compounds **6**, **7**, **8**, and **9** demonstrated significant activity against $rTAAR_1$ (Figure 1a). These compounds demonstrated specific agonistic activity at doses of 10 μM or below with the most potent analog **7**, ddE-Ami, giving an observed half maximal effective concentration (EC_{50}) of 1 μM (data not shown). The other five amiodarone derivatives (Ami, dE-Ami, dI-Ami, dEdI-Ami, and ddI-Ami) did not display any antagonistic activity when tested at 10 μM in competition with the reported agonist T_1AM at its EC_{50} concentration of 33 nM.

To extend the conclusions of amiodarone activity, the amiodarone panel was tested against another $TAAR_1$ homolog the mouse $TAAR_1$ ($mTAAR_1$). As was seen for

rTAAR$_1$ several of the amiodarones showed significant agonist activity at 10 μM concentration. A different subset of four compounds (compounds **3**, **6**, **8**, and **9)** demonstrated significant but partial or weak agonistic activity against m TAAR$_1$ (Figure 1b). Additionally, distinct from the amiodarone activity with rTAAR$_1$, several compounds in the amiodarone panel, appear to also demonstrate partial or weak antagonistic activity (> 10 μM IC$_{50}$ against mTAAR$_1$ (data not shown).

Lastly, the amiodarone panel was screened against a chimeric rat-human TAAR$_1$ (r- hTAAR$_1$). This chimera, as described previously (*11,12*), was generated by exchanging portions of the N terminus (residues 1-20), C terminus (residues 305-340), and third intracellular loop (residues 204-258) of the wild-type human sequence for that of rTAAR$_1$ to enhance expression and plasma membrane trafficking of the receptor (*11,12*). Importantly all of the transmembrane domains from the human TAAR$_1$ were retained. The chimeric r-hTAAR$_1$ receptor has been shown to respond similarly to the wild type human TAAR$_1$ (hTAAR$_1$) in regard to ligand specificity and potency (*12-14*). No published reports, however, have verified the complete ligand profile of this chimeric receptor as compared with the reported activity of wild-type hTAAR$_1$. In our screen of the r-hTAAR$_1$ receptor none of the amiodarones demonstrate any significant agonistic or antagonistic activity at any of the doses tested (Figure 1c). Despite the lack of amiodarone activity against the r-hTAAR$_1$ chimera follow-up studies with the WT receptor are warranted because of the wide ranging ligand profiles between the TAAR homologs (*10,15*). Despite our observations amiodarones could have activity with the WT hTAAR$_1$.
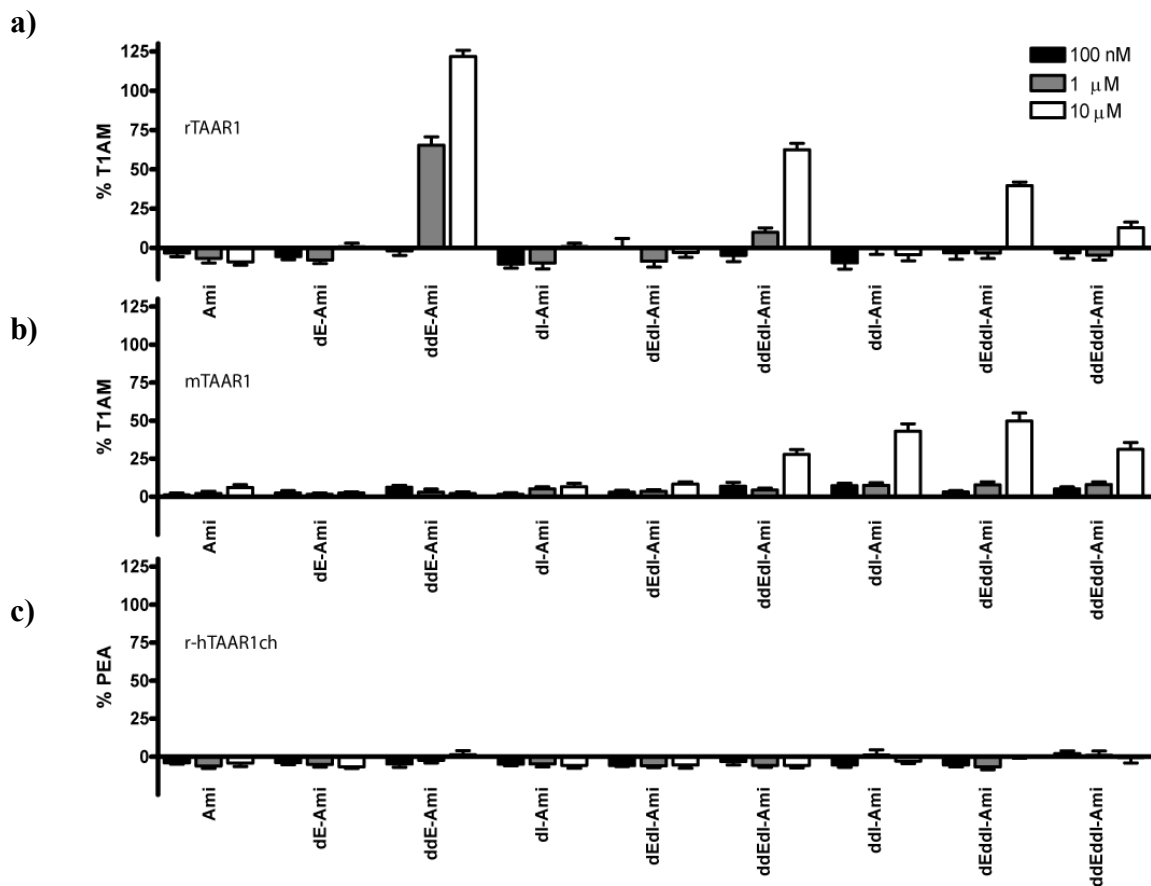
Figure 1. Amiodarone Activity with TAAR$_1$ Homologs. HEK293 cells stably transfected with either **a)** rTAAR$_1$, **b)** mTAAR$_1$, **c)** r-hTAAR$_1$, or empty pcDNA3 vector were harvested in Krebs-Ringer-Hepes buffer (KRH) and incubated in KRH with 133 μM IBMX and 3 μL of the test compound, forskolin (10 μM), or vehicle (dimethyl sulfoxide, DMSO) for 1 h at 37 °C. The cells were boiled and the cell lysate was analyzed for cAMP content by use of the Hithunter cAMP XS kit (DiscoveRX, Fremont, CA). Data were reported as percent maximal stimulation of reported agonists of each TAAR$_1$ homolog (T$_1$AM for rat and mouse TAAR$_1$ and phenethylamine (PEA) for r-hTAAR$_1$). Data were plotted and analyzed with Prism software (GraphPad, San Diego, CA). Standard error of the mean was calculated for at least three separate experiments performed in triplicate.

In summary, we synthesized several potential amiodarone metabolites, products of desethylation and/or deiodination, and found that several act as agonists against both mouse and rat $TAAR_1$ and several also weakly antagonize $mTAAR_1$. By looking at the specific compounds that demonstrated specific activity with either the rat or mouse TAAR a striking structure activity relationship was observed. As iodine content increases and ethylation state decreases compounds gain efficacy and potency with $rTAAR_1$ and amiodarones with no iodines, independent of ethylation state, are weak agonists of $mTAAR_1$. However, none of these compounds had activity against the r-$hTAAR_1$ chimera. Given that the usual therapeutic serum level of amiodarone is low micromolar, with significant accumulation in adipose and other tissues, our data potentially have clinical relevance. These results demonstrate a novel molecular target for amiodarone derivatives, at least in rodents, and suggest another family of receptors amiodarone may target *in vivo*.

Methods

In Vitro cAMP Assays

HEK293 cells stably transfected with either $rTAAR_1$, $mTAAR_1$, r-$hTAAR_1$, or empty pcDNA3 vector were grown according to standard cell culture conditions in DME-H21 media containing 10% fetal bovine serum 1X penicillin/streptomycin, and 1X Geneticin. After incubation in fresh medium for at least 2 h, cells were harvested in Krebs-Ringer-Hepes buffer (KRH) and preincubated with 200 μM 3-isobutyl-1-methylxanthine (IBMX) for 30 min at 37 °C. For agonist assays cells were then incubated in KRH with 133 μM IBMX and 3 μL of the test compound, forskolin (10 μM), or vehicle (dimethyl sulfoxide, DMSO) for 1 h at 37 °C (300 μL total volume). The cells were boiled for 20 min after addition of 100 μL of 0.5 mM sodium acetate buffer (pH ~ 6.4). The cell lysate was centrifuged (14000 rpm for 3 min) to remove cellular debris and stored at −20 °C for later analysis. For antagonist assays the cells were treated as above but with the addition of a 30 min pretreatment step with test compounds just prior to the agonist addition as described.

cAMP measurement

Cell lysate stored at −20 °C was thawed and an aliquot (30 μL) was transferred to an opaque, flat bottom 96-well plate (Corning 3917). The cAMP content of the aliquot was measured by use of the Hithunter cAMP XS kit (DiscoveRX, Fremont, CA). The plate was shaken on a titer plate shaker for 2 min after addition of 20 μL of cAMP XS antibody/lysis mix. After incubation in the dark for 1 h, 20 μL of cAMP XS ED reagent was added and the plate was shaken for 2 min. After another hour of incubation in the

dark, 40 μL of cAMP XS EA/CL substrate mix was added and the plate was shaken for 2 min. The plate was allowed to incubate for 15 h at room temperature before luminescence was measured (three readings/well at 0.33 s/reading) on a Packard Fusion microplate reader. Data were reported as percent maximal stimulation of reported agonists of each TAAR$_1$ homolog (T$_1$AM for rat and mouse TAAR$_1$ and phenethylamine (PEA) for r-hTAAR$_1$). Data were plotted and analyzed with Prism software (GraphPad, San Diego, CA). Standard error of the mean was calculated for at least three separate experiments performed in triplicate.

Synthesis of Amiodarones

(2-Butyl-benzofuran-3-yl)-[4-(2-diethylamino-ethoxy)-3,5-diiodo-phenyl]-methanone (1, amiodarone, Ami). Sigma

(2-Butyl-benzofuran-3-yl)-[4-(2-diethylamino-ethoxy)-3-iodo-phenyl]-methanone (2, deiodoamiodarone, dI-Ami). To a solution of **11** (0.24 mmol), K$_2$CO$_3$ (0.95 mmol), and NaI (0.02 mmol) in DMF (5 mL) was added **2-chloro-N, N-diethylethanamine hydrochloride (0.24 mmol).** After stirring at room temperature overnight, the reaction was quenched with water and extracted with Et$_2$O. The organic layer was washed with brine, dried over MgSO$_4$, filtered, and concentrated under reduced pressure to give the crude product. The crude product was purified via flash SiO$_2$ chromatography (EtOAc/MeOH (1:0) to (5:1) to give **2** (105 mg, 84% yield). ^{1}H NMR (400 MHz, chloroform-*d*) δ 8.32 (s, 1H), 7.82 (d, *J*=8.80 Hz, 1H), 7.48 (d, *J*=8.80 Hz, 1H), 7.33 (m,

3H), 6.91 (d, *J*=8.80 Hz, 1H), 4.76 (m, 2H), 3.56(m, 2H), 3.36(m, 2H), 2.91(m, 2H), 1.89(m, 2H), 1.79 (m, 2H), 1.52(t, *J*=7.20 Hz, 6H), 1.36(m, 2H), 0.91 (t, *J*=7.25 Hz, 3H)

(2-Butyl-benzofuran-3-yl)-[4-(2-diethylamino-ethoxy)-phenyl]-methanone (3, dideiodoamiodarone, ddI-Ami). To a solution of **10** (0.68 mmol), K$_2$CO$_3$ (2.72 mmol), and NaI (trace) in Toluene:Water (16 mL:8 mL) was added **2-chloro-N, N-diethylethanamine hydrochloride (0.24 mmol).** After stirring at room temperature overnight, the reaction was quenched with water and extracted with Et$_2$O. The organic layer was washed with brine, dried over MgSO$_4$, filtered, and concentrated under reduced pressure to give the crude product. The crude product was purified via flash SiO$_2$ chromatography (EtOAc/Hexanes (1:3) to MeOH/DCM (1:99) to (1:19) to give **3** (249 mg, 88% yield). ^{1}H NMR (400 MHz, chloroform-*d*) *δ* 7.84 (d, *J*=8.42 Hz, 2H), 7.48 (d, *J*=8.06 Hz, 1H), 7.28 (m, 3H), 6.97 (d, *J*=8.79 Hz, 2H), 4.66 (m, 2H), 3.52 (m, 2H), 3.30 (m, 2H), 2.92 (t, *J*=7.51 Hz, 2H), 1.76 (m, 2H), 1.48 (t, *J*=6.96 Hz, 6H), 1.37 (m, 2H), 0.89 (t, *J*=7.33 Hz, 3H)

(2-Butyl-benzofuran-3-yl)-[4-(2-ethylamino-ethoxy)-3,5-diiodo-phenyl]-methanone hydrochloride (4, desethyl-amiodarone, dE-Ami). To a solution of **20** (0.102 mmol) in EtCl$_2$ (3 mL) was added 1-chloroethly carbonochloride (0.03 mL). After refluxing for 2 h, the reaction was concentrated to dryness under reduced pressure. The resulting crude mixture was dissolved with MeOH (5 mL) and after refluxing for 1 h, the reaction was concentrated to dryness under reduced pressure. The residue was dissolved with EtOAc, washed with saturated NaHCO$_3$, brine, dried over MgSO$_4$, filtered, and concentrated

under reduced pressure to give the crude product. The crude product was purified via flash SiO$_2$ chromatography (EtOAc/MeOH (1:0) to (3:1). The purified product was treated with 3N HCl in EtOAc filtered and concentrated to dryness to give **4**. ^{1}H NMR (400 MHz, chloroform-*d*) *δ* 9.76 (s, 1H), 8.21 (d, *J*=1.65 Hz, 2H), 7.49 (d, *J*=8.42 Hz, 1H), 7.36 (m, 3H), 4.54 (m, 2H), 3.64 (m, 2H), 3.44 (m, 2H), 2.88 (m, 2H), 1.77 (m, 2H), 1.55 (m, 3H), 1.37 (dd, *J*=15.20, 8.06 Hz, 2H), 0.92 (t, *J*=7.60 Hz, 3H)

(2-Butyl-benzofuran-3-yl)-[4-(2-ethylamino-ethoxy)-3-iodo-phenyl]-methanone (5, desethyl-deiodo-amiodarone, dEdI-Ami). To a solution of **19** (0.267 mmol) in EtCl$_2$ (5 mL) was added 1-chloroethly carbonochloride (0.08 mL). After refluxing for 2 h, the reaction was concentrated to dryness under reduced pressure. The resulting crude mixture was dissolved with MeOH (5 mL) and after refluxing for 1 h, the reaction was concentrated to dryness under reduced pressure. The residue was dissolved with EtOAc, washed with saturated NaHCO$_3$, brine, dried over MgSO$_4$, filtered, and concentrated under reduced pressure to give the crude product. The crude product was purified via flash SiO$_2$ chromatography (EtOAc/MeOH (1:0) to (3:1). The purified product was treated with 3N HCl in EtOAc for 2 h at room temperature and concentrated to dryness under reduced pressure to give **5**. ^{1}H NMR (400 MHz, chloroform-*d*) *δ* 9.85 (s, 1H), 8.30 (d, *J*=2.01 Hz, 1H), 7.83 (dd, *J*=8.24, 2.20 Hz), 1H), 7.48 (d, *J*=7.51 Hz, 1H), 7.27 (m, 3H), 6.90 (d, *J*=8.61 Hz, 1H), 4.61 (m, 2H), 3.57 (m, 2H), 3.42 (m, 2H), 2.90 (m, 2H), 1.77 (m, 2H), 1.55 (m, 3H), 1.38 (m, 2H), 0.91 (t, *J*=7.33 Hz, 3H)

(2-Butyl-benzofuran-3-yl)-[4-(2-ethylamino-ethoxy)-phenyl]-methanone (6, desethyl-dideiodo-amiodarone, dEddI-Ami). To a solution of **18** (0.267 mmol) in EtOAc (5 mL) was added 10% Palladium on carbon (Pd/C) (15 mg). After stirring for 18 h at room temperature under $H_2(g)$ (1 atm), the Pd/C was filtered off and the solution was concentrated to dryness under reduced pressure. The crude product was purified via flash SiO_2 chromatography (EtOAc/MeOH (1:0) to (5:1). The purified product was treated with 3N HCl in EtOAc for 2 h at room temperature and concentrated to dryness under reduced pressure to give **6** (100 mg, 79% yield). ^{1}H NMR (400 MHz, chloroform-*d*) δ 7.85(d, *J*=8.42 Hz, 2H), 7.48 (d, *J*=8.24 Hz, 1H), 7.30 (m, 2H), 7.20 (d, *J*=7.69 Hz, 1 H), 6.97 (d, *J*=8.61 Hz, 2H), 4.66 (d, *J*=32.05 Hz, 2H), 3.50 (d, *J*=48.53 Hz, 2H), 3.28 (m, *J*=62.63 Hz, 2H), 1.76 (m, 2H), 1.52 (m, 3H), 1.36 (m, 2H), 0.90 (m, 3H)

[4-(2-Amino-ethoxy)-3,5-diiodo-phenyl]-(2-butyl-benzofuran-3-yl)-methanone (7, didesethyl-amiodarone, ddE-Ami). To a solution of **15** (0.11 mmol) in THF/water (5 mL/1 mL) was added PPh_3 (0.22 mmol). After refluxing for 2 h, the reaction was quenched with water and extracted with EtOAc. The organic layer was washed with brine, dried over MgSO4, filtered and concentrated under reduced pressure to give the crude product.   The crude product was purified via flash SiO_2 chromatography (EtOAc/MeOH (5:1). The purified product was treated with 3N HCl in EtOAc for 2 h then concentrated under reduced pressure to give **7** (55 mg, 80% yield). ^{1}H NMR (400 MHz, chloroform-*d*) δ 8.70 (s, 2H), 8.15 (m, 2H), 7.50 (m, 1H), 7.33 (m, 3H), 4.49 (m, 2H), 3.70(m, 2H), 2.89 (m, 2H), 1.75 (m, 2H), 1.38 (m, 2H), 0.90 (m, 3H)

[4-(2-Amino-ethoxy)-3-iodo-phenyl]-(2-butyl-benzofuran-3-yl)-methanone (8, didesethyl-deiodo-amiodarone, ddEdI-Ami). To a solution of **16** (0.22 mmol) in THF/water (5 mL/1 mL) was added PPh_3 (0.45 mmol). After refluxing for 2 h, the reaction was quenched with water and extracted with EtOAc. The organic layer was washed with brine, dried over $MgSO_4$, filtered and concentrated under reduced pressure to give the crude product. The crude product was purified via flash SiO_2 chromatography (EtOAc/MeOH (4:1). The purified product was treated with 3N HCl in EtOAc for 2 h then concentrated under reduced pressure to give **8** (82 mg, 75% yield). ^{1}H NMR (400 MHz, chloroform-d) δ 8.67 (s, 2H), 8.27 (d, J=2.01 Hz, 1H), 7.81 (dd, J=8.52, 2.11 Hz, 1H), 7.47 (d, J=8.24 Hz, 1H), 7.25 (m, 3H), 6.88 (d, J=10.80 Hz, 1H), 4.47 (m, 2H), 3.60 (m, 2H), 2.89 (m, 2H), 1.76 (m, 2H), 1.35 (m, 2H), 0.90 (t, J=7.33 Hz, 3H)

[4-(2-Amino-ethoxy)-phenyl]-(2-butyl-benzofuran-3-yl)-methanone hydrochloride (9, didesethyl-dideiodo-amiodarone, ddEddI-Ami). **13** (0.46 mmol) was dissolved in a 3N anhydrous HCl solution in EtOAc (2 mL), and the reaction mixture was stirred overnight at room temperature. The reaction was exposed to Et_2O and the resulting amine hydrochloride salts were washed with Et_2O. The Et_2O/EtOAc solution was concentrated under reduced pressure and triturated with Et_2O to give **9** (170 mg, 100% yield). ^{1}H NMR (400 MHz, chloroform-d) δ 8.50 (s, 2H), 7.72 (s, 2H), 7.41 (d, J=8.06 Hz, 1H), 7.22 (m, 3H), 6.98 (s, 2H), 4.28 (m, 2H), 3.35 (m, 2H), 2.83 (m, 2H), 1.68 (m, 2H), 1.29 (m, 2H), 0.83 (t, J=7.33 Hz, 3H)

(2-Butyl-benzofuran-3-yl)-(4-hydroxy-phenyl)-methanone (10). Sigma

(2-Butyl-benzofuran-3-yl)-(4-hydroxy-3-iodo-phenyl)-methanone (11). To a solution of **10** (5.0 mmol) in MeOH (50 mL) was added NaI (5.3 mmol) followed by 5M KOH (5 mmol). The reaction was cooled to -5 °C and sodium hypochlorite (5.5 mmol) was added dropwise over 2 h and stirred for an additional 2 h at -5 °C. The reaction was quenched with 10% HCl in water, extracted with ET2O. The organic layer was washed with 10% Na_2SO_3, brine, dried over $MgSO_4$, filtered and concentrated under reduced pressure to give the crude product. The crude product was purified via flash SiO_2 chromatography (DCM/hexanes (2:1) to (1:0) to give **11** (287 mg, 25% yield) and **12** (310 mg, 11% yield). ^{1}H NMR (400 MHz, chloroform-*d*) δ 8.23 (s, 1H), 7.77 (d, *J*=8.79 Hz, 1H), 7.40 (m, 1H), 7.33 (m, 3H), 7.05 (d, *J*=8.24 Hz, 1H), 5.74 (s, 1H), 2.90 (m, 2H), 1.77 (m, 2H), 1.37 (m, 2H), 0.91 (m, 3H)

(2-Butyl-benzofuran-3-yl)-(4-hydroxy-3,5-diiodo-phenyl)-methanone (12). To a solution of **10** (5.0 mmol) in MeOH (50 mL) was added NaI (5.3 mmol) followed by 5M KOH (5 mmol). The reaction was cooled to -5 °C and sodium hypochlorite (5.5 mmol) was added dropwise over 2 h and stirred for an additional 2 h at -5 °C. The reaction was quenched with 10% HCl in water, extracted with ET_2O, washed with 10% Na_2SO_3, brine, dried over $MgSO_4$, filtered and concentrated under reduced pressure to give the crude product. The crude product was purified via flash SiO_2 chromatography (DCM/hexanes (2:1) to (1:0) to give **11** (287 mg, 25% yield) and **12** (310 mg, 11% yield).

{2-[4-(2-Butyl-benzofuran-3-carbonyl)-phenoxy]-ethyl}-carbamic acid tert-butyl ester (13). To a solution of **10** (1.35 mmol) in DMF (15 mL) was added Cs_2CO_3 (5.44 mmol), and **24** (2.72 mmol) consecutively. After stirring the reaction overnight at 50 °C another equivalent of **24** was added and stirred for 2 days at room temperature. A fourth equivalent of **24** was added and the reaction was heated to 40 °C for 1 day and to 45 °C the following day. The reaction was diluted with EtOAc and the organic layer was washed with water, brine, dried over $MgSO_4$, filtered and concentrated under reduced pressure to give the crude product. The crude product was purified via flash SiO_2 chromatography (EtOAc/hexanes (1:9) to (3:7) to give **13** (406 mg, 68% yield). ^{1}H NMR (400 MHz, chloroform-*d*) δ 7.84 (m, 2H), 7.47 (d, *J*=8.24 Hz, 1H), 7.26 (m, 3H), 6.95 (m, 2H), 4.99 (s, 1H), 4.11 (m, 2H), 3.59 (m, 2H), 2.92 (m, 2H), 1.76 (m, 2H), 1.46 (s, 9H), 1.37 (m, 2H), 0.89 (d, *J*=7.33 Hz, 1H)

[4-(2-Bromo-ethoxy)-3-iodo-phenyl]-(2-butyl-benzofuran-3-yl)-methanone (14). To a solution of **11** (0.36 mmol), and K_2CO_3 (1.43 mmol) in DMF (10 mL) was added **1, 2-Dibromoethane (1.43 mmol)**. After stirring for 2 h at 60 °C the reaction was quenched with water and extracted with Et_2O. The organic layer was washed with brine, dried over $MgSO_4$, filtered and concentrated under reduced pressure to give the crude product. The crude product was purified via flash SiO_2 chromatography (EtOAc/hexanes (1:20) to give **14** (120 mg, 63% yield) ^{1}H NMR (400 MHz, chloroform-*d*) δ 8.32 (d, *J*=2.20 Hz, 1H), 7.83 (dd, *J*=8.50, 2.20 Hz, 1H), 7.49 (d, *J*=8.42 Hz, 1H), 7.30 (m, 3H), 6.84 (d, *J*=8.61

Hz, 1H), 4.43 (m, 2H), 3.74 (t, *J*=6.41 Hz, 2H), 2.89 (m, 2H), 1.77 (m, 2H), 1.37 (m, 2H), 0.91 (t, *J*=7.33 Hz, 3H)

[4-(2-Bromo-ethoxy)-3,5-diiodo-phenyl]-(2-butyl-benzofuran-3-yl)-methanone (15). To a solution of **12** (0.19 mmol), and K$_2$CO$_3$ (0.77 mmol) in DMF (5 mL) was added **1,2-dibromoethane (0.77 mmol)**. After stirring for 2 h at 60 °C the reaction was quenched with water and extracted with Et$_2$O. The organic layer was washed with brine, dried over MgSO$_4$, filtered and concentrated under reduced pressure to give the crude product. The crude product was purified via flash SiO$_2$ chromatography (EtOAc/hexanes (1:20) to give **14** (75 mg, 61% yield) ^{1}H NMR (400 MHz, chloroform-*d*) *δ* 8.12 (m, 2H), 7.50 (d, *J*=8.79 Hz, 1H), 7.32 (m, 3H), 4.40 (m, 2H), 3.80 (m, 2H), 2.87 (m, 2H), 1.77 (m, 2H), 1.37 (m, 2H), 0.92 (t, *J*=7.33 Hz, 3H)

[4-(2-Azido-ethoxy)-3-iodo-phenyl]-(2-butyl-benzofuran-3-yl)-methanone (16). To a solution of **14** (0.23 mmol) in DMF (5 mL) was added NaN$_3$ (0.46 mmol). After stirring for 2 h at 60 °C the reaction was quenched with water and extracted with Et$_2$O. The organic layer was washed with brine, dried over MgSO$_4$, filtered and concentrated under reduced pressure to give the crude product (70 mg, 98% yield). ^{1}H NMR (400 MHz, chloroform-*d*) *δ* 8.32 (d, *J*=2.20 Hz, 1H), 7.83 (dd, *J*=8.42, 2.20 Hz, 1H), 7.48 (m, 1H), 7.36 (m, 3H), 6.86 (d, *J* =8.61 Hz, 1H), 4.26 (m, 2H), 3.73 (m, 2H), 2.90 (m, 2H), 1.77 (m, 2H), 1.37 (m, 2H), 0.91 (t, *J*=7.33 Hz, 3H)

[4-(2-Azido-ethoxy)-3,5-diiodo-phenyl]-(2-butyl-benzofuran-3-yl)-methanone (17).

To a solution of **15** (0.11 mmol) in DMF (5 mL) was added NaN_3 (0.22 mmol). After

stirring for 2 h at 60 °C the reaction was quenched with water and extracted with EtOAc.

The organic layer was washed with brine, dried over $MgSO_4$, filtered and concentrated

under reduced pressure to give the crude product (70 mg, 100% yield). ^{1}H NMR (400

MHz, chloroform-*d*) δ 8.13 (m, 2H), 7.50 (d, *J*=7.69 Hz, 1H), 7.33 (m, 3H), 4.28 (m, 2H),

3.76 (m 2H), 2.87 (m, 2H), 1.78 (m, 2H), 1.38 (m, 2H), 0.92 (t, *J*=7.23 Hz, 3H)

{4-[2-(Benzyl-ethyl-amino)-ethoxy]-phenyl}-(2-butyl-benzofuran-3-yl)-methanone

(18). To a solution of **10** (0.74 mmol) and NaI (0.07 mmol) in DMF (5 mL) was added

22 (0.74 mmol). After stirring for 24 h at room temperature, the reaction was quenched

with water and extracted with Et_2O. The organic layer was washed with brine, dried over

$MgSO_4$, filtered, and concentrated under reduced pressure to give the crude product. The

crude product was purified via flash SiO_2 chromatography (EtOAc/hexanes (1:5) to give

18 (285 mg, 85% yield). ^{1}H NMR (400 MHz, chloroform-*d*) δ 7.80 (m, 2H), 7.47 (d,

J=8.0 Hz, 1H), 7.28 (m, 3H), 6.88 (m, 2H), 4.08 (t, *J*= 6.20 Hz, 2H), 3.70 (s, 2H), 2.92

(m, 2H), 2.68 (m, 2H), 1.75 (m, 2H), 1.36 (m, 2H), 1.11 (t, *J* = 7.0 Hz, 3H), 0.89 (t, *J*=

7.25 Hz, 3H)

{4-[2-(Benzyl-ethyl-amino)-ethoxy]-3-iodo-phenyl}-(2-butyl-benzofuran-3-yl)-

methanone (19). To a solution of **11** (0.34 mmol) and NaI (0.03 mmol) in DMF (5 mL)

was added **22** (0.41 mmol). After stirring for 24 h at room temperature, the reaction was

quenched with water and extracted with Et$_2$O. The organic layer was washed with brine, dried over MgSO$_4$, filtered, and concentrated under reduced pressure to give the crude product. The crude product was purified via flash SiO$_2$ chromatography (EtOAc/hexanes (1:5) to give **19** (155 mg, 78% yield). ^{1}H NMR (400 MHz, chloroform-*d*) δ 8.20 (s, 2H), 7.49 (d, *J*=8.06 Hz, 1H) , 7.31 (m, 4H), 4.12 (t, *J*=6.59 Hz, 2H), 3.79 (s, 2H), 3.10 (t, *J*=6.41 Hz, 2H), 2.85 (m, 2H), 2.71 (m, 2H), 1.77 (m, 2H), 1.36 (m, 2H), 1.13 (t, *J*=6.96 Hz, 3H), 0.92 (t, *J*=7.05 Hz, 3H)

{4-[2-(Benzyl-ethyl-amino)-ethoxy]-3,5-diiodo-phenyl}-(2-butyl-benzofuran-3-yl)-methanone (20). To a solution of **12** (0.28 mmol) and NaI (0.03 mmol) in DMF (5 mL) was added **22** (0.34 mmol). After stirring for 24 h at room temperature, the reaction was quenched with water and extracted with Et$_2$O. The organic layer was washed with brine, dried over MgSO$_4$, filtered, and concentrated under reduced pressure to give the crude product. The crude product was purified via flash SiO$_2$ chromatography (EtOAc/hexanes (1:10) to (1:3) to give **20** (80 mg, 40% yield). ^{1}H NMR (400 MHz, chloroform-*d*) δ 8.19 (s, 2H), 7.48 (d, *J*= 8.40 Hz, 1H), 7.31 (m, 8H), 4.12 (m, 2H), 3.78 (s, 2H), 3.09 (m, 2H), 2.84 (m, 2H), 2.71 (m, 2H), 1.77 (m, 2H), 1.37 (m, 2H), 1.13 (t, *J*= 7.0 Hz, 3H), 0.91 (t, *J*= 7.40 Hz, 3H)

2-(Benzyl-ethyl-amino)-ethanol (21). To a solution of **2-(Ethylamino)ethanol (41 mmol)** and triethylamine (82 mmol) in DCM (100 mL) was added benzyl bromide (45 mmol). After stirring for two days at room temperature under argon, the reaction was

quenched with brine and extracted with DCM. The organic layer was washed with brine, dried over MgSO$_4$, filtered, and concentrated under reduced pressure to give the crude product. The crude product was purified via flash SiO$_2$ chromatography (EtOAc/hexanes (1:5) to (1:0) to give **21** (4.2 g, 57% yield).

Benzyl-(2-chloro-ethyl)-ethyl-amine (22). To a solution of **21** (1.5 mmol) in pyridine (5 mL) at 0 °C was added **methanesulfonyl chloride (1.8 mmol). After stirring for 30 min at room temperature the reaction was quenched with water and extracted with Et$_2$O.** The organic layer was washed with brine, dried over MgSO$_4$, filtered, and concentrated under reduced pressure to give the crude product. The crude product was purified via flash SiO$_2$ chromatography (EtOAc/hexanes (1:10) to give **22** (185 mg, 63% yield). ^{1}H NMR (400 MHz, chloroform-*d*) δ 7.31 (m, 5H), 3.62 (s, 2H), 3.56 (t, *J*=5.40 Hz, 2H), 2.65 (m, 2H), 2.56 (m, 2H), 1.06 (m, 3H)

(2-Hydroxy-ethyl)-carbamic acid tert-butyl ester (23). To a solution of ethanolamine hydrochloride (10.25 mmol) in THF (35 mL) was added an aqueous solution of NaHCO$_3$ (20.50 mmol in 10 mL of water) followed by addition of di-*tert*-butyl dicarbonate (10.25 mmol). After stirring at room temperature overnight, the reaction was quenched with water and extracted with Et$_2$O. The organic layer was washed with brine, dried over MgSO$_4$, filtered, and concentrated under reduced pressure to give the crude product. The crude product was purified via flash SiO$_2$ chromatography (EtOAc/hexanes (1:10) to (1:3) to (1:1) to give **23** (1.569 g, 95% yield). ^{1}H NMR (400 MHz, chloroform-*d*) δ 4.95 (s, 1H), 3.71 (m, 2H), 3.30 (m, 2H), 2.39 (s, 1H), 1.45 (s, 9H)

Methanesulfonic acid 2-tert-butoxycarbonylamino-ethyl ester (24). To a solution of

23 (9.73 mmol) in pyridine (5 mL) at 0 °C **methanesulfonyl chloride (10.71 mmol)** was

added dropwise. The reaction was warmed to room temperature and stirred for 15 min

and then diluted with Et_2O. The organic layer was washed with water and brine, dried

over $MgSO_4$, filtered, and concentrated under reduced pressure to give the crude product.

The crude product was purified via flash SiO_2 chromatography (EtOAc/hexanes (1:4) to

(3:7) to give **24** (1.798 g, 77% yield). ^{1}H NMR (400 MHz, chloroform-*d*) δ 4.90 (s, 1H),

4.29 (m, 2H), 3.48 (m, 2H), 3.04 (s, 3H), 1.45 (s, 9H)

References

1.   Hartong, R.,Wiersinga, W. M.;Plomp, T. A. (1990) Amiodarone reduces the
        effect of T3 on beta adrenergic receptor density in rat heart, *Horm Metab Res 22*,
        85-9.

2.   Basaria, S.;Cooper, D. S. (2005) Amiodarone and the thyroid, *Am J Med 118*,
        706-14.

3.   Plomp, T. A.,van Rossum, J. M.,Robles de Medina, E. O.,van Lier, T.;Maes, R.
        A. (1984) Pharmacokinetics and body distribution of amiodarone in man,
        Arzneimittelforschung 34, 513-20.

4.   Wiersinga, W. M.;Trip, M. D. (1986) Amiodarone and thyroid hormone
        metabolism, *Postgrad Med J 62*, 909-14.

5.   Wiersinga, W. M. (1997) Towards an animal model of amiodarone-induced
        thyroid dysfunction, *Eur J Endocrinol 137*, 15-7.

6.   Latham, K. R.,Sellitti, D. F.;Goldstein, R. E. (1987) Interaction of amiodarone
        and desethylamiodarone with solubilized nuclear thyroid hormone receptors, *J Am
        Coll Cardiol 9*, 872-6.

7.   Bakker, O.,van Beeren, H. C.;Wiersinga, W. M. (1994) Desethylamiodarone is a
        noncompetitive inhibitor of the binding of thyroid hormone to the thyroid
        hormone beta 1-receptor protein, *Endocrinology 134*, 1665-70.

8.   van Beeren, H. C.,Bakker, O.;Wiersinga, W. M. (1995) Desethylamiodarone is a
        competitive inhibitor of the binding of thyroid hormone to the thyroid hormone
        alpha 1-receptor protein, *Mol Cell Endocrinol 112*, 15-9.

9.   Scanlan, T. S.,Suchland, K. L.,Hart, M. E.,Chiellini, G.,Huang, Y.,Kruzich, P. J.,Frascarelli, S.,Crossley, D. A.,Bunzow, J. R.,Ronca-Testoni, S.,Lin, E. T.,Hatton, D.,Zucchi, R.;Grandy, D. K. (2004) 3-Iodothyronamine is an endogenous and rapid-acting derivative of thyroid hormone, *Nat Med 10*, 638-42.

10.   Hart, M. E.,Suchland, K. L.,Miyakawa, M.,Bunzow, J. R.,Grandy, D. K.;Scanlan, T. S. (2006) Trace amine-associated receptor agonists: synthesis and evaluation of thyronamines and related analogues, *J Med Chem 49*, 1101-12.

11.   Lindemann, L.;Hoener, M. C. (2005) A renaissance in trace amines inspired by a novel GPCR family, *Trends Pharmacol Sci 26*, 274-81.

12.   Reese, E. A.,Bunzow, J. R.,Arttamangkul, S.,Sonders, M. S.;Grandy, D. K. (2007) Trace amine-associated receptor 1 displays species-dependent stereoselectivity for isomers of methamphetamine, amphetamine, and para-hydroxyamphetamine, *J Pharmacol Exp Ther 321*, 178-86.

13.   Navarro, H. A.,Gilmour, B. P.;Lewin, A. H. (2006) A rapid functional assay for the human trace amine-associated receptor 1 based on the mobilization of internal calcium, *J Biomol Screen 11*, 688-93.

14.   Wainscott, D. B.,Little, S. P.,Yin, T.,Tu, Y.,Rocco, V. P.,He, J. X.;Nelson, D. L. (2007) Pharmacologic characterization of the cloned human trace amine-associated receptor1 (TAAR1) and evidence for species differences with the rat TAAR1, *J Pharmacol Exp Ther 320*, 475-85.

15.   Tan, E. S.,Miyakawa, M.,Bunzow, J. R.,Grandy, D. K.;Scanlan, T. S. (2007) Exploring the structure-activity relationship of the ethylamine portion of 3-

iodothyronamine for rat and mouse trace amine-associated receptor 1, *J Med Chem 50*, 2787-98.

Appendix

Plasmid Collection

		Plasmid Collection		
name	plasmid	sequencing information	created by
SSF-rTAAR1	pIRESneo	silent mutation A45G in SSF	Aaron Snead
SSF-rTAAR4-TA	pcDNA3.1/V5-His TOPO TA		Aaron Snead
SSF-rTAAR4	pIRESneo	silent mutation A45G in SSF	Aaron Snead
SSF-rTAAR6-TA	pcDNA3.1/V5-His TOPO TA		Aaron Snead
SSF-rTAAR6	pIRESneo	silent mutation A45G in SSF	Aaron Snead
SSF-rTAAR7a	pIRESneo	silent mutation A45G in SSF	Aaron Snead
SSF-rTAAR7d-TA	pcDNA3.1/V5-His TOPO TA		Aaron Snead
SSF-rTAAR7g	pIRESneo	silent mutation A45G in SSF	Aaron Snead
SSF-rTAAR8a	pIRESneo	silent mutation A45G in SSF	Aaron Snead
SSF-rTAAR8c-TA	pcDNA3.1/V5-His TOPO TA		Aaron Snead
SSF-rTAAR8c	pIRESneo	silent mutation A45G in SSF	Aaron Snead
SSF-rTAAR9-TA	pcDNA3.1/V5-His TOPO TA		Aaron Snead
SSF-rTAAR9	pIRESneo	silent mutation A45G in SSF	Aaron Snead
hVMAT1	pcDNA3		Aaron Snead
hVMAT1	pBluescript		Edwards Lab
rVMAT2	pcDNA3.1		Edwards Lab
hVMAT2	pcDNA3.1		Edwards Lab
rDAT	pBluescript		Amara Lab
hDAT	pBluescript		Amara Lab
rNET	pBluescript		Amara Lab
hNET	pBluescript		Amara Lab
rSERT	pcDNA3		Blakely Lab
hSERT	pcDNA3		Blakely Lab
CRE-Luc			Grandy Lab

rTAAR Cell Line Collection

Stable HEK293 Cell Line Inventory
empty pIRESneo
EV B2
EV-2 A
EV-2 B2
EV-2 F
EV-2 K2

Stable HEK293 Cell Line Inventory
$TAAR_4$ (TAR_2)
2 C
2 F
2 H
2 J
2 K
2 L
2-2 A
2-2 B2
2-2 C2
2-2 D
2-2 E

Stable HEK293 Cell Line Inventory
TAAR$_6$ (TAR$_4$)
4 B3
4 C2
4 E
4 G2
4 H
4 J
4-2 B2
4-2 D2
4-2 E2
4-2 G
4-2 J
4-2 L2

Stable HEK293 Cell Line Inventory
TAAR$_{7a}$ (TAR$_8$)
8 B
8 C
8 D3
8 E
8 F2
8 G
8 H
8 I2
8 J2
8-2 B
8-2 C2
8-2 F
8-2 H
8-2 I

Stable HEK293 Cell Line Inventory
TAAR$_{7g}$ (TAR$_9$)
9 D
9 J
9 K
9 L2
9-2 A2
9-2 C
9-2 D
9-2 G2
9-2 H2
9-2 I

Stable HEK293 Cell Line Inventory
TAAR$_{8a}$ (TAR$_{11}$)
11 A
11 C3
11 D2
11 E
11-2 A3
11-2 C2
11-2 D2
11-2 E2
11-2 F
11-2 G2

Stable HEK293 Cell Line Inventory
TAAR$_{8c}$ (TAR$_{10}$)
10 B
10 C
10 D
10 E
10 F
10-2 A
10-2 C2
10-2 D2
10-2 E
10-2 F2
10-2 G2
10-2 H2
10-2 I

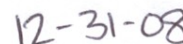| Stable HEK293 Cell Line Inventory |
| --- |
| $TAAR_9$ (TAR_3) |
| 3 B2 |
| 3 C |
| 3 G2 |
| 3-2 A2 |
| 3-2 B |
| 3-2 C |
| 3-2 D |
| 3-2 E |
| 3-2 H |
| 3-2 J2 |

Publishing Agreement

It is the policy of the University to encourage the distribution of all theses, dissertations, and manuscripts. Copies of all UCSF theses, dissertations, and manuscripts will be routed to the library via the Graduate Division. The library will make all theses, dissertations, and manuscrpts accessible to the public and will preserve these to the best of their abilities, in perpetuity.

Please sign the following statement:

I hereby grant permission to the Graduate Division of the University of California, San Francisco to release copies of my thesis, dissertation, or manuscript to the Campus Library to provide access and preservation, in whole or in part, in perpetuity.

_____
Author Signature

12-31-08
Date